

DEUTSCHES ELEKTRONEN – SYNCHROTRON **DESY**

DESY 89-043
UCLA/89/TEP/12
April 1989



The Physics of Neutrinos

R.D. Peccei
Deutsches Elektronen-Synchrotron DESY, Hamburg

ISSN 0418-9833

NOTKESTRASSE 85 · 2 HAMBURG 52

DESY behält sich alle Rechte für den Fall der Schutzrechtserteilung und für die wirtschaftliche Verwertung der in diesem Bericht enthaltenen Informationen vor.

DESY reserves all rights for commercial use of information included in this report, especially in case of filing application for or grant of patents.

To be sure that your preprints are promptly included in the
HIGH ENERGY PHYSICS INDEX,
send them to the following address (if possible by air mail):

**DESY
Bibliothek
Notkestrasse 85
2 Hamburg 52
Germany**

I. Neutrinos in the Standard Model

Neutrinos play a special role in the $SU(2) \times U(1)$ model of the electroweak interactions - the standard model [1]. As is well known, in the model the chiral fields $\Psi_L = \frac{1}{2}(1 - \gamma_5)\Psi$ and $\Psi_R = \frac{1}{2}(1 + \gamma_5)\Psi$ have different $SU(2)$ properties, with Ψ_L being part of $SU(2)$ doublets and Ψ_R being singlets. Furthermore, since the $U(1)$ properties are fixed by the electromagnetic charge identification:

$$Q = T_3 + Y, \quad (1)$$

with T_3 being the 3rd component of the $SU(2)$ generator and Y being the $U(1)$ generator, it follows that the right handed neutrino fields, ν_{Ri} , have also no $U(1)$ interactions*. Thus, these fields are sterile under $SU(2) \times U(1)$ and the electroweak interactions act only on the left handed neutrinos, ν_{Li} . Because of these circumstances, we cannot tell (up to now) if right handed neutrinos exist at all.

The statement of neutrino sterility is not quite true, since a $\nu_R - \nu_L$ Higgs coupling can exist. The Higgs doublet Φ , whose vacuum expectation value presumably is responsible for the breakdown of $SU(2) \times U(1) \rightarrow U(1)_{em}$, carries weak hypercharge of $-\frac{1}{2}$: $\Phi \sim (2, -\frac{1}{2})$. Thus an invariant coupling of Φ with a $\nu_{Li} \sim (2, +\frac{1}{2})$ and a $\nu_{Rj} \sim (1, 0)$ is allowed by $SU(2) \times U(1)$, as shown in Fig. 1. When $SU(2) \times U(1) \rightarrow U(1)_{em}$, because Φ acquires a non zero vacuum expectation value, $\langle \Phi \rangle$, these Yukawa couplings can generate a (Dirac) mass term for the neutrinos, as shown schematically in Fig. 2. No evidence exists at present for a (Dirac) mass matrix - with associated eigenvalues $(m_D)_{ij}$

$$\mathcal{L}_{mass}^{Dirac} = -\nu_{Li}(m_D)_{ij}\nu_{Rj} - \nu_{Ri}(m_D^\dagger)_{ij}\nu_{Lj} \quad (2)$$

Even if neutrino masses existed, certainly the physical mass of the neutrinos for each generation is much less than that of the corresponding charged leptons: $m_{\nu_i} \ll m_i$ **. Thus, even if right handed neutrinos existed, it is very difficult to find out about this experimentally, since all evidence for the presence of ν_{Ri} is proportional to the neutrino mass m_{ν_i} .

* Here i is a family index

** The physical masses are not necessarily the eigenvalues of m_D , if there are Majorana masses in the theory (see Sec. II). Nevertheless, these are the parameters which are important in judging the physical effects of right handed neutrinos.

The Physics of Neutrinos

R. D. Peccei*†

Deutsches Elektronen-Synchrotron DESY

Hamburg

Fed. Rep. Germany

ABSTRACT

After discussing properties of neutrinos in the standard electroweak theory, several theoretical issues related to neutrino masses are broached, including the different mass options available (Dirac and Majorana) and the see-saw mechanism. Experimental limits on neutrino masses and mixing, as well as double beta decay experiments are also reviewed. The role of neutrinos in cosmology is emphasized, both for nucleosynthesis and as possible sources of the dark matter in the Universe. Finally, several astrophysical aspects of neutrinos are touched upon, including the solar neutrino problem and the role of neutrinos in supernovas, particularly SN 1987a

* Lectures presented at the Flavor Symposium, Peking University, Beijing, Peoples Republic of China, August 1988. To appear in the Symposium Proceedings.

† Present address: Department of Physics, UCLA, Los Angeles, California, 90024-1547, USA

I.1 Charged and Neutral Current Interactions of Neutrinos

In the standard model, as we discussed above, to a very good approximation one can ignore altogether right handed neutrinos and consider only their left handed counterparts. These neutrinos, with the corresponding left handed charged leptons, form an $SU(2)$ doublet:

$$L_i = \begin{pmatrix} \nu_i \\ l_i \end{pmatrix}_L \quad (3)$$

Given this assignment, the interaction of the neutrinos with the $SU(2) \times U(1)$ gauge fields is fixed, since these interactions arise from replacing in the fermion kinetic energy terms, all derivatives by covariant derivatives. For the doublets (3), with $U(1)$ quantum numbers of $-\frac{1}{2}$, one has

$$\mathcal{L} = -\bar{L}_i \gamma^\mu \frac{1}{2} D_\mu L_i \quad (4)$$

where

$$D_\mu L_i = [\partial_\mu - ig \frac{\tau_a}{2} W_{a\mu} + i g' Y_\mu] L_i \quad (5)$$

Here $W_{a\mu}$ ($a = 1, 2, 3$) and Y_μ are the $SU(2)$ and $U(1)$ gauge fields and g and g' are their respective coupling constants. It follows from (4) and (5) that the neutrino interactions are given by

$$\mathcal{L}_{int} = g W_a^\mu J_{a\mu} + g' Y^\mu J_\mu \quad (6)$$

where the $SU(2)$ and $U(1)$ currents containing neutrinos are

$$J_a^\mu = \bar{L}_i \gamma^\mu \frac{\tau_a}{2} L_i; \quad J^\mu = -\frac{1}{2} \bar{L}_i \gamma^\mu L_i \quad (7)$$

To describe the physical interactions of neutrinos in the standard model one must take into account of two effects resulting from the $SU(2) \times U(1) \rightarrow U(1)_{em}$ breakdown. Namely, that:

- i) The mass and charge eigenstates for the gauge fields are linear combinations of the W_a^μ and Y^μ fields, with the physical excitations being:

$$W_\pm^\mu = \frac{1}{\sqrt{2}} (W_1^\mu \mp i W_2^\mu) \quad (8)$$

and

$$\begin{pmatrix} Z^\mu \\ A^\mu \end{pmatrix} = \begin{pmatrix} \cos \Theta_W & -\sin \Theta_W \\ \sin \Theta_W & \cos \Theta_W \end{pmatrix} \begin{pmatrix} W_3^\mu \\ Y^\mu \end{pmatrix} \quad (9)$$

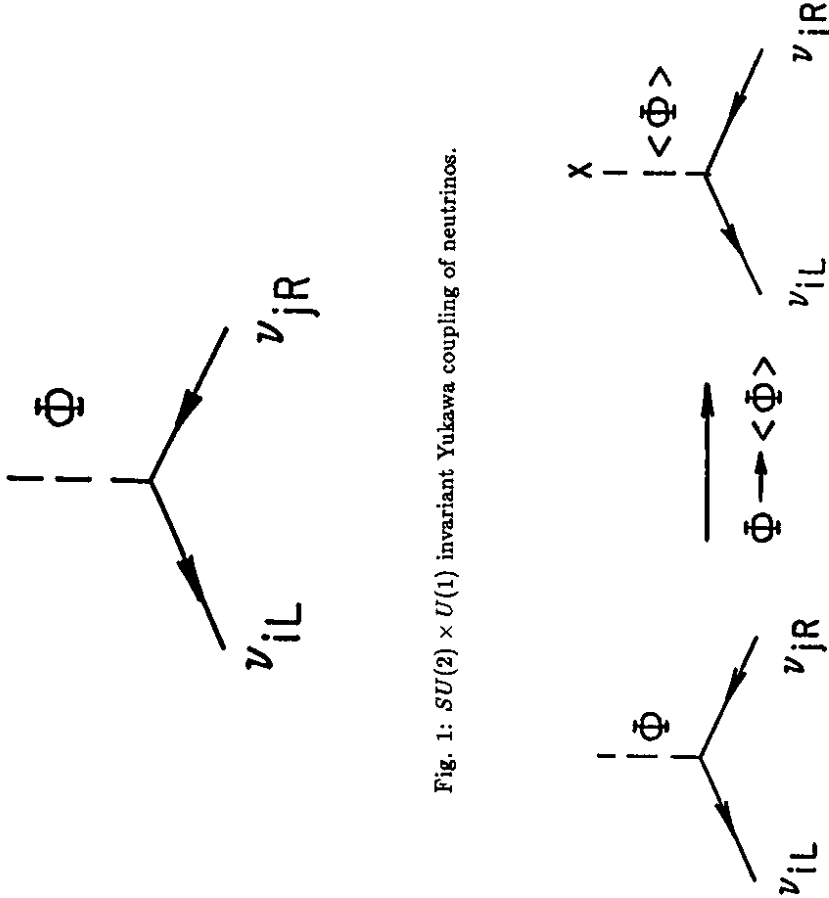


Fig. 1: $SU(2) \times U(1)$ invariant Yukawa coupling of neutrinos.

Fig. 2: Dirac mass generation for neutrinos.

Here Θ_W is the Weinberg angle, which relates the coupling constants g and g' to the electric charge e via the unification condition:

$$e = g \sin \Theta_W = g' \cos \Theta_W, \quad (10)$$

and A^μ is the photon field. These physical excitations couple to the currents which are linear combinations of J_μ^u and J_μ^d . From (6) one sees readily that

$$\mathcal{L}_{\text{int}} = \frac{e}{2\sqrt{2} \sin \Theta_W} [J_\mu^+ W_{-\mu} + J_\mu^- W_{+\mu}] + \frac{e}{2 \cos \Theta_W \sin \Theta_W} [J_{NC}^\mu Z_\mu] + e J_{em}^\mu A_\mu \quad (11)$$

where the charged currents (CC), J_\pm^μ , the neutral current (NC), J_{NC}^μ , and the electromagnetic current (EM), J_{em}^μ , are given by

$$J_\pm^\mu = 2[J_1^\mu \mp iJ_2^\mu] \quad (12)$$

$$J_{NC}^\mu = 2[J_3^\mu - \sin^2 \Theta_W J_{em}^\mu] \quad (13)$$

$$J_{em}^\mu = J_3^\mu + J^\mu \quad (14)$$

ii) As a result of the $SU(2) \times U(1)$ breakdown quarks (and charged leptons) acquire mass. However, since the quark mass eigenstates are not the same as the weak interaction eigenstates, there exists flavor mixing in the charged current interactions. For the leptonic currents, however, there is no flavor mixing in the limit that neutrino masses are neglected.

It is worthwhile to expand briefly on this last point. The Yukawa interactions of quarks and leptons with the Higgs doublet - analogous to those shown in Fig 1 - when $SU(2) \times U(1) \rightarrow U(1)_{em}$ produce mass matrices for fermions of the same charge

$$\mathcal{L}_{\text{mass}} = -\bar{u}_{iL} M_{ij}^u u_{jR} - \bar{d}_{iL} M_{ij}^d d_{jR} - \bar{\ell}_{iL} M_{ij}^\ell \ell_{jR} + h.c. \quad (15)$$

In Eq (15) no neutrino mass term is included, since by assumption here no ν_{iR} fields are considered. The matrices M_{ij}^f ($f = u, d, \ell$) are in general not diagonal. However, they can be diagonalized by a basis change on the quark and lepton fields:

$$\Psi_L^f \rightarrow U_L^f \Psi_L^f; \quad \Psi_R^f \rightarrow U_R^f \Psi_R^f \quad (16)$$

It is this basis change which produces interfamily mixing in the charged current.

Consider for definitiveness the case of three families where, before the basis change, the charged current J_μ^+ reads

$$J_\mu^+ = 2(\bar{\nu}_e \bar{\nu}_\mu \bar{\nu}_\tau)_L \gamma^\mu \mathbf{1} \begin{pmatrix} c \\ \mu \\ \tau \end{pmatrix}_L + 2(\bar{u} \bar{c} \bar{t})_L \gamma^\mu \mathbf{1} \begin{pmatrix} d \\ s \\ b \end{pmatrix}_L \quad (17)$$

After the basis change of Eq (16) this current reads

$$J_\mu^+ = 2(\bar{\nu}_e \bar{\nu}_\mu \bar{\nu}_\tau)_L \gamma^\mu U_L^+ \begin{pmatrix} c \\ \mu \\ \tau \end{pmatrix}_L + 2(\bar{u} \bar{c} \bar{t})_L \gamma^\mu (U_L^+)^t U_L^+ \begin{pmatrix} d \\ s \\ b \end{pmatrix}_L \quad (18)$$

For the quark sector the matrix entering in (18) is just the 3×3 unitary Kobayashi Maskawa mixing matrix [2]

$$V = (U_L^+)^t U_L^+ \quad (19)$$

For the lepton sector, however, since $m_{\nu_i} = 0$ the mixing matrix U_L^+ can be eliminated by a unitary redefinition of the neutrino fields

$$\nu_L \rightarrow U_L^+ \nu_L \quad (20)$$

This redefinition is possible since the neutrinos, in the limit of not including any ν_R fields, are degenerate. The form of the charged current is then

$$J_\mu^+ = 2(\bar{\nu}_e \bar{\nu}_\mu \bar{\nu}_\tau)_L \gamma^\mu \mathbf{1} \begin{pmatrix} c \\ \mu \\ \tau \end{pmatrix}_L + 2(\bar{u} \bar{c} \bar{t})_L \gamma^\mu V \begin{pmatrix} d \\ s \\ b \end{pmatrix}_L \quad (21)$$

$$J_\mu^- = (J_\mu^+)^t$$

One concludes, therefore, that neutrino CC interactions do not cause family change transitions, as long as one assumes that $m_{\nu_i} = 0$.

The basis change (16) does not affect the electromagnetic and the neutral currents, since what are involved in both currents is $(U_L^+)^t U_L^+ = (U_R^+)^t U_R^+ = \mathbf{1}$. Thus, these currents are diagonal in flavor. Using Eq (13) one finds for each fermion f in the theory

$$(J_{NC}^\mu)^f = f \gamma^\mu [Q_L^f (1 - \gamma_5) + Q_R^f (1 + \gamma_5)] f \quad (22)$$

$$(J_{em}^\mu)^f = e^f \bar{f} \gamma^\mu f \quad (23)$$

where the chiral charges $Q_{L,R}^f$ are given by

$$Q_L^f = T_3^f - e^f \sin^2 \Theta_W; \quad Q_R^f = -e^f \sin^2 \Theta_W \quad (24)$$

with T_3^f and e^f being, respectively, the eigenvalues of the $SU(2)$ generator T_3 and of the electric charge Q for the left handed components of the fermions in question:

$$T_3^f = \begin{cases} \frac{1}{2} & \nu_i, u_i \\ -\frac{1}{2} & \ell_i, d_i \end{cases}; \quad e^f = \begin{cases} \frac{2}{3} & u_i \\ 0 & \nu_i \\ -\frac{1}{3} & d_i \\ -1 & \ell_i \end{cases} \quad (25)$$

Obviously the neutrino neutral current has a pure $V - A$ form involving only ν_{Li} . For 3 generations one has

$$(J_{NC}^\mu)^{neutrinos} = \frac{1}{2} [\nu_e \gamma^\mu (1 - \gamma_5) \nu_e + \nu_\mu \gamma^\mu (1 - \gamma_5) \nu_\mu + \nu_\tau \gamma^\mu (1 - \gamma_5) \nu_\tau] \\ = \nu_{eL} \gamma^\mu \nu_{eL} + \nu_{\mu L} \gamma^\mu \nu_{\mu L} + \nu_{\tau L} \gamma^\mu \nu_{\tau L} \quad (26)$$

Because both the CC, the NC, and the EM interactions of leptons are family diagonal[c. f. Eqs. (21) and (26)] one sees that the standard electroweak model - in the absence of neutrino mass terms - conserves separately the lepton number for each family.

Except for experiments at the large $p\bar{p}$ colliders at CERN and Fermilab, where real W 's and Z 's are being produced, most other experimental investigations of the standard model have occurred in circumstances where the momentum transfer $q^2 \ll M_W^2, M_Z^2$. In this case, one can replace the weak part of the interaction Lagrangian of Eq (11) by an effective current - current Lagrangian. As shown pictorially in Fig. 3, one has

$$\mathcal{L}_{eff} = \frac{i}{2!} \int \mathcal{L}_{int} \mathcal{L}_{int} \\ \simeq \left(\frac{e}{2\sqrt{2} \sin \Theta_W} \right)^2 \frac{1}{M_W^2} J_+^\mu J_-^\mu \\ + \frac{1}{2} \left(\frac{e}{2 \cos \Theta_W \sin \Theta_W} \right)^2 \frac{1}{M_Z^2} J_{NC}^\mu J_{NC\mu} \quad (27)$$

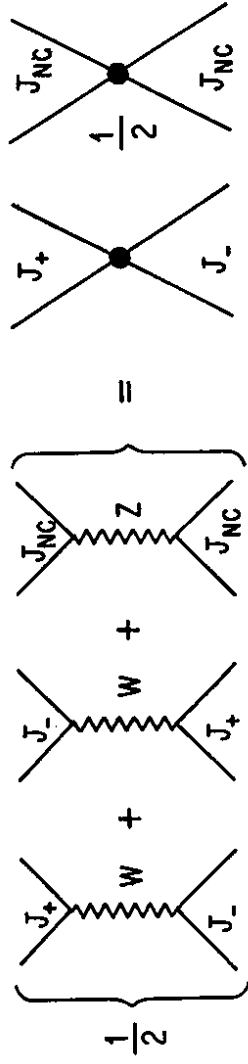


Fig. 3: Effective interactions in the limit $q^2 \ll M_W^2, M_Z^2$.

For the CC interactions, comparison with the Fermi theory identifies the Fermi constant G_F , as

$$\frac{G_F}{\sqrt{2}} = \frac{e^2}{8 \sin^2 \Theta_W M_W^2} \quad (28)$$

which provide a (lowest order) formula for the W mass, once $\sin^2 \Theta_W$ is determined experimentally*. Using Eq. (28) and defining a parameter ρ by

$$\rho = \frac{M_W^2}{\cos^2 \Theta_W M_Z^2} \quad (29)$$

one can rewrite the effective weak Lagrangian Eq (27) as

$$\mathcal{L}_{eff}^{weak} = \frac{G_F}{\sqrt{2}} \{ J_+^\mu J_-^\mu + \rho J_{NC}^\mu J_{NC\mu} \} \quad (30)$$

* Using $G_F \simeq 10^{-5} \text{ GeV}^{-2}$ and the experimental result $\sin^2 \Theta_W \simeq 0.25$ one sees that $M_W \simeq 80 \text{ GeV}$, so that indeed Eq. (27) is a very good approximation for most experiments to date.

Theoretically, it is easy to show that if the breakdown of $SU(2) \times U(1)$ to $U(1)_{em}$ is caused by an $SU(2)$ doublet vacuum expectation value, as has been assumed in the discussion so far, then the parameter ρ is fixed to be unity:

$$\rho = 1 \quad \text{doublet Higgs breakdown} \quad (31)$$

There is actually very good experimental evidence for this from experiments sensitive to the weak neutral current. In principle, these experiments in the standard model depend only on two parameters ρ and $\sin^2 \Theta_W$, which is hidden in the definition of J_{NC}^μ in Eq. (30). Thus, for the validity of the standard model, it is necessary that all experiments be fit with the same value for these parameters. Presently the most accurate experiments which determine ρ and $\sin^2 \Theta_W$ involves deep inelastic scattering of ν_μ and $\bar{\nu}_\mu$, and the direct measurement of the mass of the W and Z bosons. This data has reached a degree of precision where a correct comparison with the standard model necessitates the incorporation of electroweak radiative corrections. This is done with a particularly convenient definition of $\sin^2 \Theta_W$ suggested by Sirlin [3], which relates it to the W and Z masses via Eq (29) also to higher order in α :

$$\sin^2 \Theta_W = 1 - \frac{M_W^2}{M_Z^2 \rho} \quad (32)$$

where $\rho = 1$, if the $SU(2) \times U(1)$ breaking is done by a Higgs doublet.

Amaldi et al [4] and Costa et al [5] recently have done a global analysis of all extant neutral current experiments to deduce values for ρ and $\sin^2 \Theta_W$. They find that all experiments are in agreement with each other, fixing $\sin^2 \Theta_W$ and ρ to the per cent level, thereby testing the standard model of Glashow, Salam and Weinberg [1] to this accuracy. To give an idea of the accuracy and breadth of scope of the results, I reproduce in Table I the compilation of Amaldi et al [4] for $\sin^2 \Theta_W$ and ρ for the various experiments analyzed. I quote below also the global fit values obtained by Amaldi et al [4] *

$$\begin{aligned} \sin^2 \Theta_W(\rho = 1) &= 0.230 \pm 0.005 \\ \sin^2 \Theta_W &= 0.227 \pm 0.006 \quad ; \quad \rho = 0.998 \pm 0.009 \end{aligned} \quad (33)$$

I display in Fig. 4 the 90% C.L. allowed regions for ρ and $\sin^2 \Theta_W$, for the various experiments in question, which emerge from the global analysis of ref [4]. Clearly, the standard model very successfully correlates all existing neutral current data.

* The results of Costa et al [5] are consistent with those given in eq (33) and have a similar accuracy.

Table I: Values of $\sin^2 \Theta_W$ and ρ obtained in the global fit of Amaldi et al [4]. The error in [] is their estimate of the theoretical error

Reaction	$\sin^2 \Theta_W, \rho = 1$	$\sin^2 \Theta_W$	ρ
ν_μ DIS (Isoscalar Targets)	0.233 ± 0.003 $\pm [0.005]$	0.232 ± 0.014 $\pm [0.008]$	0.999 ± 0.013 $\pm [0.008]$
W/Z masses	0.228 ± 0.007 $\pm [0.002]$	0.228 ± 0.018 $\pm [0.003]$	1.015 ± 0.026 $\pm [0.004]$
$\nu_\mu p \rightarrow \nu_\mu p$	0.210 ± 0.033	0.205 ± 0.041	0.980 ± 0.060 $\pm [0.050]$
$\nu_\mu e \rightarrow \nu_\mu e$	0.223 ± 0.018 $\pm [0.002]$	0.221 ± 0.021 $\pm [0.003]$	0.976 ± 0.055 $\pm [0.002]$
Atomic Parity Violation	0.209 ± 0.018 $\pm [0.014]$		
Polarized eD DIS asym.	0.221 ± 0.015 $\pm [0.013]$		
Polarized $\mu^\pm C$ DIS asym.	0.250 ± 0.080		

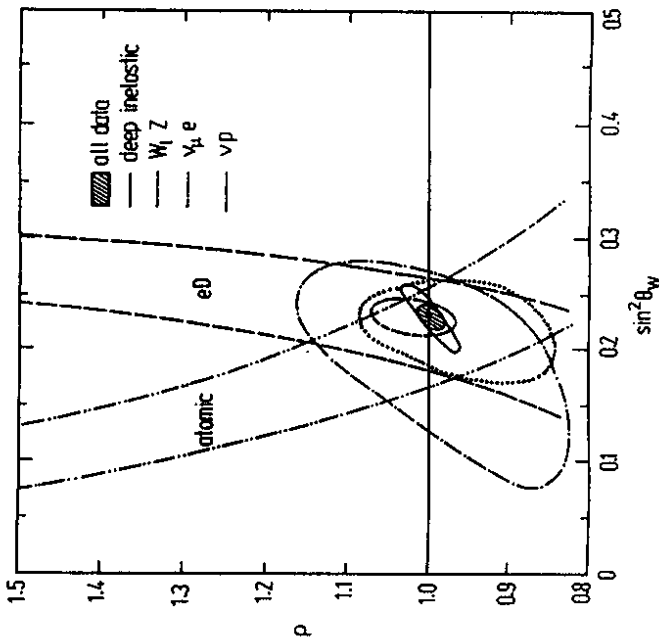


Fig. 4: 90% C.L. allowed region for the $\sin^2 \Theta_w$ and ρ for the various neutral current experiments analyzed by Amaldi et al [4].

1.2 Neutrino Counting

There is a second aspect of neutrinos in the standard model, which has been explored experimentally recently, connected with the issue of how many species of neutrinos exist. This is a very interesting question since, presumably, if one could determine the total number of neutrino species this would tell us also how many different families of quarks and leptons there are*. The idea behind neutrino counting experiments is extremely simple, since it is based on just one fact and a reasonable assumption. Namely,

- i) the coupling of the Z to all neutrino species is universal [cf Eq (26)].
- ii) Presumably all neutrino species are either massless or very light with $m_{\nu_i} \ll M_Z$.

* For this inference one must assume that all neutrinos are alike with small or vanishing masses, so that "light" neutrino counting is equivalent to counting all neutrino species.

Hence all types of neutrinos can be produced from the decay of a (real or virtual) Z boson.

Based on the above simple observations there exist now in the literature two quite strong bounds on the number of neutrino types N_ν , coming both from experiments performed at the e^+e^- colliders PEP and PETRA and from experiments at the CERN $p\bar{p}$ collider. The bounds on N_ν obtained by these particle physics experiments, which I will discuss below, turn out to be comparable to the bound on light neutrinos $m_\nu \leq 0(MeV)$ to be discussed in Section IV, which one can derive from primordial nucleosynthesis. Both bounds put the number of species of neutrinos close to the number of already known neutrinos, thereby strengthening the belief that there are probably only three (or perhaps four) generations of quarks and leptons.

1.2.1 $e^+e^- \rightarrow \gamma$ Nothing

At PEP and PETRA the production of photons unaccompanied by other charged or neutral interacting particles - the process $e^+e^- \rightarrow \gamma$ Nothing - has been studied. This reaction in the standard model can occur by pair producing neutrinos, along with some bremsstrahlung photon: $e^+e^- \rightarrow \nu_i \bar{\nu}_i \gamma$. Clearly, the more neutrino species there are, the larger the contribution one expects from this process to the total cross section for $e^+e^- \rightarrow \gamma$ Nothing. Experimentally, however, the situation is complicated, since the signal can also be faked by radiative e^+e^- production, in which the final charged particles never come out of the beam pipe. To minimize this background one must require that the produced photon comes out at a rather large angle, with respect to the incident e^+e^- direction. This cut, however, also reduces the expected signal and, typically, one is left with just a handful of events.

The two graphs that contribute to the process $e^+e^- \rightarrow \nu_i \bar{\nu}_i \gamma$ are shown in Fig. 5. Since the coupling of the Z is universal, it is obvious that the total rate will be the same for each species. There is, however, a complication for the case in which ν_i is an electron neutrino ($\nu_i = \nu_e$). For the process $e^+e^- \rightarrow \nu_e \bar{\nu}_e \gamma$, in addition to the s -channel NC contribution, there is also a t -channel CC contribution as Fig. 6 shows. For the energies of PEP and PETRA, where $\sqrt{s} \ll M_Z$, one can compute all processes in the Fermi approximation, where all gauge boson propagators are just replaced by constants. This has two consequences:

- i) The internal photon emission graph for the process $e^+e^- \rightarrow \nu_e \bar{\nu}_e \gamma$ is totally negligible, since it involves two weak propagators, and can be omitted.

ii) By means of a Fierz transformation one can recast the ν_e calculation in a similar form as that appropriate for arbitrary neutrinos.

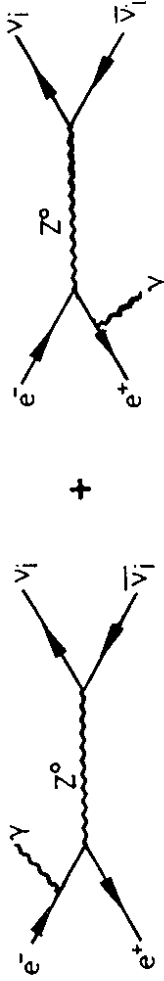


Fig. 5: Graphs contributing to the process $e^+e^- \rightarrow \nu_i \bar{\nu}_i \gamma$, with $\nu_i \neq \nu_e$.

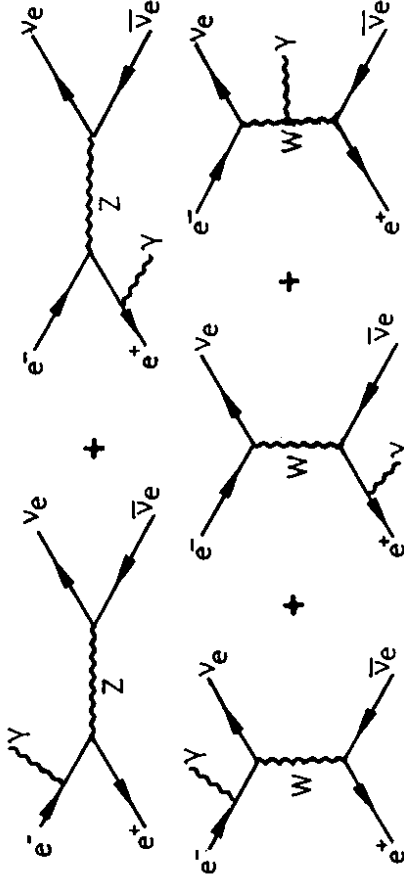


Fig. 6: Graphs contributing to the process $e^+e^- \rightarrow \nu_e \bar{\nu}_e \gamma$.

Let me expand a bit on the last point. In the Fermi approximation, the effective neutral current Lagrangian describing $e^+e^- \rightarrow \nu_i \bar{\nu}_i$ is given by [c.f. Eq(30)]*

$$\mathcal{L}_{NC}^{eff} = \frac{G_F}{\sqrt{2}} [\bar{\nu}_i \gamma^\mu (1 - \gamma_5) \nu_i] [\bar{e} (Q_L^i \gamma_\mu (1 - \gamma_5) + Q_R^i \gamma_\mu (1 + \gamma_5)) e] \quad (34)$$

where the chiral charges $Q_{L,R}^i$ are

$$Q_L^i = -\frac{1}{2} + \sin^2 \Theta_W; \quad Q_R^i = \sin^2 \Theta_W \quad (35)$$

The charged current Lagrangian, corresponding to the process $e^+e^- \rightarrow \nu_e \bar{\nu}_e$ on the other hand, is given by

$$\mathcal{L}_{CC}^{eff} = \frac{G_F}{\sqrt{2}} [\bar{\nu}_e \gamma^\mu (1 - \gamma_5) e] [\bar{e} \gamma_\mu (1 - \gamma_5) \nu_e] \quad (36)$$

This Lagrangian, however, can be rewritten as that appearing in Eq(34), after a Fierz transformation:

$$[\mathcal{L}_{CC}^{eff}]_{Fierz} = \frac{G_F}{\sqrt{2}} [\bar{\nu}_e \gamma^\mu (1 - \gamma_5) \nu_e] [\bar{e} \gamma_\mu (1 - \gamma_5) e] \quad (37)$$

Clearly, therefore, the result of the computation for producing electron neutrinos is just like that for producing any other neutrino, but with the replacement

$$Q_L^i \rightarrow (Q_L^i)_{eff} = Q_L^i + 1; \quad Q_R^i \rightarrow (Q_R^i)_{eff} = Q_R^i \quad (38)$$

The calculation of the process $e^+e^- \rightarrow \nu \bar{\nu} \gamma$ was done originally by Ma and Okada [6] and it was repeated soon after by Gaemers, Gastmans and Renard [7], who corrected some errors in the first calculation. If one denotes by x the ratio of the photon energy to the incident electron energy in the CM system: $x = \frac{2E_\gamma}{\sqrt{s}}$ and by y the cosine of the angle that the photon makes with respect to the e^- direction: $y = \cos \Theta_\gamma$ (see Fig. 7), one finds [7]

$$\frac{d\sigma}{dx dy} = \frac{G_F^2 s (1-x)}{3\pi^2 x (1-y)^2} \left[\left(1 - \frac{1}{2}x\right)^2 + \frac{1}{4}x^2 y^2 \right] F \quad (39)$$

One sees that this cross section has the typical x^{-1} behaviour of a bremsstrahlung process. The factor F , in the Fermi approximation, is simply given by

$$F = (N_\nu - 1) [(Q_L^i)_{eff}^2 + (Q_R^i)_{eff}^2] + [(Q_L^i)_{eff}^2 + (Q_R^i)_{eff}^2] \\ = N_\nu \left[\frac{1}{4} - \sin^2 \Theta_W + 2 \sin^4 \Theta_W \right] + 2 \sin^2 \Theta_W \simeq 0.126 N_\nu + 0.46 \quad (40)$$

* I have taken $\rho = 1$ here, as that is what experiment indicates.

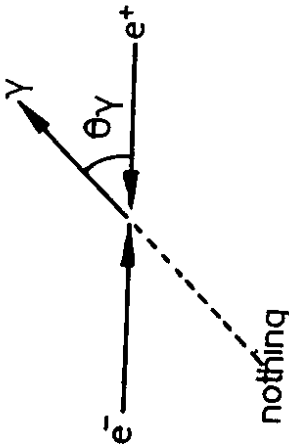


Fig. 7: Definition of the angle Θ_γ

That is, all neutrinos contribute equally, except for the electron neutrino which has just some different effective chiral charges. Unfortunately, as can be seen from Eq (40), the part in F not proportional to N_ν is rather large. Thus the difference between having three ($F \simeq 0.84$) or four ($F \simeq 0.96$) families is only about 15%.

Because of the cuts on y imposed to get rid of background at PEP and PETRA *, very few events of the type $e^+e^- \rightarrow \gamma$ *Nothing* are expected and very few are observed. Nevertheless, one has been able to set rather good limits on the number of neutrino species. The most sensitive results come from ASP at PEP [8] and CELLO at PETRA [9], giving 90 % C.L. of $N_\nu \leq 7.5$ and $N_\nu \leq 8.7$, respectively. An analysis of all e^+e^- data, done by the CELLO collaboration [9], gives a stronger combined limit

$$N_\nu < 4.6 \quad (90\% \text{ C.L.}) \quad (41)$$

I.2.2 Neutrino Counting in Collider Experiments

A bound on the number of neutrino species has also been obtained at the SpPS collider through the measurement of the ratio of the production of W bosons, decaying

* Typically $\Theta_\gamma > 20^\circ$.

into an electron and a neutrino [$W \rightarrow e\nu_e$], to that of Z bosons, decaying into e^+e^- pairs [$Z \rightarrow e^+e^-$]:

$$R = \frac{\sigma_W B(W \rightarrow e\nu_e)}{\sigma_Z B(Z \rightarrow e^+e^-)} \quad (42)$$

This ratio has been measured by both the UA1 and UA2 collaborations with the result

$$R = \begin{cases} 9.1_{-1.2}^{+1.7} & \text{UA1 [10]} \\ 7.2_{-1.2}^{+1.7} & \text{UA2 [11]} \end{cases} \quad (43)$$

This leads to an average value [12] of R :

$$\langle R \rangle = 8.4_{-0.9}^{+1.2} \quad (44)$$

and a 90 % confidence limit

$$R < 10.1 \quad (90\% \text{ C.L.}) \quad (45)$$

The ratio R depends on the number of neutrinos N_ν and on the top mass, m_t . This is easily seen by rewriting Eq (42) as a function of the total Z and W widths:

$$R = \left[\frac{\sigma_W}{\sigma_Z} \right] \left[\frac{\Gamma(W \rightarrow e\nu_e)}{\Gamma(Z \rightarrow e^+e^-)} \right] \frac{\Gamma_{tot}^Z}{\Gamma_{tot}^W} \quad (46)$$

The first two factors in square brackets above are fixed by our present theoretical knowledge. The ratio of the W and Z production cross sections is calculable in QCD, with reasonably good accuracy, while the ratio of the partial widths of $W \rightarrow e\nu_e$ to $Z \rightarrow e^+e^-$ is fixed by the $SU(2) \times U(1)$ model. The total width ratio, however, is affected by the unknown parameters in the standard model. Since Γ_{tot}^Z goes up the more neutrino species there are, it is clear that the bound on R of Eq (45) also gives a bound on N_ν . However, since the total widths depend on whether the decays $Z \rightarrow t\bar{t}$ and $W \rightarrow t\bar{b}$ are possible - and on how big their respective contributions are - the bound on N_ν depends also on the value of the t -quark mass.

To make the above remarks more quantitative, one needs to calculate the three quantities in square brackets in Eq (46). The widths $\Gamma(W \rightarrow e\nu_e)$ and $\Gamma(Z^0 \rightarrow e^+e^-)$ are straightforward to compute from the interaction Lagrangian of Eq (11). Neglecting the electron

mass, a simple calculation gives

$$\Gamma(W \rightarrow e\nu_e) = \frac{\sqrt{2}G_F M_W^3}{12\pi} \quad (47)$$

$$\Gamma(Z^0 \rightarrow e^+e^-) = \frac{\sqrt{2}G_F M_Z^3}{6\pi} [(Q_L^e)^2 + (Q_R^e)^2] \quad (48)$$

In the above, I have replaced the factor of $\frac{\alpha}{\sin^2 \Theta_W}$ which comes from a direct calculation using the Lagrangian of Eq (11), by $\frac{\sqrt{2}G_F M_W^2}{\pi}$. This replacement, effectively, takes care of the leading logarithmic radiative effects because, as can be seen in Eqs (47) and (48), both sides contain only quantities at large scales, or quantities like G_F which do not run. Using Eqs (47) and (48) one has

$$\frac{\Gamma(W \rightarrow e\nu_e)}{\Gamma(Z \rightarrow e^+e^-)} = \frac{2M_W^3}{M_Z^3 [1 - 4 \sin^2 \Theta_W + 8 \sin^4 \theta_W]} = 2.68 \quad (49)$$

The numerical value above uses a set of values for the parameters in the standard model which correspond to the central values presently measured, consistent with those given in Eq (33): $\sin^2 \Theta_W = 0.23$; $M_Z = 92 \text{ GeV}$; $M_W = 80.7 \text{ GeV}$.

To calculate the total Z width, in the standard model, one just needs to sum over the individual fermionic channels:

$$\Gamma_{tot}^Z = \sum_f \Gamma(Z \rightarrow ff) \quad (50)$$

From the UA1 bound on $m_t \geq (44 - 56) \text{ GeV}$ [13]), presumably the decay $Z \rightarrow t\bar{t}$ is not kinematically allowed. Thus the fermions f in Eq (50) include all those in the first three generations, except top, plus any extra (light) neutrinos of subsequent generations. Neglecting fermion masses again, which is an excellent approximation, and using Eqs (11) and (13) one finds

$$\Gamma(Z \rightarrow ff) = \frac{\sqrt{2}G_F M_Z^3}{6\pi} [(Q_L^f)^2 + (Q_R^f)^2] \begin{cases} 1 & \text{leptons} \\ 3(1 + \frac{2}{3}) & \text{quarks} \end{cases} \quad (51)$$

17

In the above the chiral charges Q_L^f , Q_R^f are given by [cf Eq (24)]

$$Q_L^f = T_{3f}^f - e^f \sin^2 \Theta_W; \quad Q_R^f = -e^f \sin^2 \Theta_W \quad (52)$$

where T_{3f} are the $SU(2)$ quantum numbers of the left-handed fermions and e^f are the fermion charges. The extra factor entering in Eq (51) for the quarks is a color factor of 3, times a QCD correction which accounts for the fact that, as shown in Fig. 8, a Z boson not only can decay into a $q\bar{q}$ pair but it can also have decays involving gluon emission. Using the estimate $\frac{\alpha_s(M_Z)}{\pi} = 0.04 \pm 0.01$ and the standard values of M_Z and $\sin^2 \Theta_W$ given above, one finds:

$$\Gamma(Z \rightarrow \nu\bar{\nu}) = 170 \text{ MeV} \quad (53)$$

$$\Gamma(Z \rightarrow e^+e^-) = 86 \text{ MeV} \quad (54)$$

$$\Gamma(Z \rightarrow u\bar{u}) = 306 \text{ MeV} \quad (55)$$

$$\Gamma(Z \rightarrow d\bar{d}) = 393 \text{ MeV} \quad (56)$$

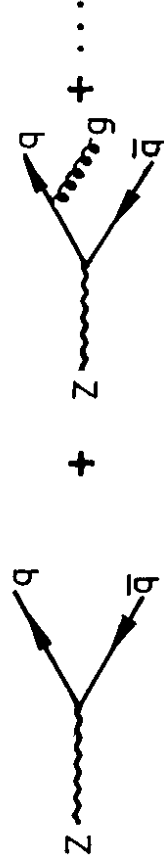


Fig. 8: QCD corrected decays of the Z boson, including gluon emission.

18

Using these results, the total Z width is

$$\Gamma_{tot}^Z = 2560 \text{ MeV} + (N_\nu - 3)170 \text{ MeV} \quad (57)$$

I note that the error on this prediction - apart from the uncertainty in M_Z which is irrelevant for our considerations, since the value of M_Z does not affect the branching ratio $B(Z \rightarrow e^+e^-)$ - is actually very small: the α_s uncertainty implies $\delta\Gamma_{tot}^Z = \pm 20 \text{ MeV}$, while the uncertainty in $\sin^2 \Theta_W$ of Eq (33), only gives $\delta\Gamma_{tot}^Z = \pm 12 \text{ MeV}$.

A similar analysis yields Γ_{tot}^W . If one again neglects all fermion masses, except m_t , then Γ_{tot}^W is independent of the Kobayashi Maskawa matrix V . A simple calculation, using Eqs (11) and (12), yields

$$\Gamma_{tot}^W = \Gamma(W \rightarrow e\nu_e) \{ 3 + 2[3(1 + \frac{\alpha_s}{\pi})] \} + \Gamma(W \rightarrow t\bar{b}) \quad (58)$$

Using the standard model parameters adopted earlier, Eq (47) implies

$$\Gamma(W \rightarrow e\nu_e) = 229 \text{ MeV} \quad (59)$$

For $W \rightarrow t\bar{b}$, on the other hand, one cannot forget phase space effects which kinematically suppress the rate. Neglecting again m_b , one finds

$$\Gamma(W \rightarrow t\bar{b}) = 3(1 + \frac{\alpha_s}{\pi}) \Gamma(W \rightarrow e\nu) \{ (1 + \frac{m_t^2}{2M_W^2})(1 - \frac{m_t^2}{M_W^2})^2 \} \quad (60)$$

The above formula implies $\Gamma(W \rightarrow t\bar{b}) = 395 \text{ MeV}$ for $m_t = 45 \text{ GeV}$, but $\Gamma(W \rightarrow t\bar{b}) \rightarrow 0$ as $m_t \rightarrow M_W$. For the standard model parameters adopted one has

$$\Gamma_{tot}^W = 2120 \text{ MeV} + \Gamma(W \rightarrow t\bar{b}) \quad (61)$$

with again little error - except for the error on M_W , but this error is irrelevant in the branching ratio that enters in R .

Collecting all the results one finds, in the standard model:

$$\frac{B(W \rightarrow e\nu_e)}{B(Z \rightarrow e^+e^-)} = \frac{\Gamma(W \rightarrow e\nu_e)}{\Gamma(Z \rightarrow e^+e^-)} \frac{\Gamma_{tot}^Z}{\Gamma_{tot}^W} = 2.68 \left\{ \frac{2560 + 170(N_\nu - 3)}{2120 + \Gamma(W \rightarrow t\bar{b})(\text{MeV})} \right\} \quad (62)$$

It is clear from the above that this ratio increases as N_ν increases and that the ratio also grows as $m_t \rightarrow M_W$, since then $\Gamma(W \rightarrow t\bar{b}) \rightarrow 0$. This behaviour is depicted in Fig. 9

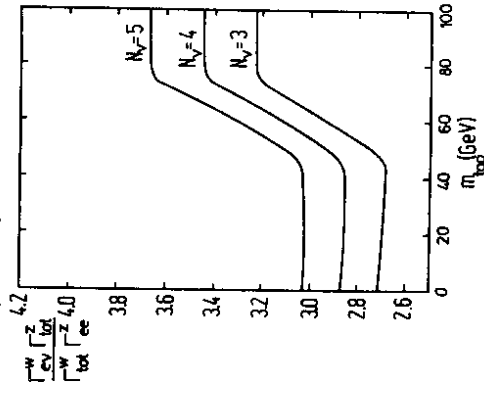


Fig. 9: The ratio of the $W \rightarrow e\nu_e$ to $Z \rightarrow e^+e^-$ branching ratios as a function of m_t , for various values of N_ν .

To complete the calculation of R one needs an estimate of the ratio $\frac{\sigma_W}{\sigma_Z}$. This is the place where the theoretical uncertainty is the largest. There are basically two sources of error in this ratio:

- i) The actual estimates for σ_W and σ_Z need values for the probability of finding u and d quarks in the proton. These probabilities are related to the corresponding structure functions and these, in turn, have some uncertainty.
- ii) In addition, the production cross sections for W and Z bosons are affected by QCD corrections, arising from either real or virtual emission of gluons- the so called K -factor.

Because one is dealing with a ratio of cross sections, it turns out that $\frac{\sigma_W}{\sigma_Z}$ is not very much affected by QCD corrections, since the W and Z K -factors tend to cancel out. On the other hand, the actual value for $\frac{\sigma_W}{\sigma_Z}$ depends to some extent on what structure functions one uses*.

Recently, Colas, Denegri and Stubenrauch [12] have done an extensive reanalysis of existing deep inelastic data from the BCDMS and EMC collaborations to try to determine $\frac{\sigma_W}{\sigma_Z}$ accurately. Their results, which are shown pictorially in Fig. 10 along with some other determinations, lead to a value

$$\frac{\sigma_W}{\sigma_Z} = 3.25 \pm 0.10 \quad (63)$$

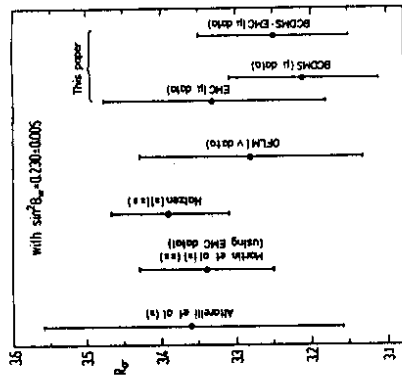


Fig. 10: Compilation of the results on $\frac{\sigma_W}{\sigma_Z}$, from [12].

Using Eqs (62) and (63) and the experimental bound on R of Eq (45), the bound on N_ν , as a function of the top quark mass, follows immediately. In effect, for the bound, what is important in the lowest value for $\frac{\sigma_W}{\sigma_Z}$ assumed. Using the 1σ value of $\frac{\sigma_W}{\sigma_Z}$ of Eq(63), $\frac{\sigma_W}{\sigma_Z} = 3.15$, Colas, Denegri and Stubenrauch obtain the results displayed in Fig. 11. One sees that for $m_t > M_W$ one has rather tight limits. These limits are displayed in a different

* σ_W requires a knowledge of $f_d \otimes f_u$, while σ_Z is proportional to $(f_d \otimes f_d) \oplus (f_u \otimes f_u)$, so there is not a complete cancellation in the ratio.

form in Fig. 12.

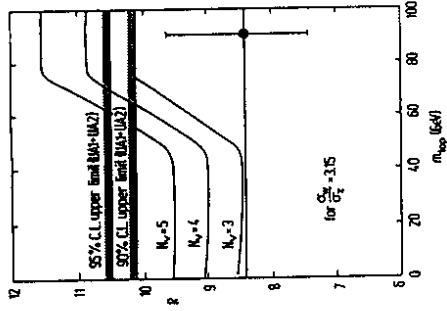


Fig. 11: Values of N_ν allowed by the combined UA1 and UA2 data on R , as a function of m_t , from [12].

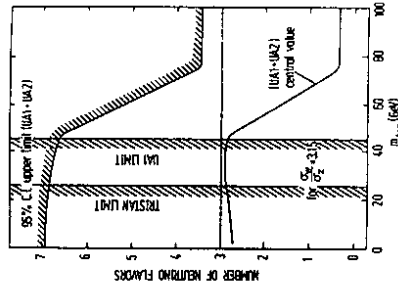


Fig. 12: Bounds on N_ν versus m_t , from [12].

From this figure, one sees that one can allow a few extra families if $m_t \simeq 50 GeV$, but there is essentially no freedom left if $m_t > 80 GeV$. To keep the above limits in perspective, however, one should note that if the minimum value assumed for $\frac{\sigma_Z}{\sigma_Z}$ goes down by 5% (i.e. $\frac{\sigma_Z}{\sigma_Z} = 3$ and not 3.15) then the allowed value for N_ν rises by one unit.

I close this Section with a remark on the future. Namely, that very accurate neutrino counting can be expected at LEP and SLC. First of all, at these colliders operating at the Z energy, one is expected to measure M_Z to an accuracy of better than 50 MeV [14]. With this measurement the actual error on Γ_{tot}^Z , due to the uncertainty in the Z mass is tiny. Hence, one can really hope to keep

$$(\delta\Gamma_{tot}^Z)_{LEP/SLC} \leq 30 \text{ MeV} \quad (64)$$

Experimentally, furthermore, one believes that one can measure Γ_{tot}^Z very accurately, with perhaps [14]

$$(\delta\Gamma_{tot}^Z)_{LEP/SLC} \leq 10 \text{ MeV} \oplus 15 \text{ MeV} \quad (65)$$

where the first error is statistical and the second is an estimate of the expected systematic error. Given Eqs (64) and (65), one should have no trouble establishing if there are any extra neutrino species, since each extra neutrino type contributes:

$$\Gamma(Z \rightarrow \nu_1 \bar{\nu}_1) = 170 \text{ MeV} >> (\delta\Gamma_{tot}^Z)_{LEP/SLC} \oplus (\delta\Gamma_{tot}^Z)_{LEP/SLC} \oplus (\delta\Gamma_{tot}^Z)_{experiment} \quad (66)$$

II Neutrino Masses - Theoretical Issues

Although neutrino masses may not exist, and if they exist certainly $m_\nu \ll m_e$, at least for the known families, it is very interesting to contemplate this possibility theoretically. Since neutrinos are neutral, it is possible to have two distinct types of mass terms: either Dirac (a particle - antiparticle mass term) or Majorana (a particle - particle mass term). Only the first kind of mass term is available for the charged leptons and the quarks, since Majorana masses, for these particles, would violate charge conservation. The possibility of having Majorana masses for neutrinos is very interesting for two reasons. First, such a mass term violates lepton number and this is an intriguing possibility, since it allows the existence of processes like neutrinoless double beta decay. Secondly, as I shall discuss, it is likely that

the existence of neutrino Majorana masses may be the physical reason why $m_\nu \ll m_e$. To discuss all of these matters, it proves useful to develop some formalism which will make the physical distinction between Dirac and Majorana masses more manifest.

II.1 Dirac and Majorana Masses

To understand the origin of Dirac and Majorana mass terms for neutrinos, it is useful to review briefly some properties of spinors of the Lorentz group [15]. In contrast to a Lorentz vector, V^μ , there are two kinds of Lorentz spinors ξ_a and $\dot{\xi}_a$. Recall that V^μ is an object which transforms in the same way as the position vector x^μ does, under Lorentz transformations. That is,

$$V^\mu \rightarrow V'^\mu = \Lambda^\mu_\nu V^\nu \quad (67)$$

where the transformation parameters Λ^μ_ν obey the constraint

$$\eta_{\mu\nu} = \Lambda^\alpha_\mu \eta_{\alpha\beta} \Lambda^\beta_\nu \quad (68)$$

with

$$\eta_{\mu\nu} = \begin{pmatrix} -1 & 0 & 0 & 0 \\ 0 & 1 & 0 & 0 \\ 0 & 0 & 1 & 0 \\ 0 & 0 & 0 & 1 \end{pmatrix} \quad (69)$$

being the metric tensor. The (Weyl) spinors ξ_a and $\dot{\xi}_a$ are two dimensional objects which transform under Lorentz transformations according to the parameters entering in a 2×2 unimodular matrix M belonging to $SL(2, C)$. To wit, one has

$$\xi_a \rightarrow \xi'_a = M_a^b \xi_b \quad (70a)$$

$$\dot{\xi}_a \rightarrow \dot{\xi}'_a = M_a^{\dot{b}} \dot{\xi}_{\dot{b}} \quad (70b)$$

Since M and M^* are not equivalent representations of $SL(2, C)$, in contrast to what happens for $SU(2)$, the "dotted" and "undotted" Weyl spinors are independent. The relation between M and Λ is easily established since the 2×2 matrix $V \sim \xi \otimes \dot{\xi}$:

$$V = \sigma^\mu V_\mu \quad (71)$$

with $\sigma^\mu = (1, \vec{\sigma})$ transforms as

$$V \rightarrow V' = MV M^\dagger \equiv \sigma^\mu V'_\mu \quad (72)$$

Hence

$$\sigma_{\alpha\dot{\alpha}}^\mu \Lambda_\nu = M_a^b \sigma_{b\dot{b}}^\nu M^{*\dot{a}c} \quad (73)$$

Because $\text{Det } M = 1$, it is easy to check that just as

$$V_\mu \eta^{\mu\nu} V_\nu \equiv V_\mu V^\mu \quad (74)$$

is a Lorentz scalar, so are

$$\xi_a \epsilon^{ab} \xi_b \equiv \xi_a \xi^a \quad (75a)$$

$$\dot{\xi}_{\dot{a}} \epsilon^{\dot{a}\dot{b}} \dot{\xi}_{\dot{b}} \equiv \dot{\xi}_{\dot{a}} \dot{\xi}^{\dot{a}} \quad (75b)$$

Here ϵ^{ab} , $\epsilon^{\dot{a}\dot{b}}$ are the two dimensional antisymmetric tensors with $\epsilon^{12} = 1$. It is also useful to define the tensors ϵ_{ab} , $\epsilon_{\dot{a}\dot{b}}$ with lower indices, so that

$$\epsilon^{ab} \epsilon_{bc} = \delta_c^a \quad (76)$$

Clearly then $\epsilon_{12} = -1$.

One can combine two Weyl spinors - a dotted and an undotted one - to form an ordinary Dirac 4-component spinor as follows:

$$\Psi_D = \begin{pmatrix} \xi_a \\ \chi^{\dot{a}} \end{pmatrix} \quad (77)$$

In this basis the appropriate Dirac γ - matrices, which obey the anticommutation relations

$$\{\gamma^\mu, \gamma^\nu\} = -2\eta^{\mu\nu}, \quad (78)$$

are written in terms of σ^μ and $\vec{\sigma}^\mu = (1, -\vec{\sigma})$ as

$$\gamma^\mu = \begin{pmatrix} 0 & \sigma^\mu \\ \vec{\sigma}^\mu & 0 \end{pmatrix} \quad (79)$$

Thus $\gamma_5 = i\gamma^0\gamma^1\gamma^2\gamma^3$ is diagonal and γ^0 is off diagonal:

$$\gamma_5 = \begin{pmatrix} -1 & 0 \\ 0 & 1 \end{pmatrix}; \quad \gamma^0 = \begin{pmatrix} 0 & 1 \\ 1 & 0 \end{pmatrix} \quad (80)$$

According to Eq (70) the dotted spinor is just proportional to the complex conjugate of the undotted spinor. Taking the proportionality constant to be unity, it follows that the adjoint Dirac spinor $\bar{\Psi}_D$ is

$$\begin{aligned} \bar{\Psi}_D &= \Psi_D^\dagger \gamma^0 = (\xi_a \chi^{\dot{a}})^* \begin{pmatrix} 0 & 1 \\ 1 & 0 \end{pmatrix} \\ &= (\chi^{\dot{a}} \xi_a) \end{aligned} \quad (81)$$

It follows from Eqs (77) (80) and (81) that the four Weyl fields $\xi_a, \chi^{\dot{a}}, \dot{\xi}_{\dot{a}}$ and χ^a can be gotten as chiral projections of Ψ_D and $\bar{\Psi}_D$. To wit,

$$\begin{aligned} \Psi_L &= \frac{1}{2}(1 - \gamma_5)\Psi_D = \begin{pmatrix} \xi_a \\ 0 \end{pmatrix} \\ \Psi_R &= \frac{1}{2}(1 + \gamma_5)\Psi_D = \begin{pmatrix} 0 \\ \chi^{\dot{a}} \end{pmatrix} \\ \bar{\Psi}_L &= \bar{\Psi}_D \frac{1}{2}(1 + \gamma_5) = (0, \dot{\xi}_{\dot{a}}) \\ \bar{\Psi}_R &= \bar{\Psi}_D \frac{1}{2}(1 - \gamma_5) = (\chi^a, 0) \end{aligned} \quad (82)$$

A Dirac mass term, of the type exemplified by Eq (2), involves always $\bar{\Psi}_L$ coupled to Ψ_R . Taking m_D to be a real parameter, one has

$$\mathcal{L}_{mass}^{Dirac} = -m_D(\bar{\Psi}_L \Psi_R + \bar{\Psi}_R \Psi_L) = -m_D \bar{\Psi}_D \Psi_D \quad (83)$$

which, in terms of the Weyl spinors, reads

$$\mathcal{L}_{mass}^{Dirac} = -m_D(\dot{\xi}_{\dot{a}} \chi^{\dot{a}} + \chi^a \xi_a) \quad (84)$$

Obviously, in view of Eq (75), this term is a Lorentz invariant. However, note that this is an invariant made out of two distinct Weyl spinors χ and ξ , and their complex conjugates. Clearly one should be able to also write a mass term involving only one Weyl spinor and its complex conjugate. Such a term is a Majorana mass term.

Consider the following four component spinor - a Majorana spinor - made up of only ξ and its complex conjugate $\bar{\xi}$:

$$\Psi_M = \begin{pmatrix} \xi_a \\ \bar{\xi}^{\dot{a}} \end{pmatrix} \quad (85)$$

Ψ_M and its adjoint $\bar{\Psi}_M = (\xi^a, \bar{\xi}_{\dot{a}})$ are really characterized by only one independent helicity projection, since they involve only one Weyl spinor. One may take these projections, for example, to be left handed projections

$$\begin{aligned} \Psi_L &= \frac{1}{2}(1 - \gamma_5)\Psi_M = \begin{pmatrix} \xi_a \\ 0 \end{pmatrix} \\ \bar{\Psi}_L &= \bar{\Psi}_M \frac{1}{2}(1 + \gamma_5) = (0, \bar{\xi}_{\dot{a}}) \end{aligned} \quad (86)$$

Then right handed spinors can be constructed from these fields by using charge conjugation. For these purposes one defines the charge conjugation matrix C obeying

$$\begin{aligned} C^\dagger &= C^{-1} = C^T = -C \\ C^\dagger \gamma^\mu C &= -(\gamma^\mu)^T \end{aligned} \quad (87)$$

The form which C takes depends on the γ^{\pm} matrix basis one uses. In the Weyl basis of Eq (79) it is not hard to convince oneself that

$$C = \begin{bmatrix} 0 & -1 & 0 & 0 \\ 1 & 0 & 0 & 0 \\ 0 & 0 & 0 & 1 \\ 0 & 0 & 1 & 0 \end{bmatrix} = \begin{bmatrix} \epsilon_{ab} & 0 \\ 0 & \epsilon^{\dot{a}\dot{b}} \end{bmatrix} \quad (88)$$

Armed with C one can construct a right handed spinor from $\bar{\Psi}_L$, namely

$$(\bar{\Psi}^c)_R = C(\bar{\Psi}_L)^T = \begin{pmatrix} 0 \\ \epsilon^{\dot{a}b} \bar{\xi}_{\dot{b}} \end{pmatrix} = \begin{pmatrix} 0 \\ \bar{\xi}^{\dot{a}} \end{pmatrix} \quad (89)$$

Clearly, one has also that

$$(\bar{\Psi}^c)_R = \Psi_L^T C = (\xi_b \epsilon_{ba}, 0) = (\xi^a, 0) \quad (90)$$

Note that these spinors are made up of the complex conjugate components of the fields in (86). They correspond therefore to the charge conjugates of Ψ_L and $\bar{\Psi}_L$. Defining the charge conjugate field Ψ^c of Ψ as

$$\Psi^c = C \bar{\Psi}^T \quad (91)$$

one sees that

$$(\Psi_L)^c \equiv (\Psi^c)_R = C(\bar{\Psi}_L)^T \quad (92)$$

The Majorana spinor Ψ_M is just the sum of Ψ_L and its charge conjugate field $(\Psi_L)^c$

$$\Psi_M = \Psi_L + (\Psi_L)^c = \begin{pmatrix} \xi_a \\ 0 \end{pmatrix} + \begin{pmatrix} 0 \\ \bar{\xi}^{\dot{a}} \end{pmatrix} = \begin{pmatrix} \xi_a \\ \bar{\xi}^{\dot{a}} \end{pmatrix} \quad (93)$$

Thus, it obeys a constraint condition [Majorana Condition]:

$$(\Psi_M)^c = C(\bar{\Psi}_M)^T = \Psi_M \quad (94)$$

One can write down a mass term for this Majorana spinor. However, this mass term will only involve one Weyl spinor and its complex conjugate, or equivalently only Ψ_L and $\bar{\Psi}_L$. In terms of the Weyl spinors, the obviously Lorentz invariant Majorana mass term reads:

$$\mathcal{L}_{mass}^{Majorana} = -\frac{1}{2} m_M^L (\bar{\Psi}_M \Psi_M) = -\frac{1}{2} m_M^L (\bar{\xi}_a \xi^a + \xi^{\dot{a}} \bar{\xi}_{\dot{a}}) \quad (95)$$

This Lagrangian can be rewritten in terms of four component spinors by using our previous identifications of Eqs (86), (89) and (90):

$$\begin{aligned} \mathcal{L}_{mass}^{Majorana} &= -\frac{1}{2} m_M^L [\bar{\Psi}_L(\Psi^c)_R + \overline{(\Psi^c)_R} \Psi_L] \\ &= -\frac{1}{2} m_M^L [\bar{\Psi}_L C(\bar{\Psi}_L)^T + \Psi_L^T C \Psi_L] \end{aligned} \quad (96)$$

It is clear from (96) that the Lorentz invariant Majorana mass term forbids the fields Ψ_L from having any conserved quantum numbers. The Majorana condition (94) is incompatible with Ψ_M having any $U(1)$ symmetry. Clearly incorporating a Majorana mass term for neutrinos will necessarily break lepton number. The Dirac mass term, on the other hand, is perfectly lepton number preserving.

II.2 Mass Generation Options for Neutrinos

Given the transformation properties of ν_L and ν_R under $SU(2) \times U(1)$, there are various ways in which neutrinos can get a mass. These mass terms can be either effective - arising from nonrenormalizable interactions in the standard model, but from renormalizable terms in an extended theory - or they may arise from renormalizable Higgs Yukawa couplings. They can also either violate or conserve lepton number, depending on whether what is being generated is a Majorana or a Dirac mass term. In view of the preceding discussion, it is useful to write down the most general neutrino mass term that can arise after $SU(2) \times U(1)$ symmetry breakdown. To simplify the notation, in what follows, I shall only consider the case of one generation. The resulting formulas, however, can be trivially generalized. One has

$$\begin{aligned} \mathcal{L}_{mass} = & -m_D[\bar{\nu}_L\nu_R + \bar{\nu}_R\nu_L] - \frac{1}{2}m_M^L|\nu_L^T C\nu_L + \bar{\nu}_L C\bar{\nu}_L^T| \\ & - \frac{1}{2}m_M^R|\nu_R^T C\nu_R + \bar{\nu}_R C\bar{\nu}_R^T| \end{aligned} \quad (97)$$

That is, one can have a Dirac mass m_D plus a Majorana mass for the left handed, m_M^L , and right handed, m_M^R , neutrino fields.

Let us investigate what can be the sources of the above mass terms. The Dirac mass m_D , as I have discussed earlier, can simply arise from a renormalizable Yukawa coupling of neutrinos with the standard model Higgs doublet $\Phi = \begin{pmatrix} \phi^+ \\ \phi^0 \end{pmatrix}$:

$$\mathcal{L}_{Yukawa} = -\Gamma^\nu(\bar{\nu}, \bar{\ell})_L \Phi \nu_R - \Gamma^{\nu^*} \bar{\nu}_R \Phi^\dagger \begin{pmatrix} \nu \\ \ell \end{pmatrix}_L \quad (98)$$

where ℓ is the lepton associated with the neutrino ν in question. Clearly then *

$$m_D = \Gamma^\nu < \phi^0 > \quad (99)$$

Obviously, this mass term is lepton number conserving since \mathcal{L}_{Yukawa} is invariant under

$$\begin{pmatrix} \nu \\ \ell \end{pmatrix}_L \rightarrow \begin{pmatrix} \nu' \\ \ell' \end{pmatrix}_L = e^{i\alpha} \begin{pmatrix} \nu \\ \ell \end{pmatrix}_L \quad (100a)$$

$$\nu_R \rightarrow \nu'_R = e^{i\alpha} \nu_R \quad (100b)$$

Note, however, that in the many generation case above m_D is a matrix and one does not expect any more separate conservation of L_e, L_μ and L_τ . The presence of a Dirac mass matrix for neutrinos implies lepton mixing, just as in the quark case. Note also that since $< \phi^0 > \simeq 180$ GeV, to get neutrino masses in the eV range - as we know to be the case, at least for electron neutrinos (see Sec. III) - requires Yukawa couplings which are ridiculously small: $\Gamma^\nu \sim 10^{-10} - 10^{-11}$!

The Majorana mass m_M^R is allowed by $SU(2) \times U(1)$ since the right handed neutrinos are singlets. In contrast to the Dirac mass m_D , which is connected to the scale of the $SU(2) \times U(1)$ breaking $< \phi^0 > \sim 180$ GeV, m_M^R is an independent scale altogether. It is clear that the presence of m_M^R breaks lepton number since the combinations $\nu_R^T C\nu_R$ and $\bar{\nu}_R C\bar{\nu}_R^T$ have $L = +2$ and $L = -2$, respectively.

Although m_M^R can be just an explicit renormalizable mass term, it can also arise from a Yukawa coupling with some $SU(2) \times U(1)$ singlet Higgs field, σ , which acquires a non zero vacuum expectation value. Thus

$$m_M^R = \begin{cases} m_M^R & \text{explicit mass} \\ \frac{\Lambda}{\sqrt{2}} < \sigma > & \text{spontaneous mass} \end{cases} \quad (101)$$

* We take here without loss of generality both Γ^ν and $< \phi^0 >$ to be real, as any phase in m_D can be rotated away by a phase redefinition of the lepton doublet in (98).

Here h is a coupling constant. In the case of spontaneous mass generation, one can further distinguish between the cases when lepton number is explicitly violated or when it is spontaneously broken. If σ carries lepton number, then the Yukawa coupling of σ with the ν_R fields can be lepton number conserving and lepton number is only broken spontaneously by the σ vacuum expectation value $\langle \sigma \rangle$. In this latter case, unless lepton number is gauged, there always appears a Goldstone boson in the theory, known as a Majoron [16]. I will discuss this interesting possibility further in Sec. II.4.

The Majorana mass m_M^L cannot be an explicit mass term, as it violates $SU(2) \times U(1)$. It can, however, arise after the breaking of $SU(2) \times U(1)$. If one insists that m_M^L be the result of renormalizable interactions, then it is necessary to introduce an $SU(2)$ triplet Higgs field $\vec{\Delta}$ in the theory [17]. From the Yukawa interaction

$$\mathcal{L}_\Delta = -\frac{g}{\sqrt{2}} \left[(\nu, \ell)_L^T C \vec{\tau} \cdot \vec{\Delta} \begin{pmatrix} \nu \\ \ell \end{pmatrix} \right] + h.c. \quad (102)$$

and the assumption that the zero charge component of $\vec{\Delta}$ acquires a non zero vacuum expectation value $\langle \Delta^0 \rangle$, one has

$$m_M^L = \sqrt{2}g \langle \Delta^0 \rangle \quad (103)$$

Again here, as in the case of m_M^R , one must distinguish between the possibility of explicit or spontaneous lepton number violation. Clearly, if $\vec{\Delta}$ carries no lepton number, then Eq (102) breaks lepton number explicitly. However, if $\vec{\Delta}$ has $L = -2$ then Eq (102) is lepton number preserving. Of course, in this case, the expectation $\langle \Delta^0 \rangle \neq 0$ breaks lepton number spontaneously and a Majoron [17] will appear in the theory. I shall return to this kind of Majoron also in Sec. II.4.

Note that the mass m_M^L , according to Eq (103), is associated to a new scale connected with the triplet vacuum expectation value $\langle \Delta^0 \rangle$. In contrast to m_M^R or $\langle \sigma \rangle$, the vacuum expectation value $\langle \Delta^0 \rangle$ is rather well bounded by experiment. Recall that in our discussion of Sec. I we found that, experimentally, ρ was perfectly consistent with unity [cf Eq (33)]. The presence of a triplet Higgs field expectation value, however, changes the prediction for ρ and one has now

$$\rho \simeq 1 - 2 \left(\frac{\langle \Delta^0 \rangle}{\langle \phi^0 \rangle} \right)^2 \quad (104)$$

Hence the 1% accuracy obtained for ρ implies

$$\langle \Delta^0 \rangle \gtrsim 12 \text{ GeV} \quad (105)$$

The mass scale m_M^L could also arise from some L -violating non renormalizable, beyond the standard model, interaction signaling the presence of new physics at a scale Λ :

$$\mathcal{L}_{L \text{ viol}}^{eff} = \frac{1}{\Lambda} [\Phi^T C \vec{\tau} \Phi] \cdot [(\nu, \ell)_L^T C \vec{\tau} \begin{pmatrix} \nu \\ \ell \end{pmatrix}] + h.c. \quad (106)$$

When $\Phi \rightarrow \langle \Phi \rangle$ the above yields a Majorana mass

$$m_M^L = \frac{2 \langle \phi^0 \rangle^2}{\Lambda} \quad (107)$$

One sees that m_M^L is small if Λ is big. For instance, if one wants $m_M^L \leq eV$ then one needs $\Lambda \geq 6 \times 10^{13}$ GeV. So the presence of a small left handed neutrino Majorana mass could signal the presence of new physics at very large scales.

II.3 The See Saw Mechanism

Given the great variety of possible sources for neutrino masses and the fact that, if these masses exist, $m_\nu \ll m_\ell$, one wants to see if there is a natural mass generation mechanism which explains why neutrino masses turn out to be so small. We saw already [cf Eq (107)] that new physics at a scale $\Lambda \gg M_W$ can produce small Majorana neutrino masses for ν_L : $m_M^L \sim \frac{m_\nu^2}{\Lambda}$. This formula, it turns out, is quite general and one can always adduce the smallness of neutrino masses to the presence of some new large scale in the theory. This is the famous see saw mechanism of Yanagida [18] and Gell Mann Ramond and Slanski [19].

Let me, again for simplicity, discuss the idea behind the see saw mechanism for the case of one family. It proves convenient for these purposes to rewrite the general neutrino mass of Eq (97) in a more symmetrical form, by making use of the conjugate spinor ν^c . Using the results of Sec. II.1, one has that

$$\overline{(\nu^c)}_L (\nu^c)_R = \nu_R^T C C D_L^T = -\nu_R^T \nu_L^T = \nu_L \nu_R \quad (108)$$

Thus one can rewrite

$$\nu_L \nu_R = \frac{1}{2} [\nu_L \nu_R + \overline{(\nu^c)_L} (\nu^c)_R] \quad (109)$$

Furthermore

$$\nu_R^T C \nu_R = \overline{(\nu^c)_L} \nu_R \quad (110a)$$

and

$$\nu_L C (\nu_L)^T = \nu_L (\nu^c)_R \quad (110b)$$

Hence, Eq (97) can be rewritten as

$$\mathcal{L}_{mass} = -\frac{1}{2} [\nu_L, \overline{(\nu^c)_L}] \begin{pmatrix} m_M^L & m_D \\ m_D & m_M^R \end{pmatrix} \begin{pmatrix} (\nu^c)_R \\ \nu_R \end{pmatrix} + h.c. \quad (111)$$

The mass matrix

$$\mathcal{M} = \begin{pmatrix} m_M^L & m_D \\ m_D & m_M^R \end{pmatrix} \quad (112)$$

clearly has two eigenvalues, m_1 and m_2 , and the eigenstates of Eq (112) are Majorana neutrino states. It is pretty obvious that one can build a hierarchy between these two eigenvalues if there is a hierarchy in \mathcal{M} itself. Remembering that m_M^L is connected to the vacuum expectation value of a triplet Higgs field $\overline{\Delta}$ (with $\langle \Delta^0 \rangle \leq 12$ GeV), or is inversely proportional to a large scale Λ , it is more sensible to try to build a hierarchy via m_M^R instead. Thus a natural hierarchy to imagine for \mathcal{M} is that

$$m_M^R \equiv M \gg m_D \gg m_M^L \simeq 0 \quad (113)$$

In these circumstances then

$$\mathcal{M} \simeq \begin{pmatrix} 0 & m_D \\ m_D & M \end{pmatrix} \quad (114)$$

and its eigenvalues are, approximately,

$$m_1 \simeq -\frac{m_D^2}{M}; \quad m_2 \simeq M \quad (115)$$

In this case, one sees that one neutrino is superheavy $m_2 \simeq M \gg m_D$, while the other is superlight * : $m_1 \simeq \frac{m_D^2}{M} \ll m_D$.

The matrix \mathcal{M} is diagonalized via a unitary transformation

$$U^\dagger \mathcal{M} U = \begin{pmatrix} m_1 & 0 \\ 0 & m_2 \end{pmatrix} \quad (116)$$

and if $M \gg m_D$ then it is easy to see that

$$U \simeq \begin{pmatrix} 1 & \frac{m_D}{M} \\ -\frac{m_D}{M} & 1 \end{pmatrix} \quad (117)$$

The diagonalization of \mathcal{M} corresponds to a basis change for the left handed and right handed neutrino fields:

$$\begin{pmatrix} (\nu^c)_R \\ \nu_R \end{pmatrix} = U \begin{pmatrix} \nu_{1R} \\ \nu_{2R} \end{pmatrix} \quad (118a)$$

$$(\nu_L, \overline{(\nu^c)_L}) = ((\nu_1^c)_L, \overline{(\nu_2^c)_L}) U^\dagger \quad (118b)$$

and one has, approximately,

$$\nu_R \simeq \nu_{2R} - \frac{m_D}{M} \nu_{1R} \quad (119)$$

and

$$\nu_L \simeq (\nu_1^c)_L + \frac{m_D}{M} (\nu_2^c)_L \quad (120)$$

That is, ν_R is mostly made up of the heavy neutrino field ν_2 , while ν_L is mostly the light neutrino field ν_1 .

In terms of ν_1 and ν_2 the mass Lagrangian reads

$$\mathcal{L}_{mass} = -\frac{1}{2} m_1 \overline{[(\nu_1^c)_L \nu_{1R} + \nu_{1R} (\nu_1^c)_L]} - \frac{1}{2} m_2 \overline{[(\nu_2^c)_L \nu_{2R} + \nu_{2R} (\nu_2^c)_L]} \quad (121)$$

* The sign of m_1 in (115) is irrelevant, as it can be again rotated away through a redefinition of the neutrino fields.

which are Majorana mass terms for these fields. Indeed, one can define Majorana fields η_1 , and η_2 by

$$\begin{aligned}\eta_1 &= (\nu_1^c)_L + \nu_{1R} = (\eta_1)^c \\ \eta_2 &= (\nu_2^c)_L + \nu_{2R} = (\eta_2)^c\end{aligned}\quad (122)$$

so that Eq (121) can be rewritten as

$$\mathcal{L}_{mass} = -\frac{1}{2}m_1(\bar{\eta}_1\eta_1) - \frac{1}{2}m_2(\bar{\eta}_2\eta_2)\quad (123)$$

Corresponding to Eqs (119) and (120) we now have

$$\nu_R \simeq \eta_{2R} - \frac{m_D}{M}\eta_{1R}\quad (124)$$

and

$$\nu_L \simeq \eta_{1L} + \frac{m_D}{M}\eta_{2L}\quad (125)$$

so that ν_L is mostly η_1 and ν_R is mostly η_2 . If m_2 is sufficiently heavy, one would not have seen any evidence yet for η_2 . However, the see saw mechanism allows a light neutrino η_1 to exist, which for all practical purposes is essentially the same as the (massless) left handed neutrino of the standard model.

II.4 Majorons

It is unlikely, but possible, that lepton number is an exact global symmetry which is, however, spontaneously broken. The resulting physics is quite amusing since Goldstone's theorem [20] requires that there should exist an $m = 0$ Goldstone boson in the low energy spectrum of the theory. As I have mentioned earlier, these Goldstone bosons for the case of spontaneously broken lepton number have been dubbed Majorons [16] [17]. Having $m = 0$ bosons in the theory appears very dangerous, at first sight, since one would naively expect that their exchange in matter would give rise to a long range force. This turns out not to be the case, since as I shall show below, Goldstone boson exchange gives rise to a tensorial r^{-3} potential rather than a Coulomb potential. The proof of this statement is rather simple [21]. It is based on the fact that Goldstone bosons interact with matter only

via derivative couplings. Hence, for example, the most general interaction of a Goldstone boson Π with two fermions is:

$$\mathcal{L}_{GB} = i\frac{\partial^\mu \Pi}{V_G} \bar{f}_1 [a\gamma_\mu + b\gamma_\mu \gamma_5] f_2\quad (126)$$

In the above V_G is the scale parameter associated with the breakdown and a and b are numbers (which presumably are of $O(1)$). The above can be rewritten, using the fermion equations of motion as

$$\mathcal{L}_{GB} = \frac{\Pi}{V_G} \bar{f}_1 [a(m_1 - m_2) + b\gamma_5(m_1 + m_2)] f_2\quad (127)$$

One sees that a Goldstone boson couples to the same species of fermions ($f_1 = f_2$) only via an effective γ_5 coupling. This in turn means that Goldstone boson exchange will only give rise to a tensorial spin-spin interaction. Taking the nonrelativistic limit of the effective interaction

$$\begin{aligned}\mathcal{L}_{GB}^{eff} &= i\frac{m_f}{V_\Pi} \bar{f} \gamma_5 f \Pi \\ &\rightarrow (\chi_f^* \frac{\vec{\sigma} \cdot \vec{\nabla}}{V_\Pi} \chi_f) \Pi\end{aligned}\quad (128)$$

one sees that the γ_5 coupling reduces to a $\vec{\sigma} \cdot \vec{p}$ interaction among two component spinors. This leads to an r^{-3} spin-spin long range potential for the exchange of Goldstone bosons:

$$V_{GB} = \frac{1}{4\pi V_\Pi^2} \left\{ \frac{3(\vec{\sigma}_1 \cdot \vec{r})(\vec{\sigma}_2 \cdot \vec{r}) - r^2 \vec{\sigma}_1 \cdot \vec{\sigma}_2}{r^5} \right\}\quad (129)$$

The presence of such additional interactions has been bounded by Feinberg and Sucher [22] who looked for any evidence of non magnetic dipole-dipole interactions in matter. These authors found that as long as

$$V_\Pi \geq TeV\quad (130)$$

the effects of Eq (129) would not have been visible. Thus Majorons could exist, as long as the above bound is satisfied.

As our discussion of the previous subsection indicated, there are two possible types of Majoron models, depending on whether ν_R or ν_L gets a Majorana mass. In the former case (CMP Majoron [16]) this excitation is connected with the $SU(2)$ singlet field σ , while in the latter case (GR Majoron [17]) it is connected to the $SU(2)$ triplet field $\vec{\Delta}$. I want to briefly describe the properties of both models here.

II.4.1 CMP Majoron

Here one introduces a lepton number conserving coupling of the $SU(2) \times U(1)$ singlet field σ to ν_R by endowing σ itself with lepton number:

$$\mathcal{L}_{CMP} = -\frac{h}{\sqrt{2}}[\nu_R^T C \sigma \nu_R] + h.c. \quad (131)$$

Obviously, if under a lepton number transformation

$$\begin{aligned} \nu_R &\rightarrow \nu'_R = e^{i\alpha} \nu_R \\ \sigma &\rightarrow \sigma' = e^{-2i\alpha} \sigma, \end{aligned} \quad (132)$$

then the CMP Lagrangian is invariant under this transformation. Lepton number is spontaneously broken, however, if σ obtains a vacuum expectation value $\langle \sigma \rangle = \frac{1}{\sqrt{2}} v_R$. Then ν_R acquires a Majorana mass

$$m_M^R = h v_R \quad (133)$$

and a zero mass Majoron appears in the theory. If one writes the complex field σ as

$$\sigma = \frac{1}{\sqrt{2}}[v_R + \rho + i\chi] \quad (134)$$

it is not difficult to convince oneself that χ is the Majoron field.

Provided m_M^R is sufficiently big, the effects of the CMP Majoron are essentially unobservable. If $m_M^R \equiv M \gg m_D$, we have a see saw mechanism, with the heavy Majorana state η_2 , of mass M , being essentially ν_R and the light Majorana state η_1 , of mass $\frac{m_D^2}{M}$, being

identified with ν_L . Obviously the Majoron χ couples to η_2 with the full strength h , but its coupling to η_1 is very suppressed by mixing. One has

$$\mathcal{L}_\chi^{neutrinos} = \frac{h}{2} \bar{\eta}_2 \gamma_5 \eta_2 \chi + \frac{h}{2} \left(\frac{m_D}{M}\right)^2 \bar{\eta}_1 \gamma_5 \eta_1 \chi \quad (135)$$

The CMP Majoron χ couples to charged fermions only as a result of virtual neutrino loops, as shown in Fig. 13. A simple calculation [16] shows that*

$$\mathcal{L}_\chi^{fermion} = \frac{m_f}{V_\Pi} \bar{f} \gamma_5 f \chi \quad (136)$$

where

$$V_\Pi = \frac{16\pi^2}{h G_F m_\nu} \simeq \frac{10^{16} \text{ GeV}}{h \left(\frac{m_\nu}{eV}\right)} \quad (137)$$

Obviously for the CMP Majoron, the Feinberg Sucher bound of Eq. (130) is well satisfied, even for GeV neutrinos!

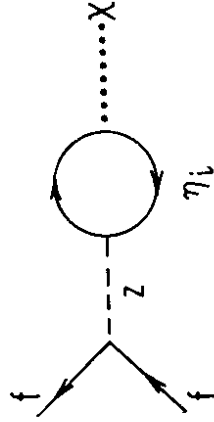


Fig. 13: Coupling of the CMP Majoron to matter.

* For the leptons there is an additional contribution due to a CC loop also, so that Eq (137) is not quite correct.

Because of its extremely weak coupling to matter and to light neutrinos, the CMP Majoron model is essentially untestable. However, as we shall discuss in Section V, the CMP Majoron could have some cosmological significance. It could also have some theoretical importance in certain schemes [23] where it is essentially identified as the invisible axion.

II.4.2 The GR Majoron

The Majoron model of Gelmini and Roncadelli [17] has a few more direct experimental consequences. The model makes use of the Higgs triplet field $\vec{\Delta}$ and the interaction Lagrangian (102). This Lagrangian is clearly invariant under a lepton number transformation, provided $\vec{\Delta}$ carries $L = -2$:

$$\begin{aligned} \begin{pmatrix} \nu \\ \ell \end{pmatrix}_L &\rightarrow \begin{pmatrix} \nu \\ \ell \end{pmatrix}'_L = e^{i\alpha} \begin{pmatrix} \nu \\ \ell \end{pmatrix}_L \\ \vec{\Delta} &\rightarrow \vec{\Delta}' = e^{-2i\alpha} \vec{\Delta} \end{aligned} \quad (138)$$

Again, if $\vec{\Delta}$ gets a vacuum expectation value then lepton number is broken spontaneously, ν_L gets a Majorana mass, and an $m = 0$ Majoron will appear in the theory. Let us write

$$\vec{\Delta} \cdot \vec{\Delta} = \begin{pmatrix} \Delta^0 \\ \frac{\Delta^-}{\sqrt{2}} \\ \frac{\Delta^+}{\sqrt{2}} \end{pmatrix} \begin{pmatrix} \Delta^0 \\ \Delta^- \\ \Delta^+ \end{pmatrix} \quad (139)$$

and take $\langle \Delta^0 \rangle = \frac{1}{\sqrt{2}} v_T$. Then

$$m_M^L = m_\nu = g v_T \quad (140)$$

The Goldstone boson associated with the L breakdown is in Δ^0 . If one writes

$$\Delta^0 = \frac{1}{\sqrt{2}} (v_T + \rho + i\chi) \quad (141)$$

then χ is the GR Majoron. As we shall see, the scalar field ρ is also interesting because, even though it is not massless, it is very light.

The presence of the GR Majoron is more amenable to experimental constraint. I will discuss some of these constraints here and some in the next section, when I will talk about double beta decay. It turns out that these experiments put both a bound on the neutrino Majorana mass (hence on $g v_T$), as well as a direct bound on g itself. We saw earlier that the ρ parameter put a bound on $\langle \Delta^0 \rangle \leq 12$ GeV, which implies

$$v_T \leq 17 \text{ GeV} \quad (142)$$

Amazingly enough, this bound is of the same order of magnitude as that provided by the Feinberg Sucher bound (130). The GR Majoron, since it carries $SU(2) \times U(1)$ quantum numbers, mixes in general slightly with the $SU(2)$ doublet Higgs. This produces a direct coupling of χ with ordinary fermions which is suppressed by a factor of $\frac{v_T}{v}$, where v is related to the doublet expectation value $\langle \phi^0 \rangle = \frac{v}{\sqrt{2}}$ [17]

$$\mathcal{L}_\chi^{\text{fermion}} = i \frac{m_f}{v} \left(\frac{v_T}{v} \right) \bar{f} \gamma_5 f \chi \quad (143)$$

Thus for the GR model

$$V_\pi = \frac{v^2}{v_T} \quad (144)$$

and the Feinberg Sucher bound implies $v_T \leq 60$ GeV.

One can get very much stronger bounds on v_T from astrophysical considerations related to star cooling. The process $e\gamma \rightarrow e\chi$ cools stars since Majorons are so weakly interacting that they freely leave the star's interior, carrying out energy. The cooling rate is proportional to the cross section for the above process and hence to v_T^2 . Obviously, by requiring that the Majoron cooling rate be less than the star's power output for the lifetime of the star allows one to set an upper bound on v_T . I give below the results quoted in a recent compilation of Cheng [24] for the bounds on v_T , obtained from various astrophysical objects:

$$v_T \leq \begin{cases} 5 \text{ MeV} & (\text{Sun}) \\ (20 - 50) \text{ KeV} & (\text{Red Giants / Neutron Stars}) \end{cases} \quad (145)$$

These bounds are very much stronger than those obtained earlier. However, I should note that, for the Red Giants and Neutron Stars bounds, the theoretical uncertainties are also quite big.

The GR Majorons are impacted quite strongly by neutrino counting experiments. Since $\bar{\Delta}$ is an $SU(2)$ triplet, there is a $Z\bar{\Delta}\Delta$ coupling, so that the Z boson can decay into the fields contained in $\bar{\Delta}$. There are three possible Z decay channels and one, in particular, involves Majorons [25]. One has: $Z \rightarrow \Delta^{++}\Delta^{--}$, $Z \rightarrow \Delta^+\Delta^-$ and $Z \rightarrow \rho\chi$. The first two of these decays may or may not happen, depending on the masses of Δ^{++} and Δ^+ . However, the $\rho\chi$ decay mode will always be allowed kinematically. This can be seen by analyzing the Higgs potential involving Δ , where one finds that [25]

$$m_{\Delta^{++}} = \sqrt{2}m_{\Delta^+} \sim 0(v) \quad (146)$$

while

$$m_\rho \sim 0(v_T) \quad (147)$$

In view of the bounds in Eq (145), one sees that the scalar partner of the GR Majoron is very light, so that the decay $Z \rightarrow \chi\rho$ is always permitted. In fact, it is easy to check that [25]

$$\Gamma(Z \rightarrow \chi\rho) = 2\Gamma(Z \rightarrow \nu_L\nu_L) \simeq 340 \text{ MeV} \quad (148)$$

Thus, if GR Majorons exist, they count as two extra neutrino species. Our discussion of neutrino bounds from the $p\bar{p}$ collider [cf Fig. 12] gives $N_\nu \leq 3$ if m_i is heavy. Thus these bounds already can rule out the existence of the GR Majorons. This may still be premature at this stage, since we really do not know m_i and there are some other theoretical uncertainties. However, when LEP and SLC turn on we will know for sure whether it is possible for the GR Majorons to exist.

III Neutrino Masses - Experimental Results

In 1980 great excitement in neutrino physics was caused by two reports:

- i) Some evidence for neutrino oscillations was seen in an experiment at the Savannah River reactor [26]
- ii) The ITEP group in Moscow [27] reported a finite value for the electron antineutrino mass, from a measurement of the end point spectrum in Tritium beta decay.

Unfortunately, (or fortunately?) in 1988 both these phenomena are in serious doubt:

- i) Many experiments looked for neutrino oscillations in the region of parameter space claimed by the Savannah River experiment, but failed to confirm their effect.

- ii) Although a revised experiment from ITEP [28] still claims evidence for a neutrino mass ($m_{\nu_e} \sim 20 \text{ eV}$), competing experiments do not confirm this result, while indirect evidence from double beta decay is (probably) in contradiction with the ITEP claim.

In what follows, I shall discuss both the neutrino mass issue as well as neutrino oscillations and double beta decay experiments.

III.1 Neutrino Mass Limits

Mass limits on ν_τ , ν_μ and ν_e follow essentially from simple kinematical constraints, involving decays where neutrinos are involved in the final state.

III.1.1 ν_τ Mass Bound

The best bound to date on m_{ν_τ} has been obtained by the ARGUS collaboration. They have studied the 5π decay of τ leptons ($\tau \rightarrow \nu_\tau 5\pi$) and fitted the invariant mass spectrum near the τ mass to obtain a bound on ν_τ . However, the data is affected by some backgrounds and is not highly statistically significant. The 5π signal is extracted by looking at a sample of $\tau^+\tau^-$ events, where one τ decays into a single prong and the other goes into 5π . This signal can be faked by purely hadronic events in which 6π are produced. However, for the ARGUS experiment operating near $\sqrt{s} = 10 \text{ GeV}$, for $M_{5\pi}$ near 1-2 GeV, a cut on $P_\pi \leq 3 \text{ GeV}$ removes most of the background. The new limit reported by ARGUS at the Munich conference [29], at 95% C.L. is

$$m_{\nu_\tau} \leq 35 \text{ MeV} \quad (149)$$

III.1.2 ν_μ Mass Bound

The best limit here comes from studying the two body π decay [$\pi \rightarrow \mu + \nu_\mu$] and the limit one obtains is only momentum resolution limited. The most recent result, obtained at PSI (ex SIN) at 90% C.L. is [30]

$$m_{\nu_\mu} \leq 250 \text{ KeV} \quad (150)$$

III.1.3 ν_e Mass Bound

The best limits (observation?) on m_{ν_e} comes from the end point spectrum of Tritium beta decay: ${}^3\text{H} \rightarrow {}^3\text{He} + e^- + \nu_e$. This reaction has a very low Q value ($Q = 18.6 \text{ KeV}$) and the idea is to look for departures from linearity in the Kurie plot. The electron intensity, $I(E)$, is proportional to $(Q - E)^2$ if the electron antineutrino is massless. Otherwise, since $I(E)$ is proportional to the product of the antineutrino energy times its momentum, one has

$$I(E) \sim \frac{d\Gamma}{dE} \sim (Q - E) [(Q - E)^2 - m_{\nu_e}^2]^{\frac{1}{2}} \quad (151)$$

Thus, in a plot of $\sqrt{I(E)}$ versus E - the Kurie plot - one expects departures from linearity near $E = Q$ if $m_{\nu_e} \neq 0$. This is shown schematically in Fig. 14.

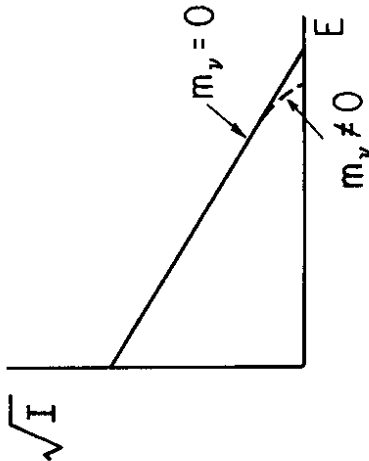


Fig. 14: Kurie plot for zero and non zero electron antineutrino masses.

However, because m_{ν_e} if it exists at all is very small ($m_{\nu_e} < 100\text{eV}$), the effect one is looking for is very tiny. This is illustrated very nicely in Fig. 15, where the actual intensity for the Tritium beta decay is plotted, with the last 100 eV near the end point blown up. One sees from this figure that the distinction between $m_{\nu_e} = 0$ and $m_{\nu_e} = 35 \text{ eV}$ is quite small. Furthermore, the fraction of events between 18.5 and 18.6 KeV is very small ($f \approx 3 \times 10^{-7}$), so one needs substantial statistics to dig out a possible neutrino mass.

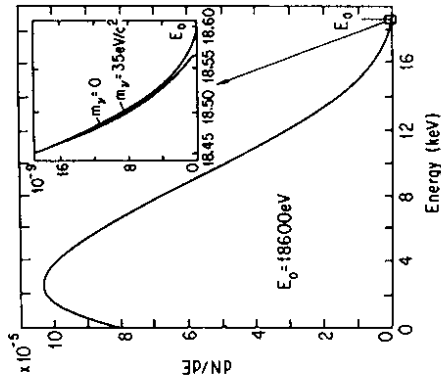


Fig. 15: Intensity for Tritium beta decay plotted versus E , with end point blown up. From [31]

Besides large statistics a Tritium beta decay experiment needs to have good control of systematic uncertainties, if it wants to probe m_{ν_e} below 50 eV. The systematic errors, in fact, are difficult to control and may determine the ultimate accuracy achievable by the experiment. There are at least three principal systematic sources of error, which one needs to minimize [32]:

- i) Errors connected with the spectrometer resolution function, which influence $\frac{\Delta E}{E}$.
- ii) Possible energy losses inside the source, which are sources of spurious energy losses, ΔE .
- iii) Energy excitations of the final states for Tritium embedded in some molecular compound, since atomic transitions can fake the effect of a neutrino mass.

At present there are 6 experiments which have results below 50 eV. I give below a table which was presented by Daniel at the Munich conference [31], summarizing the present status on this important issue.

Table II: Present Status of m_ν measurements [31]

Experiment	Source	Thickness	No. Events < 100eV	Result
IITEP Moscow	$C_5H_{11}NO_2$ (Valine)	$\sim 2 \frac{\mu g}{cm^2}$	1.3×10^5	$25_{-6}^{+6} eV$
Zurich SIN	CH_3T	$1-2 \frac{\mu g}{cm^2}$	10^5	$< 18 eV$
INS Tokyo	$C_{30}H_{40}O_2$ (C.d. calib.)	$0.6 \frac{\mu g}{cm^2}$	1.4×10^4	$< 28 eV$
Los Alamos	T_2 beam	$0.2 \frac{\mu g}{cm^2}$	10^3	$< 27 eV$
IAE Beijing	Solid Compound			$< 30 eV$
TUM Munich	T diff. into $HF O_2$	Evap. on single Xtal		$15_{-16}^{+32} eV$

Only the IITEP experiment makes a positive claim. Statistically this experiment - along with that performed in Zurich - is the most significant. However, one must worry about systematics. Furthermore, the Zurich source is better than Valine, which is a complicated compound. Of course, from this point of view the best source is the Tritium beam at Los Alamos. Unfortunately, this experiment, as well as the one performed at the INS in Tokyo are statistically limited. The TUM Munich experiment is just beginning and one cannot make very strong statements yet. Thus, the situation still remains unclear and it is difficult to see how it can be really clarified in the near future!

Although the experimental situation with the electron neutrino mass remains uncertain, there is an interesting numerical observation that one can make, related to the see saw mechanism. We saw that, for one generation, $m_\nu = \frac{m_D^2}{M}$, where m_D is the neutrino

Dirac's mass. The simplest generalization of this formula for the case of three generations is to take M to be universal and assume $m_{D_i} = m_D$. That is, the neutrino Dirac masses for each generation are just equal to the masses of the corresponding leptons. Given this assumption and the universality of M , then the formula

$$m_{\nu_i} = \frac{m_D^2}{M} \quad (152)$$

implies, for $m_\nu \approx 20 eV$, that $M \approx 10 GeV$. In turn, it follows that $m_{\nu_e} \approx 1 MeV$ and $m_{\nu_\mu} \approx 300 MeV$. Amazingly enough, these latter values are near the level where today's present bounds for m_{ν_e} and m_{ν_μ} exist! However, as I will discuss in some detail later, having such "heavy" neutrinos is in conflict with cosmological bounds, which forbid (stable) neutrinos of mass of $0(MeV)$ to exist.

III.2 Neutrino Mixing and Oscillations

An indirect manifestation of the presence of neutrino masses is the possibility of neutrino mixing which can lead to the phenomena of neutrino oscillations. If the masses of neutrinos are non vanishing, the charged weak currents in the leptonic sector will involve a mixing matrix, which is the analogue of the quark Kobayashi Maskawa matrix. Let me denote this matrix by U . Then one has

$$(J_{\pm}^{\mu})_{lept.} = 2(\nu_e \nu_\mu \nu_\tau)_L \gamma^{\mu} U \begin{pmatrix} e \\ \mu \\ \tau \end{pmatrix}_L \quad (153)$$

One can look for the presence of the mixing matrix U in a number of ways. For instance:

- 1) Besides the usual $\pi \rightarrow \mu \nu_\mu$ decay mode, now it is also possible to have the decays $\pi \rightarrow \mu \nu_e$ and $\pi \rightarrow \mu \nu_\tau$. Obviously if m_{ν_e} is in the MeV range, this latter decay will give rise to a kinematic peak which is not the one usually expected for the $\pi \rightarrow \mu \nu_\mu$ mode.
- ii) Heavy neutrinos produced in beam dumps can decay into light neutrinos, via the process shown in Fig. 16, which is proportional to the amount of mixing. The non observation of unusual e^+e^- pairs downstream in the dump can then provide bounds on the mixing.

iii) The presence of massive neutrino admixtures to ν_e can cause distortions of the lepton spectra in nuclear beta decay. Hence, for example, the Tritium bounds we just discussed are also bounds on admixed heavy neutrinos.

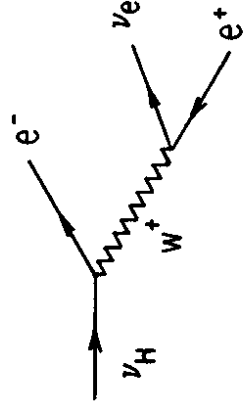


Fig. 16: Heavy neutrino decay via mixing.

Fig. 17 shows a compilation by Eichler [32] of bounds for $|U_{ie}|^2$ and $|U_{i\mu}|^2$ as function of the neutrino masses m_{ν_i} . As one can see, for "heavy neutrinos" these bounds are particularly strong.

Another interesting connected phenomena which arises if neutrinos have mass is neutrino oscillations. Just as in the quark case, the neutrino weak interaction eigenstates - the states that couple to the W and a given charged lepton - are not the same as the mass eigenstates. For instance, the weak interaction eigenstates connected with the electron, $(\nu_e)^{WI}$, is a superposition of the mass eigenstates ν_i :

$$(\nu_e)^{WI} = \sum_i U_{ei}^\dagger \nu_i \quad (154)$$

In what follows, for simplicity of exposition, I will consider only the case of two neutrino species and write the decomposition of the weak interaction eigenstates $(\nu_e)^{WI}$ and $(\nu_\mu)^{WI}$ into the mass eigenstates ν_1 and ν_2 as

$$\begin{pmatrix} \nu_e \\ \nu_\mu \end{pmatrix}^{WI} = \begin{pmatrix} \cos\theta & \sin\theta \\ -\sin\theta & \cos\theta \end{pmatrix} \begin{pmatrix} \nu_1 \\ \nu_2 \end{pmatrix} \quad (155)$$

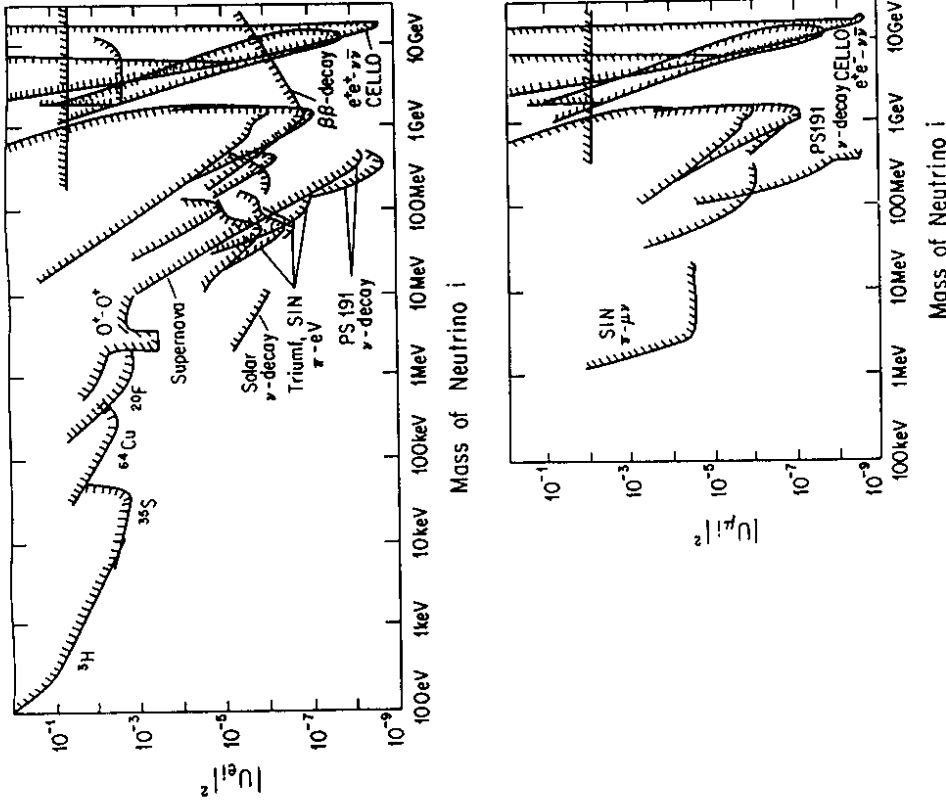


Fig. 17: Limits on $|U_{ie}|^2$ and $|U_{i\mu}|^2$ as a function of the mass of the i th neutrino. Taken from [32], where more details on the various experiments are given.

In a Schrodinger picture, the evolution in time of the mass eigenstates ν_i is characterized by a simple exponential dependence.

$$|\nu_i(t)\rangle = e^{-iE_i t} |\nu_i(0)\rangle \quad (156)$$

with $E_i = \sqrt{p^2 + m_i^2}$. Because $m_1 \neq m_2$, however, a given weak interaction eigenstate

which is a superposition of ν_1 and ν_2 , evolves in time to a superposition of both weak interaction eigenstates. That is a ν_e^{WI} state can oscillate in time to a ν_μ^{WI} state. Since what are produced by the weak interactions are precisely the weak interaction eigenstates and these states, in turn, can give rise to specific charged leptons (i.e. ν_μ^{WI} always gives a μ), the existence of these neutrino oscillations is a directly observable phenomena.

Let me discuss this a bit more quantitatively. Imagine for definitiveness that at $t = 0$ a ν_e^{WI} state is produced, so that:

$$|\nu(0)\rangle \equiv |\nu_e\rangle = \cos\theta|\nu_1(0)\rangle + \sin\theta|\nu_2(0)\rangle \quad (157)$$

At a later time this state, since $m_1 \neq m_2$, evolves into a linear superposition of ν_e^{WI} and ν_μ^{WI} . Specifically, at time t , one has

$$\begin{aligned} |\nu(t)\rangle &> = \cos\theta|\nu_1(t)\rangle + \sin\theta|\nu_2(t)\rangle \\ &= \cos\theta e^{-iE_1 t}|\nu_1(0)\rangle + \sin\theta e^{-iE_2 t}|\nu_2(0)\rangle \end{aligned} \quad (158)$$

Using that ν_μ^{WI} is the orthogonal combination to ν_e^{WI} , so that

$$|\nu_\mu^{WI}\rangle > = -\sin\theta|\nu_1(0)\rangle + \cos\theta|\nu_2(0)\rangle, \quad (159)$$

one has that

$$\begin{aligned} |\nu(t)\rangle > &= (\cos^2\theta e^{-iE_1 t} + \sin^2\theta e^{-iE_2 t})|\nu_e\rangle + \nu_e^{WI} \\ &\quad + \cos\theta \sin\theta (e^{-iE_2 t} - e^{-iE_1 t})|\nu_\mu\rangle + \nu_\mu^{WI} \end{aligned} \quad (160)$$

Hence one can calculate immediately what is the probability that a ν_e^{WI} state oscillates in a time t to a ν_μ^{WI} state:

$$\begin{aligned} P(\nu_e^{WI} \rightarrow \nu_\mu^{WI}; t) &= |\langle \nu(t) | \nu_\mu^{WI} \rangle|^2 \\ &= \frac{1}{2} \sin^2 2\theta [1 - \cos(E_1 - E_2)t] \end{aligned} \quad (161)$$

One sees from the above that to have neutrino oscillations, one needs both mixing ($\theta \neq 0$) and a mass difference ($E_1 - E_2 \neq 0$) among the neutrinos. Furthermore, since in all

practical experiments $m_{\nu_i} \ll p$, one can approximate

$$E_i = \sqrt{p^2 + m_i^2} \simeq p + \frac{m_i^2}{2p} \quad (162)$$

and take the time directly proportional to the distance travelled: $t \simeq L$. Hence,

$$(E_1 - E_2)t \simeq \left(\frac{m_1^2 - m_2^2}{2p} \right) L = \frac{\Delta m^2 L}{2p} \quad (163)$$

and the oscillation probability becomes

$$P(\nu_e^{WI} \rightarrow \nu_\mu^{WI}; L) = \sin^2 2\theta \sin^2 \frac{\Delta m^2 L}{4p} \quad (164)$$

Note that, obviously,

$$P(\nu_e^{WI} \rightarrow \nu_e^{WI}; L) = 1 - P(\nu_e^{WI} \rightarrow \nu_\mu^{WI}; L) \quad (165)$$

Oscillation experiments - in the simplified two neutrino species limit considered - are sensitive therefore to the combined effect of the amount of mixing ($\sin^2 2\theta$) and of the actual mass difference between the neutrinos (Δm^2). I note that, numerically,

$$\frac{\Delta m^2 L}{4p} \simeq 1.27 \left[\frac{\Delta m^2 (eV^2) L(m)}{p(MeV)} \right] \quad (166)$$

The compilation of neutrino oscillation limits shown in Fig. 18, taken from the report of Eichler at the 1987 Hamburg conference [32], shows that a fairly large area in the $\Delta m^2 - \sin^2 2\theta$ plane is excluded for various possible oscillations ($\nu_e \rightarrow \nu_\mu$; $\nu_e \rightarrow \nu_\tau$; etc). Typically, what is excluded are regions where

$$\begin{aligned} \Delta m^2 &\geq 1 - 10 \text{ eV} \\ \sin 2\theta &\geq 10^{-1} \end{aligned}, \quad (167)$$

but small values of Δm^2 and of the mixing angle θ are allowed. The area shaded in Fig. 18 corresponds to a reported positive signal observed in an experiment at the Bugey reactor [33]. The collaboration, however, presented a reanalysis at the Munich conference and now no effect is claimed [34]. So also in the case of neutrino oscillations, one has only limits at the moment!

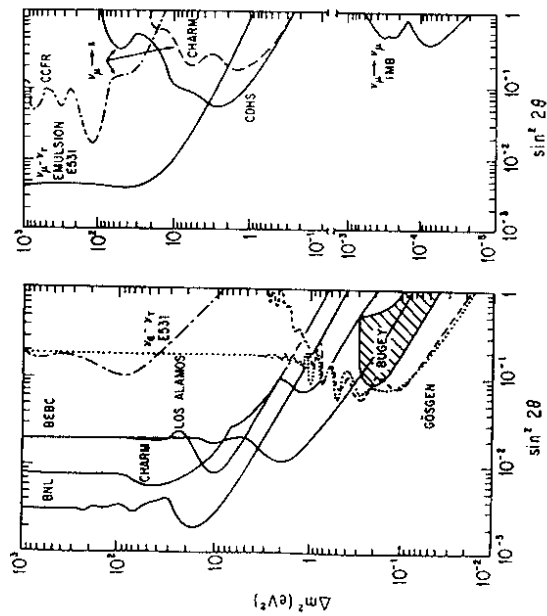


Fig. 18: Neutrino oscillation limits compiled by Eichler [32]. The positive evidence from the Bugey reactor now has disappeared.

III.3 Double Beta Decay

The observation of a finite neutrino mass, in general, does not mean that lepton number is violated*. To actually violate lepton number one needs a Majorana mass term for neutrinos, which as we saw then implies that the neutrinos themselves are Majorana particles. The Majorana nature of neutrinos could be established if one could observe evidence for neutrinoless double beta decay $[2\beta(0\nu)]$. Ordinary double beta decay, accompanied by the emission of two neutrinos $[2\beta(2\nu)]$, is a second order weak process in which a nucleus Z decays into another nucleus with two additional units of charge: $Z \rightarrow Z+2 + e^- + e^- + \nu_e + \nu_e$. This is an extremely rare process ($\tau_{2\beta} \geq 10^{20}$ years) which can only occur in nuclei where the ordinary β decay process ($Z \rightarrow Z+1 + e^- + \nu_e$) is energetically forbidden. However, as is shown schematically in Fig. 19a, such a process is perfectly lepton number conserving. In contrast, neutrinoless double beta decay $[2\beta(0\nu)]$ can only proceed if there is a lepton number violating Majorana mass term. As shown schematically in Fig. 19b, the neutrino Majorana mass term can absorb two units of lepton number. If Majorons of the Gelmini Roncadelli [17] type exist, a further double beta decay process $[2\beta(M)]$, involving Majoron emission, can take place: $Z \rightarrow Z+2 + e^- + e^- + X$. This process is shown schematically in Fig. 19c. This latter possibility is actually a lepton number conserving reaction, since the Majoron carries away two units of lepton number.

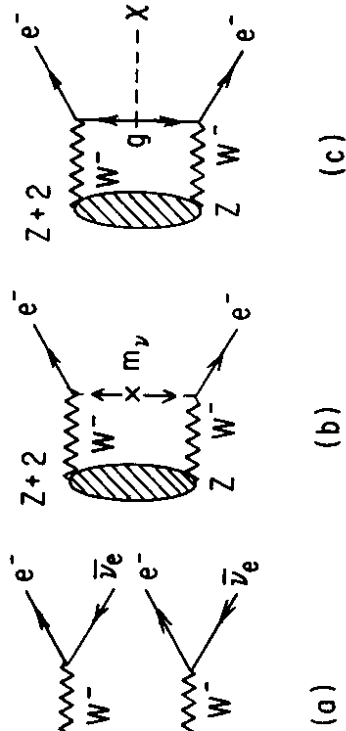


Fig. 19: Possible double beta decay processes: a) $2\beta(2\nu)$; b) $2\beta(0\nu)$; c) $2\beta(M)$.

* However, since mixing is now allowed, obviously individual electron, muon and tau number are violated.

Kinematically, neutrinoless double β decay is favored over the other two processes because of the three body phase space. Indeed, for this case, since one has only the two electrons aside for the remnant nucleus in the final state, the electron sum energy spectra is a δ -function at the value of the allowed energy release. The spectrum of emitted electrons for both the $2\beta(2\nu)$ and $2\beta(M)$ processes, on the other hand, leads to a continuous sum energy spectrum. Furthermore, since the phase space for these two processes is different, one can use the shape of this spectrum to differentiate among these two cases. This is illustrated in Fig. 20, which shows that the peak in the sum energy spectrum for the Majoron emission process is clearly at a higher value than that for ordinary double β decay.

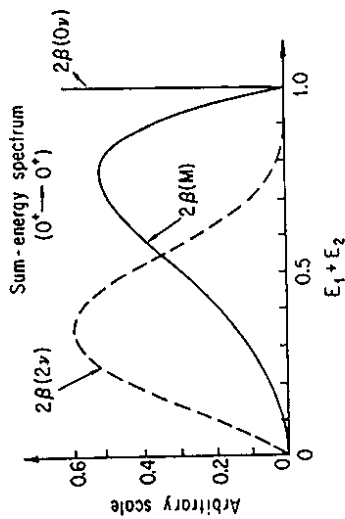


Fig. 20: Sum energy spectrum for the various double β decay process.

To calculate the rate for the three β decay processes requires a calculation of the nuclear matrix element of the weak Hamiltonian causing the transition, convoluted with the appropriate leptonic factors. As can be gathered from Fig. 19, the $2\beta(0\nu)$ and the Majoron emission processes are closely related to each other. Indeed, as observed by Georgi, Glashow and Nussinov [25], the nuclear matrix elements for the processes are actually the same. Thus, apart from phase space effects, the only other difference in the total rates is that the $2\beta(0\nu)$ rate is proportional to m_ν^2 , while the $2\beta(M)$ ratio is proportional to the Majoron coupling constant g^2 .

Until this year one had only geological evidence for double beta decay. However, finally, the first direct evidence for the $2\beta(2\nu)$ process, was obtained by a group at the University of California at Irvine, [35]. They studied ^{82}Se double beta decay and found the sum energy spectrum for the two electrons shown in Fig. 21, which is in agreement in shape

with the expectations for the $2\beta(2\nu)$ process. However, the lifetime observed

$$\tau[2\beta(2\nu)] = 1.1 \times 10^{20} \text{ years} \quad (168)$$

is about an order of magnitude longer than what had been expected theoretically [36]. This raises the question whether other nuclear matrix elements in double beta decay reactions have also been over estimated in the literature. At any rate, just from the shape of the spectrum in Fig. 21, one can infer that the $2\beta(M)$ process has a considerably weaker rate. Indeed these results can be used to set a strong bound on the Majoron coupling [37].

$$g \leq 1.9 \times 10^{-4} \quad (169)$$

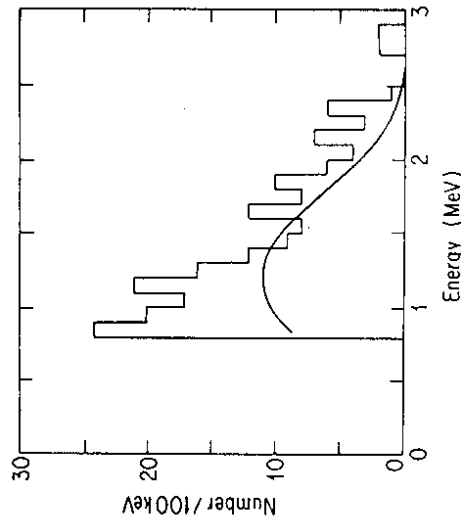


Fig. 21: Observed sum energy spectrum in ^{82}Se . From [35].

The best limits for neutrinoless double beta decay come from experiments looking for this decay in ^{76}Ge . Part of the reason for this is that ^{76}Ge is approximately 8% of natural Ge .

Furthermore, germanium detectors have excellent energy resolution and are very pure. Thus, one has the ideal situation in which the source itself is also the detector! In the decay



which leads to a sum peak energy of 2.04 MeV, the most difficult task is to reduce background. Many groups have been studying this process. At the present moment, the most stringent $\beta(0\nu)$ limits come from three different experiments, which study both the $0^+ \rightarrow 0^+$ and the $0^+ \rightarrow 2^+$ transitions. These results are summarized in Table III, taken from [38]. The ITEP - Yerevan experiment is relatively a new one entering into this field. However, since the experiment runs with 35% enriched Ge, already their results are among the most accurate.

Table III: Summary of most significant $2\beta[0\nu]$ experiment

Experiment	$\tau \times 10^{23}$ yrs($0^+ \rightarrow 0^+$)	$\tau \times 10^{23}$ yrs($0^+ \rightarrow 2^+$)
Caltech Sin	>3	>0.7
Neuchatel		
ITEP Yerevan	>4	
UCSB	>7	>2
LBL		

The combined limit for all experiments, quoted by Withereil [38] is

$$\tau[2\beta(0\nu)] > 8 \times 10^{23} \text{ yrs} \quad (171)$$

One can use the above ${}^{76}\text{Ge}$ result on $\tau[2\beta(0\nu)]$ to obtain a bound on the neutrino Majorana mass. The precise bound depends on the calculation of the nuclear matrix element for the process in question which, in view of the ${}^{82}\text{Se}$ $2\beta(2\nu)$ discrepancy between theory and experiment, has some uncertainty. Thus, it is useful to cite the extremes among the range

of values obtained by various theoretical calculations found in the literature [39]. Using the result (171) one has

$$< m_{\nu_e} > \leq \begin{cases} 0.57 \text{ eV} & [40] \\ 6 - 7 \text{ eV} & [41] \end{cases} \quad (172)$$

What is quoted here is not directly a bound on the electron neutrino Majorana mass, since what enters in the computation of the graph in Fig. 19b, if there is mixing, is

$$< m_{\nu_e} > = \sum_i \lambda_i |U_{ei}|^2 m_{\nu_i}, \quad (173)$$

where λ_i is a possible sign[42]. However, it appears very reasonable- to me, at least! - that

$$m_{\nu_e} \simeq < m_{\nu_e} > \leq \text{few eV} \quad (174)$$

This result casts some doubts on the ITEP claim of a direct measurement of m_{ν_e} [$m_{\nu_e} = 25_{-5}^{+6}$ eV]. This, of course, is not a direct contradiction since a Dirac neutrino mass would not contribute to double beta decay. However, it is difficult to imagine that an electron neutrino with a mass in the eV range is not a Majorana neutrino. In the Dirac case one must answer why

$$(m_{\nu_e})_{\text{Dirac}} < < m_e, \quad (175)$$

while in the Majorana case the see saw mechanism nicely sidesteps this question. Here, very naturally, one has

$$(m_{\nu_e})_{\text{Majorana}} \simeq \frac{m_e^2}{M} < < m_e \quad (176)$$

by requiring the existence of a large mass scale M, associated with some new physics. It is possible that within the next few years the controversy relating to the direct measurement of m_{ν_e} can be settled. However, technically, it appears difficult to improve the $2\beta(0\nu)$ bounds much below $< m_{\nu_e} > \leq \text{eV}$ in the near future.

The double beta decay experiments in ${}^{82}\text{Se}$ and ${}^{76}\text{Ge}$ provide quite stringent limits for the GR Majoron model [17]. Recall that in this model $m_{\nu} = g\nu_T$, so that from Eq (174) this product is bound by

$$g\nu_T \leq \text{eV} \quad (177)$$

In Fig. 22 I display this bound, along with the ^{82}Se bound on g and the astrophysical bounds on ν_T discussed in the last section [cf Eq (145)]. One sees from this figure that the allowed region in the parameter space for the GR model is pushed to uncomfortably small values. For instance, it is natural to ask how does a hierarchy like $\frac{\nu_T}{\nu} < 10^{-7}$ come about in the model?

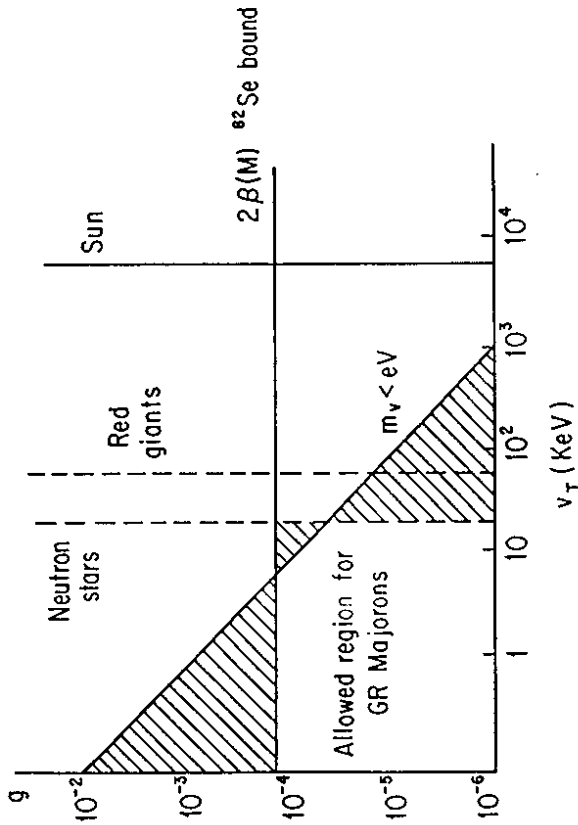


Fig. 22: Combined bounds for the GR Majoron model.

IV Neutrinos in Cosmology

Important information on neutrino properties can be gathered by cosmological arguments. Conversely, it is possible that neutrinos have a fundamental role in the Universe, since they could be the agents that helped trigger galaxy formation and/or they could be the dark matter that closes the Universe. Before we can examine the cosmological role of neutrinos, we need to discuss a few of the main features of the standard model of cosmology: The Big Bang Model [43].

On a large scale the Universe is homogenous and isotropic and so it can be described by the Robertson Walker metric. This metric is characterized by a scale factor $R(t)$. Since all proper distances are determined by $R(t)$, the expansion of the Universe is embodied in the growth of $R(t)$ with time. Describing the energy momentum tensor of matter by that of a perfect fluid, Einstein's equations for the Robertson-Walker metric reduce to Friedman's equation for the evolution of $R(t)$:

$$\left(\frac{\dot{R}}{R}\right)^2 + \frac{k}{R^2} = \frac{8\pi G_N}{3}\rho \quad (178)$$

plus an equation of energy conservation

$$\frac{d}{dt}(\rho R^3) = -p \frac{d}{dt}(R^3) \quad (179)$$

In the above ρ and p are, respectively, the total energy density and the pressure of the fluid, while k is the curvature factor [$k > 0$ corresponding to a spacetime which has a positive spatial curvature and is finite in extent].

One may use Eq (179) to characterize the dependence of the energy density on the scale factor $R(t)$ in two interesting limits. In the radiation dominated era - corresponding to a relativistic gas - $p = \frac{1}{3}\rho$ and it follows that

$$\rho \sim R^{-4} \quad (\text{rad. dom. era}) \quad (180)$$

In the case that matter dominates, on the other hand, the pressure is negligible with respect to the energy density and one has

$$\rho \sim R^{-3} \quad (\text{matter dom. era}) \quad (181)$$

It is usual to introduce the Hubble parameter H as

$$H(t) = \frac{\dot{R}}{R} \quad (182)$$

to describe the evolution of the Universe. The value of the Hubble parameter at present is the Hubble constant H_0 . This constant is known within a factor of two uncertainty, typified by a parameter h [$h = \frac{1}{2} - 1$]:

$$H_0 = 100h \frac{km}{sec Mpc} \simeq 2.2 \times 10^{-42} h GeV \quad (183)$$

Another useful number is the, so called, critical density, ρ_c . This is the density corresponding to our Universe being flat [$k=0$]. Knowing H_0 , Friedman's equation gives the critical density now as

$$\rho_c = \frac{3H_0^2}{8\pi G_N} \simeq 1.9 \times 10^{-29} h^2 \frac{g}{cm^3} \simeq 1.1 \times 10^4 h^2 \frac{eV}{cm^3} \simeq h^2 10^{-46} GeV^4 \quad (184)$$

One often defines a parameter

$$\Omega = \frac{\rho}{\rho_c} \quad (185)$$

Clearly $\Omega \rightarrow 1$ as $\rho \rightarrow \rho_c$, so that the statement that $\Omega = 1$ is equivalent to that of having a flat Universe.

At early times, the Universe was dominated by radiation. All species of particles were extremely relativistic and in thermal equilibrium with one another. Thus, apart from

certain kinematical factors related to the spin, the energy density of each type of excitation at this time can be characterized by the temperature T of the Universe. One has *

$$\rho = \frac{g}{2\pi^2} \int_0^\infty \frac{E^3 dE}{1 \pm e^{E/T}} = \frac{\pi^2}{30} g T^4 \begin{cases} 1 & \text{Bosons} \\ \frac{7}{8} & \text{Fermions} \end{cases} \quad (186)$$

where g is the spin degeneracy factor [$g = 2$ for photons and spin $\frac{1}{2}$ fermions]. Since in the radiation dominated era $\rho \sim R^{-4}$, it follows that

$$R(t) \sim \frac{1}{T}, \quad (187)$$

so that as the Universe expands it cools. In the early Universe, the curvature factor is irrelevant, being only proportional to R^{-2} . Thus Friedman's equation reduces to

$$H^2 \simeq \frac{8\pi G_N}{3} \rho = \frac{8\pi G_N}{3} \left[\frac{\pi^2}{30} g \right] T^4 \quad (188)$$

where

$$g^* = \sum_{\text{bosons}} g_b + \frac{7}{8} \sum_{\text{fermions}} g_f \quad (189)$$

characterizes the number of effective degrees of freedom present in the Universe. Clearly the Hubble parameter decreases quadratically as the temperature of the Universe cools. Writing Newton's constant in terms of the Planck mass

$$G_N = \frac{1}{M_P^2} \quad (190)$$

with $M_P \simeq 1.2 \times 10^{19}$ GeV, one finds for H the (mnemonically simple) expression

$$H \simeq 1.66 [g^*]^{1/2} \frac{T^2}{M_P} \quad (191)$$

* I use units where the Boltzman constant $k_B = 1$.

The last important concept we shall need for our discussion is that of decoupling. In the early Universe particles will remain in equilibrium as long as the interaction rates, Γ , are larger than the Universe's rate of expansion, typified by the Hubble parameter. Now the interaction rates by which relativistic particles maintain themselves in equilibrium are function both of the number density of these particles in the Universe and their interaction cross sections:

$$\Gamma = \langle \sigma n \rangle \quad (192)$$

For weakly interacting relativistic particles, like neutrinos, the interaction cross sections depend quadratically on T :

$$\sigma \sim G_F^2 T^2 \quad (193)$$

Since $n \sim T^3$, the interaction rate depends very strongly on the temperature

$$\Gamma \sim G_F^2 T^6 \quad (194)$$

Although $\Gamma \gg H$ in the early Universe, when the temperature is very high, eventually since $H \sim T^2$ but $\Gamma \sim T^6$, the interaction rate will fall below the Universe expansion rate. When this happens, the particular particle species in question decouples from the rest of the other excitations, since the Universe is expanding at a much greater rate than the processes which would allow the decoupled excitations to communicate with the rest of the other excitations. After decoupling, which can be taken to occur at temperatures below those for which $\Gamma \simeq H$, the number density of the decoupled particles just decreases proportionally to the Universe's scale factor cubed:

$$n(t) = n(t_{dec}) \left[\frac{R(t_{dec})}{R(t)} \right]^3 \quad (195)$$

IV.1 Neutrino Bounds from Nucleosynthesis

Helium is present abundantly in the Universe, with its mass fraction Y being about 30%. Although some of this Helium is generated in stars, the bulk of the mass fraction Y is believed to have been generated primordially by nucleosynthesis, with the primordial mass fraction generally taken to be about [44].

$$Y_P \simeq 0.22 - 0.26 \quad (196)$$

The idea of primordial nucleosynthesis was suggested long ago by Gamow [45]. However, it took the pioneering calculation of Peebles and of Wagoner, Fowler and Hoyle [46] to demonstrate that the Helium abundance Y_P was indeed calculable and of the right order of magnitude in the Big Bang scenario. Indeed, primordial nucleosynthesis provides one of the main tests for the Big Bang model.

Although I do not want to discuss this subject in great detail, I want to indicate why Y_P can serve to put a bound on the number of light neutrino species. As we shall see, in fact, an accurate determination of Y_P in the Big Bang model depends mainly on two parameters:

$$i) \eta = \frac{n_B}{n_\gamma} \sim 10^{-9} - 10^{-10} \text{ - the baryon to photon ratio in the Universe at the present time}$$

and

$$ii) N_\nu, \text{ the number of light neutrinos, where "light" in this context means } m_\nu \leq 0(\text{MeV}).$$

Clearly it is this last parameter which we are most interested in, in these lectures.

To see where the above dependences of Y_P come from, it is useful to describe the process of nucleosynthesis in a sequence of three time frames [47].

Frame 1: $T \simeq 10 \text{ MeV}$ ($t_{\text{univ}} \simeq 10^{-2} \text{ sec}$)

At this time the energy density of the Universe is dominated by the particles which are present and are still relativistic. These are the photons, the electrons, and the positrons and the "light" neutrinos and antineutrinos. Thus, at this temperature,

$$g^* = 2 + \frac{7}{8} \cdot 4 + \frac{7}{8} \cdot 2N_\nu = \frac{43 + 7(N_\nu - 3)}{4} \quad (197)$$

Note that neutrinos and antineutrinos, since they only have one effective interacting degree of freedom, have a degeneracy factor of 1. In view of Eq (191), the Hubble parameter is a function of g^* and hence of the number of light neutrino species.

At this stage in the development of the Universe, thermal equilibrium is maintained by the weak and electromagnetic interactions, whose reaction rates for processes like $e^+e^- \rightarrow \nu_i\bar{\nu}_i$, $e^+n \leftrightarrow p\bar{\nu}_e$, etc, are much greater than the Hubble parameter: $\Gamma_W \sim G_F^2 T^6 \gg H \sim T^2/M_P$. In particular, since the neutrons and protons are in thermal equilibrium still, the neutron to proton ratio is fixed by the Boltzman factor:

$$\frac{n}{p} = e^{-\frac{\Delta m}{T}}; \quad \Delta m = m_n - m_p \simeq 1.3 \text{ MeV} \quad (198)$$

Frame 2: $T^* \simeq 1 \text{ MeV}$ ($t_{\text{univ}} \sim 1 \text{ sec}$)

At about this temperature $\Gamma_W \simeq H$ and neutrinos, which have only weak interactions, decouple. Thereafter their density just decreases like R^{-3} [cf Eq (195)]. At this time also the n/p ratio ceases to follow the equilibrium value since the $n \leftrightarrow p$ weak conversion is proceeding too slowly compared to the Universe's expansion. Thus the n/p ratio "freezes" out at a value

$$\left(\frac{n}{p}\right)_{\text{freeze out}} = e^{-\frac{\Delta m}{T^*}} \simeq \frac{1}{6} \quad (199)$$

[Here the numerical value is the one obtained by a more detailed calculation [47]]. This value then only decreases due to the decay of some neutrons by the usual beta process:

$n \rightarrow p\bar{\nu}_e$, so that

$$\left(\frac{n}{p}\right) = e^{-\frac{\Delta m}{T}} \left(\frac{n}{p}\right)_{\text{freeze out}} \quad (200)$$

with τ being the neutron lifetime.

Frame 3: $T_N \sim 0.1 \text{ MeV}$ ($t_{\text{univ}} \sim 3 \text{ min}$)

Around this time nucleosynthesis begins in earnest, since now there are enough deuterons being formed via the process $n + p \rightarrow D + \gamma$. The number density of deuterons, which is tiny at higher temperatures, now catches up with the baryon number density. At $T = T_N$ one requires that

$$\frac{n_D}{n_B} = \frac{n_B}{n_\gamma} e^{-\frac{\Delta m}{T}} = \eta e^{\frac{2\Delta m}{T}} \simeq 1 \quad (201)$$

Since $\eta \sim 10^{-9} - 10^{-10}$ indeed one sees that $T_N \sim 0.1 \text{ MeV}$. At T_N essentially all the neutrons present at this time [$n/p \simeq \frac{1}{7}$, due to some neutron decays] are transformed to deuterons and then quickly into the even more stable ${}^4\text{He}$ nucleus, although some trace amounts of deuterium and ${}^3\text{He}$ remain unburned. Synthesis of elements beyond ${}^4\text{He}$ is prevented by lack of stable isotopes and the Coulomb barrier*.

The primordial ${}^4\text{He}$ yield is essentially determined by the neutron to proton ratio at T_N :

$$Y_P = 2 \left[\frac{n}{n+p} \right]_{T_N} \simeq \frac{1}{4}, \quad (202)$$

where the numerical value corresponds to taking $(\frac{n}{p})_{T_N} = \frac{1}{7}$. To determine Y_P accurately, therefore, one must know $(\frac{n}{p})_{T_N}$ accurately. Since

$$\left(\frac{n}{p}\right)_{T_N} = \left(\frac{n}{p}\right)_{T^*} e^{-\frac{(t_N - t^*)}{\tau}}, \quad (203)$$

* Traces of ${}^7\text{Li}$ are synthesized by ${}^3\text{H}$ and/or ${}^3\text{He}$ reactions with ${}^4\text{He}$.

this means in turn that one needs precise values for T^* and T_N^{**} . The value of the "freeze out" temperature T^* is determined by setting the reaction rate $\Gamma_W \sim T^{*5}$ equal to the expansion rate $H \sim (g^*)^{1/2} T^{*2}$. One sees, therefore, that T^* depends on g^* and N_ν , as

$$T^* \sim [g^*]^{1/2} \sim [43 + 7(N_\nu - 3)]^{1/2} \quad (204)$$

Hence, if $N_\nu > 3$, T^* rises. Since $(\frac{n}{p})_{T^*} \simeq e^{-\frac{m_n}{kT^*}}$, more neutrino species imply a larger value for $(\frac{n}{p})_{T^*}$ and hence a higher Y_P . Thus, an upper bound on the primordial helium fraction corresponds directly to a bound on N_ν .

The value for the nucleosynthesis temperature T_N^{**} , as Eq (201) indicates, depends on η . If the baryon to photon ratio η is larger, then T_N^{**} itself can be larger. Thus as η increases one expects a larger value for $(n/p)_{T_N^{**}}$ and hence for Y_P . This behavior is, however, opposite for the trace nuclei ${}^3\text{He}$ and D^{***} . The higher η is, the more ${}^4\text{He}$ is processed and hence the less one expects of the trace materials to survive. The fact that the behavior of these latter abundances goes oppositely with η to that of ${}^4\text{He}$ is important, since it helps to set bounds on the allowed region of η .

I summarize below and in Fig. 23 the results of the careful analysis of nucleosynthesis yields done by Yang, Turner, Steigman, Schramm and Olive [48]. The estimate of the primordial fraction of nucleosynthesized elements is difficult, but they lie in the range [48]:

$$\begin{aligned} 0.22 \leq Y_P \leq 0.26 \\ \frac{D}{H} \geq 10^{-6} \\ 8 \times 10^{-5} \geq \frac{D + {}^3\text{He}}{H} \\ 10^{-10} \leq {}^7\text{Li} \leq 2 \times 10^{-10} \end{aligned} \quad (205)$$

** In fact, one also needs an accurate value for the neutron lifetime which today is still only known to 2%!

*** The situation for ${}^7\text{Li}$ is more complicated since its nucleosynthesis involves two different reactions.

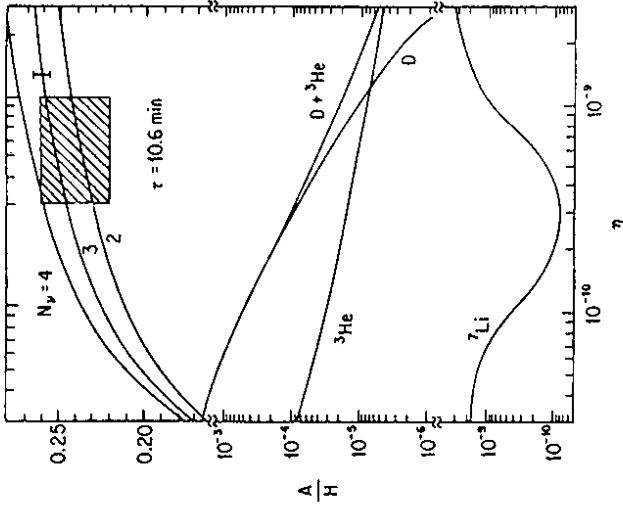


Fig. 23: Predicted abundances for ${}^4\text{He}$, D , ${}^3\text{He}$ and ${}^7\text{Li}$ from [48]. The abundance for ${}^4\text{He}$ is Y_P . That for the other nuclei is the number ratio with respect to H . The error bar on the ${}^4\text{He}$ prediction is the effect of the neutron lifetime uncertainty. For Y_P different values of N_ν , are also shown.

The last three numbers are consistent if

$$3 \times 10^{-10} \leq \eta \leq (7 - 10) \times 10^{-10} \quad (206)$$

This region, along with restriction (196) on Y_P , is shown cross-hatched in Fig. 23. It implies that

$$N_\nu \leq 4, \quad (207)$$

perfectly in agreement with the particle physics bounds we discussed earlier.

IV.2 Neutrino Mass Bounds

Marx and Szalay [49] and Cowsik and McClelland [50] pointed out long ago that one could use the fact that the present energy density in the Universe is near the critical energy density, ρ_c , to set a limit on neutrino masses. Their argument is quite simple and yet very powerful. After neutrinos decouple, at temperatures of $0(1 \text{ MeV})$, since $\Gamma W \leq H$, the neutrino number density just decreases because of the Universe's expansion as $n_\nu \sim R(t)^{-3}$ [cf Eq (195)]. At decoupling the temperature of the neutrinos and that of the photons is the same, since they are still in equilibrium. Thus, at the time of decoupling $n_\nu \sim T_\nu^3 \sim T_\gamma^3$. Even though after decoupling neutrinos are out of thermal equilibrium, the neutrino density effectively continues to track the photon temperature:

$$n_\nu \sim T_\gamma \quad (208)$$

This is the case because, as we saw earlier, for radiation the temperature decreases inversely proportional to the Universe scale factor: $T_\gamma \sim R(t)^{-1}$. Hence, since $n_\nu \sim R(t)^{-3}$ after decoupling, Eq (208) holds also. Thus one can continue to characterize neutrinos by a temperature $T_\nu = T_\gamma$, also after decoupling.

Actually, this is not exactly correct. The photon temperature does not quite follow $R(t)^{-1}$, since there is a jump in T_γ after the electrons and positrons go out of thermal equilibrium [$\Gamma(e^+e^- \leftrightarrow \gamma) \leq H$]. Entropy conservation at this latter decoupling implies

$$(g^* RT_\gamma^3)_{\text{before}} = (g^* RT_\gamma^3)_{\text{after}} \quad (209)$$

or

$$\left(\frac{T_\gamma}{T_\nu}\right)_{\text{after}} = \left[\frac{g_{\text{before}}^*}{g_{\text{after}}^*}\right]^{1/3} = \left[\frac{11/2}{2}\right]^{1/3} = \left[\frac{11}{4}\right]^{1/3} \quad (210)$$

Thus the neutrino temperature later on in the Universe is slightly lower than that of the photons:

$$T_\nu = \left(\frac{4}{11}\right)^{1/3} T_\gamma \quad (211)$$

So the $3^\circ K$ photon black body radiation today [$T_\gamma \simeq 2.7^\circ K$] implies a neutrino temperature today of $T_\nu = 1.9^\circ K$.

If neutrinos are massless, then their contribution to the Universe energy density is given by [cf Eq (186)]:

$$\begin{aligned} \rho_\nu &= \frac{\pi^2}{30} \left[\frac{7}{8}\right] 2N_\nu T_\nu^4 \\ &\simeq N_\nu (8 \times 10^{-35} \frac{g}{\text{cm}^3}) \end{aligned} \quad (212)$$

where the second line corresponds to taking $T_\nu = 1.9^\circ K$. Obviously massless neutrinos make a negligible contribution to the Universe's energy density. [$\rho_\nu \ll \rho_c \simeq 1.9 \times 10^{-29} h^2 \frac{g}{\text{cm}^3}$]. If neutrinos have mass, however, one can get a much larger contribution to ρ_ν , since one can only redshift the neutrino energy to m_ν . That is,

$$\rho_\nu \sim \begin{cases} T_\nu^4 & (m_\nu = 0) \\ m_\nu T_\nu^3 & (m_\nu \neq 0) \end{cases} \quad (213)$$

More precisely

$$\rho_\nu = \sum_i m_{\nu_i} n_i \quad (214)$$

where n_i is the density of the i^{th} species of neutrinos, which is fixed by the effective neutrino temperature $T_\nu = \left(\frac{4}{11}\right)^{1/3} T_\gamma$:

$$n_{\nu_i} = \frac{g}{2\pi^2} \int_0^\infty \frac{E^2 dE}{1 + e^{E/T_\nu}} = \frac{3\zeta(3)}{2\pi^2} T_\nu^3 \quad (215)$$

In the above g is the degeneracy factor which, if we take into account of both neutrinos and antineutrinos, equals 2. Hence, for massive neutrinos one has

$$\rho_\nu = \frac{3\zeta(3)}{2\pi^2} \left[\sum_i m_{\nu_i} \right] T_\nu^3 \simeq 109 \left[\sum_i m_{\nu_i} \right] \text{cm}^{-3} \quad (216)$$

Clearly, one can get a bound on (the sum of) neutrino masses by requiring that $\rho_\nu \leq \rho_c \simeq 1.1 \times 10^4 h^2 \text{ eV cm}^{-3}$. This yields the bound

$$\sum_i m_{\nu_i} \leq 100 h^2 \text{ eV} \quad (217)$$

Although the controversy regarding the value of the Hubble parameter is not totally settled yet [$\frac{1}{2} \leq h \leq 1$], the most likely modern value for h is $h \simeq 0.8$ [51]. So for a flat Universe [$k = 0, \Omega = 1$] the most likely bound on neutrino masses is

$$\sum_i m_{\nu_i} \leq 65 \text{ eV} \quad (218)$$

The above bound does not apply for very heavy neutrinos. One can understand this qualitatively rather simply. If the mass of the heavy neutrinos m_{ν_H} is much greater than the decoupling temperature

$$m_{\nu_H} \gg T^* \simeq 1 \text{ MeV} \quad (219)$$

then the density of these neutrinos at decoupling is suppressed by a Boltzman factor and is much less than the density of relativistic neutrinos at decoupling

$$n_{\nu_H}(T^*) \sim e^{-\frac{m_{\nu_H}}{T^*}} \ll n_\nu(T^*)|_{rel} \sim T^{*3} \quad (220)$$

Obviously, if m_{ν_H} is big enough

$$\rho_{\nu_H} \sim \left(e^{-\frac{m_{\nu_H}}{T^*}} \right) m_{\nu_H} \left(\frac{T^*}{T^*} \right)^3 < \rho_c, \quad (221)$$

so that very heavy neutrinos are not subjected to any cosmological bound.

Actually, Eq (221) is too rough an approximation. The Boltzman factor $e^{-\frac{m_{\nu_H}}{T^*}}$ not only changes the number density at decoupling, but it also changes the neutrino interaction rate and hence T^* itself. So the actual upper bound on neutrino masses allowed by

cosmology requires a bit more care, as first emphasized by Lee and Weinberg [52]. The correct treatment [53] needs a numerical solution of the rate equation, which follow from Boltzman's equation:

$$\frac{dn_{\nu_H}}{dt} = -3Hn_{\nu_H} - \langle \sigma v \rangle \{ n_{\nu_H}^2 - n_{eq}^2 \} \quad (222)$$

In the above $\langle \sigma v \rangle$ is the thermal average of the annihilation rate, with $\langle \sigma v \rangle \sim G_F^2 m_{\nu_H}^2$, while n_{eq} is the equilibrium number density, $n_{eq} \sim e^{-\frac{m_{\nu_H}}{T}}$. It turns out that for neutrinos in the GeV range, the solution to Eq (222) yields, approximately, that $n_{\nu_H} \sim m_{\nu_H}^{-3}$, rather than the exponential cut off given in Eq (220). A recent analysis of Kolb [54] gives the following expression for the present energy density of heavy neutrinos:

$$\rho_{\nu_H} \simeq 5.7 \times 10^4 C_{\nu_H} \frac{\left[1 + \frac{3}{28} \ln m_{\nu_H}(\text{GeV}) \right] \text{ eV}}{m_{\nu_H}^2(\text{GeV})^2 \text{ cm}^3} \quad (223)$$

where the constant $C_{\nu_H} = 1$ for Dirac neutrinos, but $C_{\nu_H} \simeq 3.3$ for Majorana neutrinos*. Requiring that $\rho < \rho_c$ and taking $h = 0.8$ implies

$$m_{\nu_H} \geq \begin{cases} 8 \text{ GeV} & \text{(Dirac neutrinos)} \\ 14.4 \text{ GeV} & \text{(Majorana neutrinos)} \end{cases} \quad (224)$$

The above results indicate that cosmology has a forbidden gap for neutrino masses in the range between above 65 eV and either 8 GeV or 14.4 GeV. The present upper limits for ν_μ and ν_τ from particle physics experiments [$\nu_\mu \leq 250 \text{ KeV}$; $\nu_\tau \leq 35 \text{ MeV}$] allow these masses to be in this forbidden region. Thus, cosmology strongly constrains the value of the ν_μ and ν_τ neutrino masses. Furthermore, I note that if one takes the ITEP value for m_{ν_e} [$m_{\nu_e} = 25_{-8}^{+6} \text{ eV}$] as a real observation, then roughly 40% of the mass density of the Universe is in the form of ν_e 's!

Neutrinos in the forbidden cosmological region can exist provided they are unstable, have a sufficient short lifetime and decay into innocuous modes. The effect of instability is simple to take into account if the neutrinos decay into massless excitations [e.g. $\nu_H \rightarrow \nu_e \gamma$]

* These differences are due to the different interaction rates for both cases.

- although this is an unsafe mode, as will be discussed below]. Basically, in this case, the temperature dependence of the energy density for ν_H is that of a massive particle from the time of decoupling to the decay time, but then it switches to that of a massless particle, since the decay products's energy can be redshifted down towards zero. Hence if t_D is the decay time and T_D the decay temperature

$$\rho(t_0) = \rho(t_D) \left(\frac{T_0}{T_D} \right)^4 \quad (225)$$

with

$$\rho(t_D) = \rho(t^*) \left(\frac{T_D}{T^*} \right)^3 \quad (226)$$

So the result for the energy density in this case is the stable particle result, multiplied by an extra redshift factor of $\frac{T_D}{T^*}$:

$$\rho(t_0) = \left[\rho(t^*) \left(\frac{T_0}{T^*} \right)^3 \right] \left(\frac{T_0}{T_D} \right) \quad (227)$$

Since in a radiation dominated universe $t \sim T^{-2}$, the extra redshift factor is equivalent to the square root of the ratio of the neutrino lifetime to that of the Universe's. So for unstable neutrinos, decaying to massless excitations, the bound of Eq (218) reduces to

$$\sum m_{\nu_i} \left[\frac{\tau_i}{\tau_{\text{univ}}} \right]^{\frac{1}{2}} \leq 65 \text{ eV} \quad (228)$$

Obviously, for sufficiently short-lived neutrinos, one can penetrate the previously forbidden region.

Unstable neutrinos will also alter the large mass bounds of Eq (224) and one is lead to a shrinking of the cosmological forbidden region. I show in Fig. 24, taken from a recent paper of Harari and Nir [55], a two dimensional forbidden zone in the $m_\nu - \tau_\nu$ plane,

which accounts for the effects of decaying neutrinos. One sees that if neutrino lifetimes were shorter than about one year, then no cosmological forbidden zone would survive.

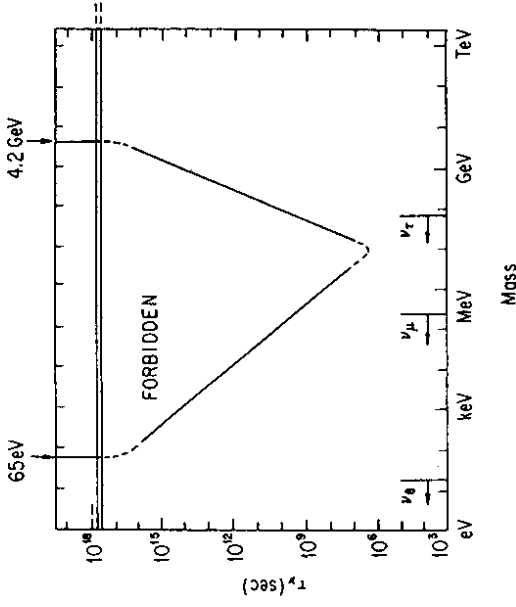


Fig. 24: Cosmological forbidden zone in the $m_\nu - \tau_\nu$ plane, from [55]. Note that the large mass bounds are slightly different than those given in Eq (224), due to the somewhat differing assumptions employed for the interacting cross sections.

Although the above results are interesting there are two serious practical problems that one must address [55]:

- i) It is difficult theoretically to get so short neutrino lifetimes, in the standard model. Typically, decays like $\nu_\tau \rightarrow \nu_\mu \gamma$, $\nu_\mu \rightarrow \nu_e \nu_e \nu_e$, etc, have lifetimes larger than the age of the Universe!
- ii) If the decay byproducts contain either photons or e^+e^- pairs there will be substantial reheating when the ν_H decay, disturbing the $3^0 K$ background radiation. So these are not allowed final states, unless τ_ν is really very short ($\tau_\nu < 10^4$ sec [56]).

Harari and Nir [55], in their rather extensive analysis, found only two very small windows where unstable neutrinos could exist, and escape from any cosmological bounds. One of these windows concerns ν_τ 's in the range $10 \text{ MeV} \leq m_{\nu_\tau} \leq 25 \text{ MeV}$, which decay via $\nu_\tau \rightarrow \nu_e e^+ e^-$, with a lifetime $\tau_{\nu_\tau} < 10^4 \text{ sec}$. The second Harari-Nir window in the cosmological forbidden zone is more speculative, since it necessitates the existence of a CMP Majoron and it involves the decay: $\nu_\mu \rightarrow \nu_e X$. In our original work on Majorons and their effects on the cosmology of neutrinos [57], we assumed that the $\nu_\mu \nu_e X$ coupling was of order of the Cabibbo angle. Then essentially all ν_μ masses are allowed cosmologically. However, our assumption was overly generous, as Schechter and Valle [58] pointed out, since this coupling must vanish as $m_{\nu_\mu} \rightarrow 0$. In the analysis of Harari and Nir, this limiting behavior is incorporated by taking the $\nu_\mu \nu_e X$ coupling to be proportional to $m_D(e) m_D^3(\mu) / M^4$, with m_D being the neutrino Dirac mass ($m_D(e) \sim m_e$, etc). Then there is a small window for m_{ν_μ} allowed: $70 \text{ KeV} \leq m_{\nu_\mu} < 250 \text{ KeV}$, provided $M < M_W$. This is certainly in accord with the Feinberg Sucher bound [22], as long as M itself does not become too light.

IV.3 Neutrinos as Dark Matter

Recall that the calculations of nucleosynthesis of ^4He , D , ^3He and ^7Li were in agreement with observations for a range of $\eta = \frac{n_B}{n_\gamma}$:

$$3 \times 10^{-10} \leq \eta \leq (7 - 10) \times 10^{-10} \quad (229)$$

One can use this number to calculate the Universe energy density in baryons, and compare it to ρ_c . One finds

$$\Omega_B = \frac{\rho_B}{\rho_c} = \frac{m_B \eta}{\rho_c} \left[\frac{\pi^2}{15} T_\gamma^4 \right] = 3.6 \times 10^7 \frac{\eta}{h^2} \quad (230)$$

Since $0.5 < h < 1$, using (229) one arrives at a range for Ω_B :

$$0.01 \leq \Omega_B \leq 0.14 \quad (231)$$

Thus, the Universe is not closed by baryonic matter. This is an interesting observation since, if one believes on theoretical grounds that $\Omega = 1$ as follows from the inflationary Universe scenario [59], then there must exist some dark matter. There are, in fact, further observational and theoretical arguments for dark matter.

The two most compelling observational indications for dark matter come from two sources:

- i) Flat galactic rotation curves, where one finds that the velocity of stars beyond the luminous part of galaxies does not decrease with the radius, $v^2 \sim \frac{1}{r}$, as one would expect from elementary considerations. The amount of dark matter one would infer from these observations [60] gives

$$\Omega_{\text{dark}} \simeq 0.005 \quad (232)$$

- ii) The mass to light ratio of various astronomical objects, which one can estimate via virial theorem considerations, appears to be larger at larger scales. This gives the following dark matter estimates [61]:

$$\Omega_{\text{dark}} = 0.0016 \pm 0.0008 \quad (\text{Solar neighborhood}) \quad (233a)$$

$$\Omega_{\text{dark}} = 0.008 - 0.017 \quad (\text{Center of galaxies}) \quad (233b)$$

$$\Omega_{\text{dark}} = 0.05 - 0.15 \quad (\text{Binaries and small groups}) \quad (233c)$$

$$\Omega_{\text{dark}} = 0.25 - 0.8 \quad (\text{Clusters of galaxies}) \quad (233d)$$

I note that all estimates of Ω_{dark} , except for the last estimate which is quite uncertain, could be due to nonluminous baryonic matter, since these values do not exceed the upper bound of Eq (231).

On the theoretical side, besides appealing to the inflationary Universe scenario, where $\Omega = 1$ is a natural consequence, the strongest evidence for dark matter comes from the growth of fluctuations in the Universe. The argument, succinctly put, is as follows [62]. In a baryon dominated Universe the growth of density fluctuations, needed for galaxy formation, is slow:

$$\frac{\delta \rho}{\rho} \sim R(t) \sim T^{-1} \quad (234)$$

Furthermore, the growth of these fluctuations does not start until the time of Hydrogen formation- the recombination time, t_R , at a temperature $T_R \sim 3 \times 10^3 \text{ }^\circ\text{K}$. From the (lack

of) anisotropy in the microwave background radiation [63], one can put a bound on the density fluctuations at recombination

$$\left(\frac{\delta\rho}{\rho}\right)_{t_R} = 3\left(\frac{\delta T}{T}\right)_{t_R} \leq 3(2.5 \times 10^{-5}) \quad (235)$$

This number, given the slow growth rate of the density fluctuations (234), is not enough to get $\frac{\delta\rho}{\rho} \simeq 1$ sufficiently far in the past, to give a realistic scenario for galaxy formation. The presence of dark matter (e.g. massive neutrinos) helps in this regard in two ways. With dark matter the era of matter domination starts sooner and, in general, the dark matter also facilitates the formation of structure. I want to describe briefly below some of the advantages, and some of the disadvantages, of neutrinos as dark matter.

A nontrivial advantage (in my opinion) of neutrinos as a dark matter candidate over other proposed candidates [photinos, axions, quark nuggets, etc.] is that neutrinos are known to exist! Given that for $\Omega = 1$, one needs most of the mass density to be in dark matter - and hence, for the case of neutrinos one needs $\sum_i m_{\nu_i} \simeq 65 \text{ eV}$ [cf Eq (218)] - it is probable that this dark matter is made mostly of ν_r . Obviously, even taking the ITEX value as real, the mass of ν_e is not sufficient to close the Universe. Hence, it is much more likely that $m_{\nu_e} \simeq 65 \text{ eV}$, with the other neutrino masses being much smaller, according to a see saw hierarchy:

$$m_{\nu_r} : m_{\nu_\mu} : m_{\nu_\tau} \sim m_r^2 : m_\mu^2 : m_\tau^2 \quad (236)$$

Apart from the above prejudicial advantage, neutrinos have a kinematical advantage over other dark matter candidates in that they cluster on larger scales [64], where the dark matter is needed. Recall in this respect that the Ω value inferred for clusters of galaxies [61] [$\Omega_{\text{dark}} \simeq 0.25 - 0.8$] was much greater than that inferred for an individual galaxy [$\Omega_{\text{dark}} \simeq 0.01$]. One can show rather straightforwardly, in terms of energetics, that 65 eV neutrinos tend to give rise to rather large structures, of the size of a supercluster. For fluctuations of a certain linear dimension ℓ to grow, one needs that the self gravitational energy should exceed the thermal energy associated with the fluctuation. For neutrinos, this leads to the inequality

$$\frac{G_N(\rho_\nu \ell^3)^2}{\ell} > \rho_\nu \ell^3 \quad (237)$$

or

$$\ell > \left[\frac{1}{G_N \rho_\nu} \right]^{\frac{1}{2}} \quad (238)$$

Associated with this minimal dimension - the so called Jean's length - beyond which neutrinos do not erase fluctuations, there is a mass [the Jean's mass]

$$M_J \simeq \rho_\nu \ell_J^3 \simeq \frac{1}{G_N^{3/2} \rho_\nu^{1/2}} \quad (239)$$

Now neutrino dominance occurs at a temperature T of order $T \sim m_\nu$ (i.e. when the neutrinos are still largely relativistic), so that $\rho_\nu \sim m_\nu T^3 \sim m_\nu^4$. Hence the Jean's mass of the fluctuations which are not erased by neutrinos is

$$M_J \simeq \frac{1}{G_N^{3/2} \rho_\nu^{1/2}} \simeq \frac{M_P^2}{m_\nu^2} \simeq 10^{16} M_\odot \quad (240)$$

where the numerical value is that appropriate for 65 eV neutrinos.

Although the, so called, free streaming of neutrinos [64] has the property of erasing all perturbations of mass below the Jean's mass, this is somewhat of a mixed blessing. On the one hand, it is true that one would like to associate dark matter with large structures. Yet, forming big structures first means that, in this scenario, galaxies can form only by the collapse of superclusters - the pancake formation mechanism of Zeldovich [65]. The trouble is that detailed studies seem to show [66] that the collapse of superclusters only happens very late and may be in contradiction with the existence of quasars of large red shift. However, much recent work has been going on to avoid this impasse, by appealing to cosmic strings [67]. The idea here is to use cosmic strings as galaxy seeds, since they are not erased by the neutrino free streaming. Obviously, a proper treatment of this fascinating subject is both beyond the scope of these lectures and my own expertise. Nevertheless, I conclude that there remains a reasonable possibility that neutrinos are the dark matter which closes the Universe. Although a neutrino dominated Universe scenario is not totally watertight, the recent discovery of filaments and voids [68] in the Universe - prototypical structures of Zeldovich's pancake scenario - is rather encouraging.

V Astrophysical Neutrinos

Neutrino astronomy came of age on February 23, 1987, when neutrino events from the supernova burst arising from SN 1987a were discovered by the Kamiokande [69] and IMB [70] detectors. The potential for exploring neutrino properties with astrophysical experiments is very exciting. Indeed, as I shall discuss below, already the observation of neutrinos from SN 1987a has provided interesting mass and lifetime limits for neutrinos. Conversely, by studying neutrinos of astrophysical origin, much can be learned of the detailed processes involved in stellar structure. The only disadvantage that I can see in the new scientific discipline of neutrino astronomy is that, unfortunately, one cannot control either the "quality" or the time structure of the source!

V.1 The Solar Neutrino Puzzle

R. Davis and collaborators [71] have been involved for almost 20 years in an extremely challenging experiment to detect neutrinos originating from the thermonuclear reactions in the sun. Their experiment uses a tank of approximately 400,000 liters of C_2Cl_4 and looks for the conversion of (minute amounts) of chlorine nuclei via the process



initiated by solar neutrinos. The produced amount of ^{37}Ar is measured by radiochemical techniques, which are necessarily very sophisticated since only about one atom of ^{37}Ar is produced per day! The usual unit used in describing this, and other soon to be detailed, solar neutrino experiments is the SNU [Solar Neutrino Unit]. This corresponds to 10^{-36} captures/atom-sec. For the experiment of Davis et al [71] 1 SNU is equivalent to the conversion of about 0.23 atoms of ^{37}Ar per day. Their observations are consistent with a signal of about 2 SNU (~ 0.5 atoms/day) which is much greater than their estimate of the cosmic ray induced background in their detector, which yields about 0.08 atoms/day. Given these very small numbers, it is not surprising that their detailed results have fluctuated through the years. Nevertheless, taking all their data from 1970 to 1985 into account, the average conversion rate [71] is

$$< \text{}^{37}\text{Cl} >_{exp} = (2.1 \pm 0.3) \text{ SNU} \quad (242)$$

This number, which per se represents a fantastic experimental achievement, is below the predictions of the Standard Solar Model (SSM) [72], which expects a rate roughly a factor of three greater:

$$< \text{}^{37}\text{Cl} >_{SSM} = (7.9 \pm 2.6) \text{ SNU} \quad (243)$$

This, roughly 3σ contradiction between experiment and theory, constitutes the solar neutrino puzzle. Its resolution could lie in one of three possible explanations:

- i) The experiment of Davis et al [71], somehow, has consistently failed to measure a sizable fraction of the expected conversions.
- ii) The prediction of the Standard Solar Model is in error and the model overestimates the flux of neutrinos coming into Davis's experiment.
- iii) Some new physics phenomena associated with neutrinos is at play, which accounts for the discrepancy.

I have little to comment on the first possibility, except to note that the experiment is extremely challenging. Furthermore, as I shall discuss below, at least the 1987 observations of Davis are confirmed by the Kamiokande experiment. Note, however, that the 1987 data of Davis et al [73] yield a value

$$< \text{}^{37}\text{Cl} >_{exp} |_{1987} = (5.1 \pm 1) \text{ SNU} \quad (244)$$

which is about a factor of two above the 1970-85 average.

The possibility that the Standard Solar Model itself could be wrong, at least for its predictions of the yield for the ^{37}Cl experiment, is not too far fetched. The SSM is being rather severely tested by the Davis et al experiment, since the ^{37}Cl capture rate depends on the minor (and therefore more uncertain) ^8B cycle in the sun*. Fig. 25 shows the spectrum of neutrinos emerging from the sun, arising from the various nuclear cycles. Because the threshold for the $^{37}\text{Cl} + \nu_e \rightarrow \text{}^{37}\text{Ar} + e^-$ reaction is $E_{th} = 0.814$ MeV, the experiment of Davis et al is insensitive to the dominant pp cycle [$p+p \rightarrow D + e^+ + \nu_e$; $E_{max} = 0.42$ MeV]. Furthermore, since the dominant transition in the ν_e capture in ^{37}Cl is the excitation of the $3/2^+$ ground state to the 4.99 MeV $3/2^+$ excited state of ^{37}Ar (capture rate $\sim 69\%$ [72]), one sees from the figure that the experiment of [71] is mostly sensitive to the energetic neutrinos coming from the small ^8B cycle [$^7\text{Be} + p \rightarrow \text{}^8\text{B} + \gamma$; $^8\text{B} \rightarrow \text{}^8\text{Be}^* + e^+ + \nu_e$; $E_{max} = 14.1$ MeV]. Indeed, according to Bahcall et al [72], the 7.9 SNU predicted for the

* One should note that the predictions of the SSM have varied monotonically downward with time [72], although this was mostly due to uncertainties - later resolved - in nuclear cross sections. So one may hope that the SSM predictions will eventually asymptote to the Davis et al [71] answer!

^{37}Cl experiment have the following breakdown, in terms of the sun's various cycles:

$$pp = 0; \text{ } ^7\text{Be} = 0.2; \text{ } ^8\text{B} = 1.1; \text{ } \text{CNO} = 0.4; \text{ } ^8\text{B} = 6.1 \quad (245)$$

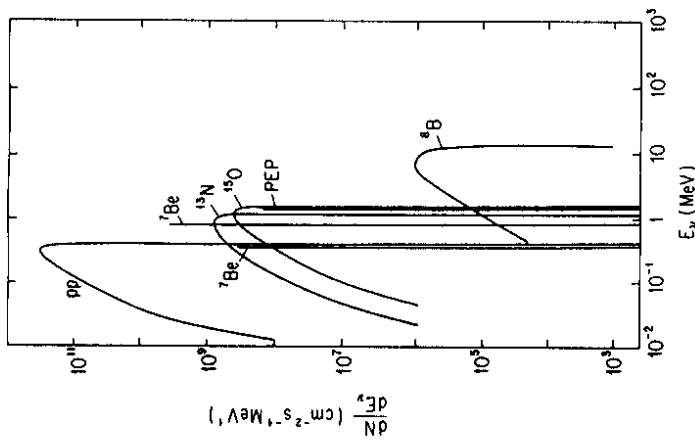


Fig. 25: Solar neutrino spectrum, from [72], for the various cycles in the sun.

The ^8B rate, which is crucial for the Davis et al experiment, depends quite sensitively on the temperature of the sun in its core region. This is illustrated in Fig. 26, which shows that the ^8B flux comes mostly from a region around $R = 0.05R_{\odot}$.

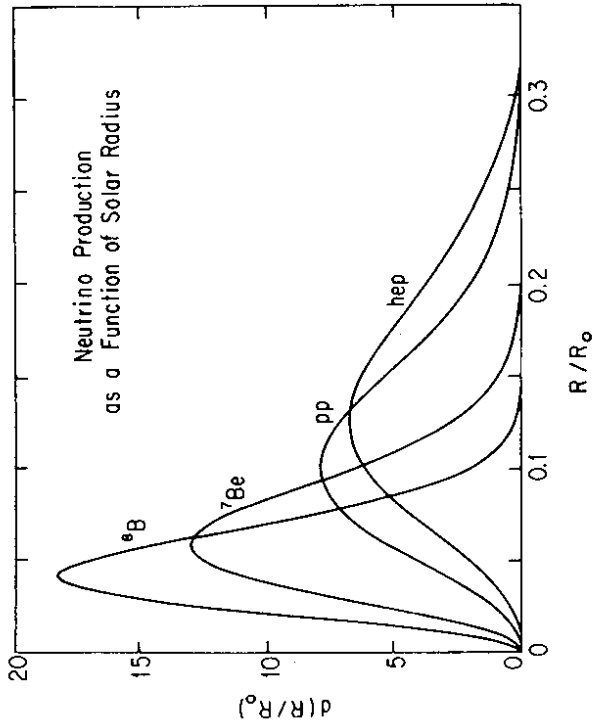


Fig. 26: Neutrino production as a function of the solar radius, from [74].

Because the ^8B neutrinos are produced so centrally, their rate depends crucially on the core temperature of the sun, where it is quite uncertain*. The theoretical error [72] on the 7.9 SNU quoted in Eq (243) is supposed to take into account of all these uncertainties. However, it would clearly be desirable if:

- i) One could get a confirmation of the Davis et al experiment by some other means.
- ii) One could perform other experiments not so sensitive to the ^8B cycle.

I will address both these points below.

The Kamiokande II detector has recently presented the first direct evidence for a non zero solar neutrino flux [75], confirming the results of the radiochemical ^{37}Cl experiment

* Indeed, the original motivation of the Davis experiment was to measure this core temperature!

[71]. However, these results are somewhere in between the predictions of the SSM and the long-term average results of the Davis et al experiment, Eq (242). The Kamiokande detector is a 3000 tons water Cherenkov detector, which is sensitive to the high energy end of the solar neutrino spectrum. What is being measured is the elastic scattering process $e^- \nu_e \rightarrow e^- \nu_e$, above a threshold energy of $E_e^{th} = 9.5$ MeV. Hence, Kamiokande II is only sensitive to neutrinos from the ^8B cycle. To eliminate spurious background sources only a fiducial volume of 680 tons was considered in the experiment. Furthermore, to dig out the signal from the background, use was made of the directionality of the scattered electron signal, with respect to the sun. As can be seen from Fig. 27, taken from [75], there is indeed a considerable peaking at zero angle, over a flat background.

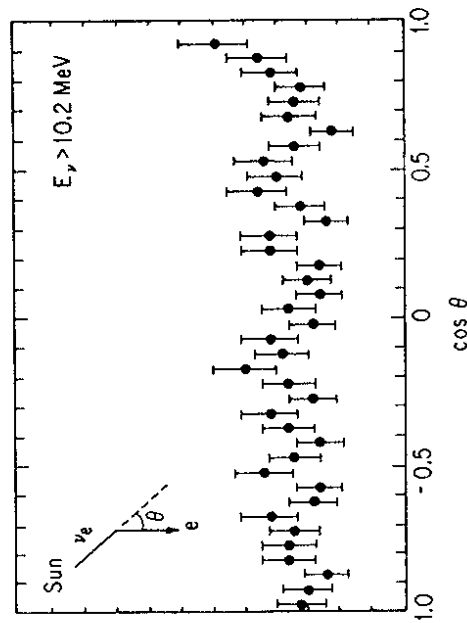


Fig.27: Angular dependence of the scattered electrons with respect to the sun direction, for $E_e > 10.2$ MeV, from [75].

These observations allow the Kamiokande collaboration to give a (preliminary) value for the ^8B neutrino flux observed of

$$\Phi_\nu(^8\text{B}) = (2.6 \pm 0.8) \times 10^6 \text{ cm}^{-2} \text{ sec}^{-1}, \quad (246)$$

which one should compare to the prediction of the SSM

$$\Phi_\nu^{SSM}(^8\text{B}) = (5.8 \pm 1.7) \times 10^6 \text{ cm}^{-2} \text{ sec}^{-1} \quad (247)$$

Obviously, the discrepancy between theory and experiment is smaller here. It is difficult to translate the above result so as to make a direct comparison with the ^{37}Cl experiment. A sensible attempt, perhaps, would be to multiply the 6.1 SNU's expected from the ^8B cycle by the ratio of Φ_ν observed to Φ_ν^{SSM} and add to it the remaining 1.8 SNU's from the other cycles. Then the equivalent Kamiokande II result would be

$$\langle ^{37}\text{Cl} \rangle > \text{Kamiokande eq} = 4.55 \pm 0.83 \text{ SNU} \quad (248)$$

This value is about a factor of two larger than the average value of the Davis et al [71] experiment, Eq. (242). It is, however, comparable to the Davis et al data [73] taken in the same time period (1987), Eq (244). It is unclear what to make of this latter observation, except to point out [76] an amusing anticorrelation of the Davis et al data with the number of sun spots. This anticorrelation persists for the new 1987 data, both from the Kamiokande and the ^{37}Cl experiment, as Fig. 28 shows.

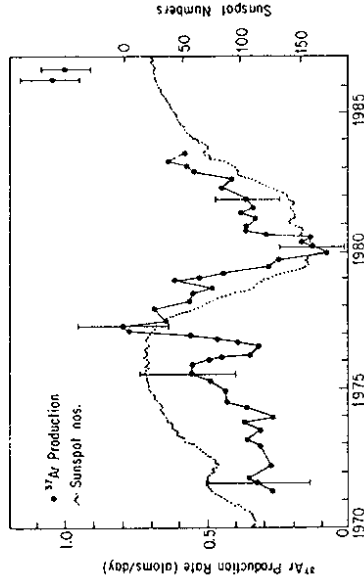
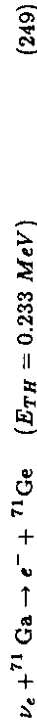


Fig. 28: Comparison of solar neutrino data with sun spot number, from [76].

It is clearly very important to ascertain if the solar neutrino puzzle is a problem of the solar model or a particle physics problem (or maybe no problem at all!).

In this respect the results of experiments to be performed in the coming years will be crucial. In the near future, two detectors using Gallium will begin operation, one in the Soviet Union at Baksam, and the other in Italy, in the Gran Sasso tunnel. At Baksam a US - USSR collaboration (SAGE) has installed a detector with 30 tons of metallic gallium and eventually hopes to grow to 60 tons, with first physics results expected in 1989. In the Gran Sasso Tunnel the Gallex collaboration has 30 tons of gallium in $\text{GaCl}_3 - \text{HCl}$, and they hope for first results in 1989/90. The interesting aspect of these gallium based experiments is that they will be sensitive to neutrinos from the dominant pp cycle, because of the low threshold for the neutrino capture reaction



In the Standard Solar Model one expects a rate of 132^{+20}_{-17} SNU [72], of which about half arises from the pp cycle. This rate corresponds to about 1 event/day for 30 tons of Ga, so that these experiments are in the difficulty class of the experiment of Davis and collaborators! Nevertheless, the solar uncertainty is in much better control and these experiments can provide an important check of new physics ideas [see Sec. V.2].

On a larger term scale (early to middle 1990's) two other powerful detectors may yield an order of magnitude more information [77]. ICARUS, in the Gran Sasso, is a planned 3000 tons liquid Argon calorimeter, while the SNO experiment in Sudbury, Canada, envisages having a 1000 ton D_2O detector. Both of these planned experiments are sensitive once again to neutrinos in the upper end of the solar spectrum, because of their high thresholds. Hence, they will be detecting neutrinos from the ${}^8\text{B}$ cycle, along with neutrinos from the small hep cycle (${}^3\text{He} + p \rightarrow {}^4\text{He} + e^+ + \nu_e$) which has almost a 14 MeV top energy. As Fig. 26 indicates, these two processes probe different regions in the interior of the sun.

Both ICARUS and SNO are direct detection experiments, which will be able to measure the actual energy spectrum of solar neutrinos, in contrast to the Davis et al experiment, which is only sensitive to integrated data. In ICARUS one expects about 20 events/day arising equally from capture in Argon and from elastic neutrino scattering. The Sudbury experiment will be principally triggered by the neutrino disintegration of the deuteron:



and one expects about 30 events/day here also. Obviously, one is eagerly awaiting the results from the gallium experiments and one can only look forward to the commissioning of these latter (3^{rd} generation) experiments.

V.2 The MSW Effect

The solar neutrino puzzle may in the end be only a problem of the SSM or of the existing experiments. Nevertheless, there is also a very beautiful and interesting possibility for diluting the flux of solar neutrinos: the Mikheyev - Smirnov - Wolfenstein (MSW) effect [78] [79]. The simple idea here is that the flux of solar neutrinos is reduced due to neutrino oscillations in the sun. However, the important physics point raised by the MSW effect is that, in contrast to neutrino oscillations in vacuum, in matter one can have large effects also for small mixing angles! I want to spend a little time elucidating this point, since it is both interesting and beautiful (and it might be true, in real life!).

We have discussed briefly neutrino oscillations in vacuum in Sec. III.2. The extra ingredient in matter, not present in vacuum, is the contribution of the CC process $\nu_e e^- \rightarrow e^- \nu_e$, in addition to the NC process, to neutrino scattering (see Fig. 29). This extra scattering process adds a "phase" to the ν_e components of the neutrino wave function.

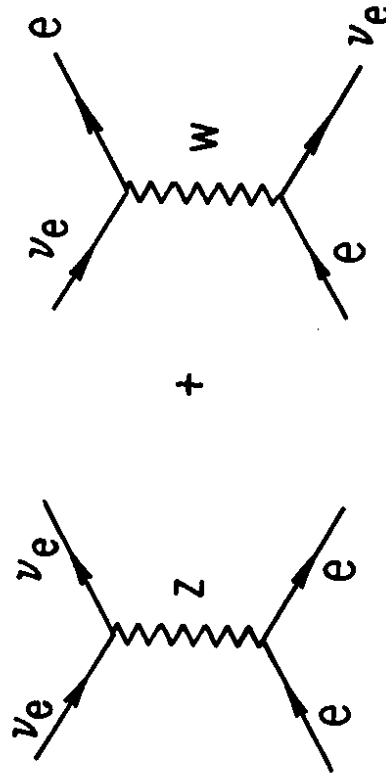


Fig. 29: NC and CC processes contributing to $e^- \nu_e \rightarrow e^- \nu_e$ scattering

One can think of neutrino scattering in matter as being equivalent to producing an index of refraction for the propagation of the neutrinos. The presence of the second process in

Fig. 29, which is peculiar to $\nu_e e^-$ scattering, will produce a different index of refraction for a ν_e compared to that for a ν_μ , or a ν_τ : $n_e \neq n_\mu = n_\tau$. Thus, neutrino oscillations in matter can be different to those in vacuum.

Let me consider for simplicity the case of two species of neutrinos. Then, as we discussed earlier [c.f. Eq (155)], there is a linear relation between the mass eigenstates ν_1 and ν_2 and the weak interaction eigenstates ν_e^{WI} and ν_μ^{WI} , characterized by a mixing angle θ . If one examines the time development of a state which was born originally as a ν_e^{WI} (or a ν_μ^{WI}), there will be now two sources for its time dependence. In matter, just as in vacuum, the mass eigenstates $|\nu_i(t)\rangle$ will oscillate as

$$|\nu_i(t)\rangle \sim e^{-iEt} \sim e^{-ip_e t} e^{-i\frac{m_i^2}{2p} t} \quad (251)$$

where I have expanded the energy to first order in the mass parameters. However, in addition to this the $|\nu_e^{WI}\rangle$ state will pick up an extra phase factor relative to the $|\nu_\mu^{WI}\rangle$ state, since its forward scattering amplitude, due to the presence of the CC process, is different than that of the $|\nu_\mu^{WI}\rangle$ state:

$$T(0)_{\nu_e e} \neq T(0)_{\nu_\mu e} \quad (252)$$

If n_{rel} is the relative index of refraction between $|\nu_e^{WI}\rangle$ and $|\nu_\mu^{WI}\rangle$, one has that [78]

$$1 - n_{rel} = -\frac{2\pi n_e}{p^2} [T(0)_{\nu_e e} - T(0)_{\nu_\mu e}] \quad (253)$$

$$= \frac{\sqrt{2} G_F n_e}{p}$$

where n_e is the electron density in the media.

The time development of $|\nu_e^{WI}(t)\rangle$ and $|\nu_\mu^{WI}(t)\rangle$ in matter is governed by a 2×2 Schroedinger equation

$$i \frac{\partial}{\partial t} \begin{pmatrix} |\nu_e^{WI}(t)\rangle \\ |\nu_\mu^{WI}(t)\rangle \end{pmatrix} = H_{matter} \begin{pmatrix} |\nu_e^{WI}(t)\rangle \\ |\nu_\mu^{WI}(t)\rangle \end{pmatrix} \quad (254)$$

Here H_{matter} contains the usual vacuum mixing Hamiltonian, plus a piece taking into account of the difference in the relative index of refraction between $|\nu_e^{WI}\rangle$ and $|\nu_\mu^{WI}\rangle$:

$$H_{matter} = H_{vac} + p(1 - n_{rel}) \begin{pmatrix} 1 & 0 \\ 0 & 0 \end{pmatrix} \quad (255)$$

where

$$H_{vac} = \frac{1}{2p} \begin{vmatrix} m_1^2 \cos^2 \theta + m_2^2 \sin^2 \theta & (m_2^2 - m_1^2) \sin \theta \cos \theta \\ (m_2^2 - m_1^2) \sin \theta \cos \theta & m_1^2 \sin^2 \theta + m_2^2 \cos^2 \theta \end{vmatrix} \quad (256)$$

Using Eq (253), one sees that the evolution in matter of $|\nu_e^{WI}(t)\rangle$ and $|\nu_\mu^{WI}(t)\rangle$ is governed by the slightly modified Hamiltonian (with respect to Eq (256)):

$$H_{matter} = \frac{1}{2p} \begin{vmatrix} m_1^2 \cos^2 \theta + m_2^2 \sin^2 \theta + p\sqrt{2} G_F n_e & (m_2^2 - m_1^2) \sin \theta \cos \theta \\ (m_2^2 - m_1^2) \sin \theta \cos \theta & m_1^2 \sin^2 \theta + m_2^2 \cos^2 \theta \end{vmatrix} \quad (257)$$

One can use the above Schroedinger equation to compute the transition probability for a ν_e^{WI} state to oscillate into a ν_μ^{WI} state. The result will have the same form as that given in Eq (164), except that the mixing angle and the eigenstates are reinterpreted:

$$P(\nu_e^{WI} \rightarrow \nu_\mu^{WI}) = \sin^2 2\theta_M \sin^2 \frac{L}{4p} (\Delta m^2)_M \quad (258)$$

A straightforward calculation, using Eq (257), secures the following formulas for the mixing angle factor in matter, $\sin^2 2\theta_M$, and for the matter mass difference squared, $(\Delta m^2)_M$:

$$\sin^2 2\theta_M = \sin^2 2\theta \left[\frac{\Delta m^2}{(\Delta m^2)_M} \right] \quad (259)$$

$$(\Delta m^2)_M = [(D - \Delta m^2 \cos 2\theta)^2 + (\Delta m^2 \sin 2\theta)^2]^{\frac{1}{2}} \quad (260)$$

where

$$D = 2\sqrt{2}G_F n_e p \quad (261)$$

Note that as $n_e \rightarrow 0$, the matter quantities θ_M and $(\Delta m^2)_M$ reduce to those in vacuum. Furthermore, it is also easy to deduce that the two mass eigenstates in matter are:

$$m_{\mp}^2 = \frac{1}{2} [m_1^2 + m_2^2 + D \mp (\Delta m^2)_M] \quad (262)$$

From the above results one arrives at two principal conclusions:

i) In matter the two neutrino system experiences a resonance phenomena. There is a critical density, n_e^{crit} , which depends on the momentum of the neutrinos, given by

$$D = 2\sqrt{2}G_F n_e^{crit} p = \Delta m^2 \cos 2\theta, \quad (263)$$

where the matter mixing angle factor goes to unity: $\sin^2 2\theta_M \rightarrow 1$. Thus, maximum mixing occurs independently of the value of the vacuum mixing angle θ .

ii) At the same critical density, a level crossing phenomena occurs and the neutrino mass eigenstates switch identities. That is, at n_e^{crit} given by

$$n_e^{crit} = \frac{\Delta m^2 \cos 2\theta}{2\sqrt{2}G_F p}, \quad (264)$$

a $|\nu_e^{WI} >$ state is converted 100% into a $|\nu_\mu^{WI} >$ state!

This level crossing phenomena is illustrated in Fig. 30. This is the MSW effect [78] [79]. Neutrinos produced as ν_e^{WI} 's, in a region of high electron density, oscillate totally into ν_μ^{WI} 's as the density goes below the critical density n_e^{crit} .

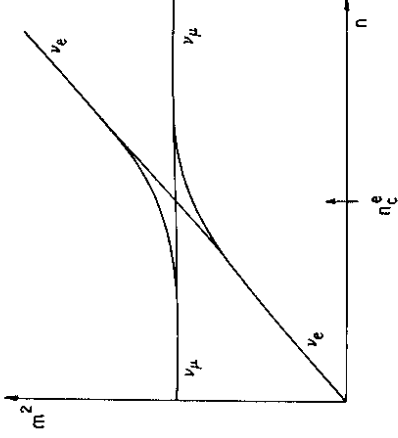


Fig. 30: Level crossing at the critical density.

The MSW effect offers, obviously, a possible explanation of the solar neutrino puzzle. Electron neutrinos produced in the sun core at $n_e > n_e^{crit}(p)$, as they move out of the center of the sun to regions of lesser density, get totally converted into other neutrinos. The only ν_e 's which survive to be detected in the earth's experiments are electron neutrinos with sufficiently small energy, so that even in the sun's core, the critical density $n_e^{crit}(p)$ is always greater than the core electron density. To compute the number of neutrinos expected at earth one must integrate over the neutrino spectrum, with the MSW effect providing an effective high energy cut off.

One can estimate the allowed region in the $\Delta m^2 - \sin 2\theta$ plane for which the MSW effect will cause a depletion in the solar neutrino flux as follows [80]. First of all, the resonance condition (264) on the critical density will not be satisfied unless Δm^2 is small enough. Taking $p = p_{max} \simeq 14$ MeV for the ^8B cycle and setting the critical density n_e^{crit} equal to the central density in the sun, $n_e^{crit} \simeq 100 \frac{\rho}{\text{cm}^3} N_A$, yields

$$(\Delta m^2)_{max} \simeq 10^{-4} (\text{eV})^2 \quad (265)$$

So for the MSW effect to be operative, one needs very small neutrino mass differences. Unless there is some kind of fine tuning conspiracy, this argues then also for small individual neutrino masses (i.e. $m_\nu < 10^{-2} \text{eV}$).

However, not all values of (Δm^2) below $(\Delta m^2)_{\max}$ will give rise to an effect. The total conversion of ν_e^{WI} into ν_μ^{WI} as the electron neutrinos go through the critical density region, $n_e \simeq n_e^{\text{crit}}$, will only happen in practice if the change in the environment is not too rapid. This requirement of adiabaticity [81] can be stated more precisely as a requirement that the change in the matter mixing angle θ_M be slow compared to the frequency of oscillation:

$$\left. \frac{d\theta_M}{dr} \right|_{n_e^{\text{crit}}} < \frac{\Delta m^2 \sin 2\theta}{2p} \quad (266)$$

Since

$$\left. \frac{d\theta_M}{dr} \right|_{n_e^{\text{crit}}} \simeq \frac{1 \sin 2\theta}{2 \cos 2\theta} \frac{1}{n_e} \frac{dn_e}{dr} \Big|_{n_e^{\text{crit}}} \quad (267)$$

the adiabatic condition requires that

$$\frac{1}{n_e} \frac{dn_e}{dr} \Big|_{n_e^{\text{crit}}} < \frac{\Delta m^2 \sin^2 2\theta}{p \cos 2\theta} \quad (268)$$

Typically, in the Sun [82]

$$\frac{1}{n_e} \frac{dn_e}{dr} \simeq \frac{10}{R_\odot} \simeq 1.4 \times 10^{-15} \text{ eV} \quad (269)$$

so that the adiabatic constraint implies that

$$\frac{\Delta m^2 \sin^2 2\theta}{\cos 2\theta} > 2 \times 10^{-8} \text{ (eV)}^2 \quad (270)$$

If we add to the two conditions, (265) and (270), a trivial constraint that the mixing angle $\sin \theta$ cannot be bigger than $\frac{1}{\sqrt{N_e}} = \frac{1}{\sqrt{3}}$, one sees that the MSW effect for the ^8B neutrinos can only make sense if the parameters Δm^2 and $\frac{\sin^2 2\theta}{\cos 2\theta}$ lie in the triangular region roughly sketched in Fig. 31 below.

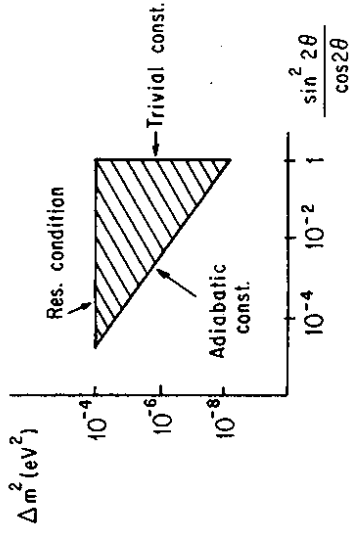


Fig. 31: Schematic allowed region for the MSW effect.

This result is verified by more detailed calculations. As an example, I show in Fig. 32 the results of a careful recent study by Parke and Walker [83] for the allowed region in the $\Delta m^2 - \frac{\sin^2 2\theta}{\cos 2\theta}$ plane. The shaded region in the figure corresponds to the values of these parameters which would reproduce the results of the ^{37}Cl experiment. Also shown in this picture are contour lines for the number of SNU's to be expected for the gallium experiments, if the MSW effect is the explanation of the solar neutrino puzzle. Clearly, one awaits with interest the results from SAGE and Gallex!

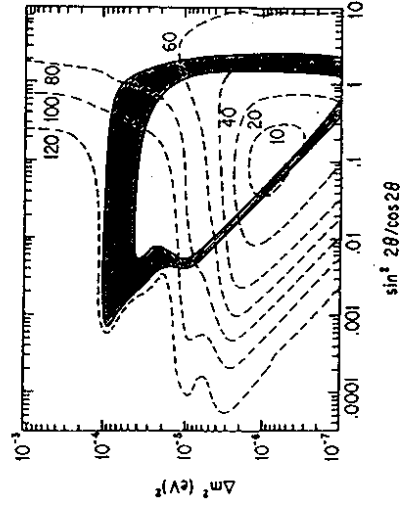


Fig. 32: Allowed region in the $\Delta m^2 - \frac{\sin^2 2\theta}{\cos 2\theta}$ plane, from [83].

V.3 Neutrinos from SN 1987a

The neutrino burst observed by the Kamiokande [69] and IMB [70] detectors, arising from the supernova explosion in the large Magellanic cloud (LMC) in February 1987, has provided important information on neutrinos and a confirmation of the theoretical mechanisms associated with gravitational collapse. I shall discuss first some preliminaries of the events observed by the Kamiokande and IMB detectors. I will, however, discount here the data of Mt. Blanc [84] since these observations are not in coincidence with the other experiments and the energetics appear to be wrong.

I display in Fig. 33 the combined time sequence of events from IMB and Kamiokande. Since, unfortunately, there was not a coincident time measurement, I have taken the liberty to overlay these events so that the initial main burst, corresponding to $\Delta t \sim 3 - 4$ sec, in both detector's overlaps. As the detectors have different energy thresholds, [IMB: $E \sim 30$ MeV; Kamiokande: $E \sim 7.5$ MeV], the apparent higher average energy given by IMB [$E > \text{IMB} \approx 35$ MeV] compared to that of the Kamiokande experiment [$E > \text{Kamiokande} \approx 15$ MeV] may be entirely a result of this threshold cut.

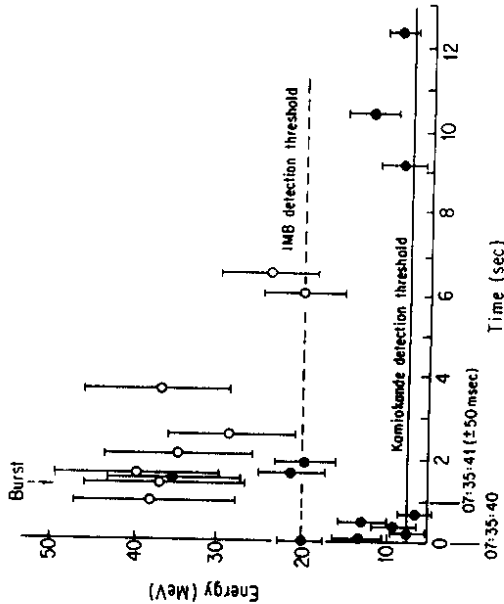


Fig. 33: Neutrino event structure for the IMB (open circles) and Kamiokande (closed circles) detectors.

In Fig. 34, I display the angular distribution of the events compared to the direction of the Magellanic cloud ($\theta = 0$). It is clear that this angular distribution shows some correlation with the supernova position. Indeed, particularly the first two events seen by the Kamiokande detector [69] appear to point directly back to the LMC direction [$\theta_1 = 18^\circ \pm 18^\circ$; $\theta_2 = 15^\circ \pm 27^\circ$]

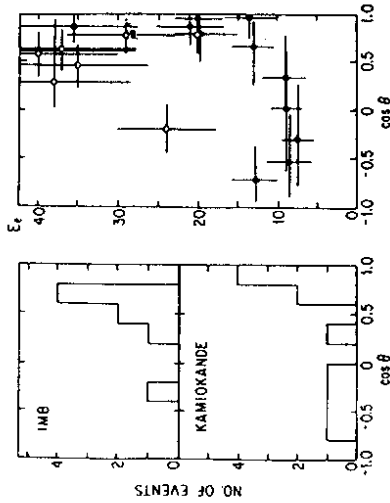


Fig. 34: Distribution of events and of the electron's recoil energy E_e as a function of $\cos \theta$, as observed by the Kamiokande and IMB detectors.

Water Cherenkov detectors like IMB and Kamiokande are sensitive to neutrinos either through the NC scattering off electrons $\nu_e \rightarrow \nu_e$ ($\nu_i = \nu_e, \nu_\mu, \nu_\tau$), or via the inverse β decay process $\bar{\nu}_e p \rightarrow e^+ n$. The second process, however, has a much larger cross section:

$$\sigma(\bar{\nu}_e) \approx 7 \times 10^{-42} \text{ cm}^2 \left(\frac{E_\nu}{10 \text{ MeV}} \right)^2 \quad (271)$$

$$\sigma(\nu_e) \approx 10^{-43} \text{ cm}^2 \left(\frac{E_\nu}{10 \text{ MeV}} \right) \quad (272)$$

As one expects the flux of all neutrinos from the supernova to be roughly the same (I shall discuss this further, below), the inference is that the bulk of the events observed by both detectors are $\bar{\nu}_e$.

Simple kinematical considerations of the events from SN 1987a can immediately serve to restrict neutrino properties.

Neutrino Lifetime

Since the neutrino burst travelled the approximately 150,000 light years from the large Magellanic cloud to earth, it follows that the neutrinos are not unstable. Indeed, using that $\langle E_\nu \rangle \approx 15 \text{ MeV}$, it follows that the electron antineutrino lifetime is longer than

$$\tau_{\nu_e} \geq 3 \times 10^5 \text{ sec} \left(\frac{m_{\nu_e}}{\text{eV}} \right) \quad (273)$$

The above result provides the first direct evidence that solar neutrinos can get to the earth without decaying first. Hence, it rules out neutrino decay as a possible solution of the solar neutrino puzzle [85].

Neutrino Mass

Obviously, massive neutrinos originating from SN 1987a would arrive at earth with a certain time spread, since they would travel at different velocities.

$$\beta = \frac{1}{\sqrt{1 - \left(\frac{E_\nu}{m_\nu}\right)^2}} \approx 1 - \frac{1}{2} \frac{m_\nu^2}{E_\nu^2} \quad (274)$$

Unfortunately, one cannot directly interpret the time spread of the neutrino signal, shown in Fig. 33, as evidence for a neutrino mass. The supernova emission process itself has some time and energy spread and so its analysis is not so straight forward. Furthermore, the recoil energy observed is not directly the energy of the incoming neutrinos, adding another element of uncertainty.

The time delay of a massive neutrino, relative to that of a massless neutrino, is simply*

$$\Delta t = \frac{d}{2c} \left(\frac{m_\nu}{E_\nu} \right)^2 \approx 2.6 \text{ sec} \left(\frac{m_\nu}{10 \text{ eV}} \right)^2 \left(\frac{10 \text{ MeV}}{E_\nu} \right)^2 \quad (275)$$

Since the average neutrino energies are around 10 MeV, one sees from the above that the time spread expected is of the right order of magnitude to probe 10 eV neutrino masses. One way to try to estimate a possible neutrino mass is to plot the pulse dispersion as a function of m_ν^2 [86] and to look for maximal overlap regions. The resulting picture for the Kamiokande events is shown in Fig. 35, which takes into account the 1σ errors on the energies.

* The numerical value below, in fact, has some error since the distance of SN 1987a from earth is not totally well determined: $d = 55 \pm 15 \text{ Kpc}$

The least dispersion here appears around $m_{\nu_e} \approx 20 \text{ eV}$, but one should really fold in the supernova time and energy profile for a more reliable analysis. This has been done by a great number of people to try to extract a neutrino mass bound from SN 1987a*. The result, which is already understandable from our naive discussion, is that

$$m_{\nu_e} \leq 5 - 30 \text{ eV} \quad (276)$$

This is interesting, in that it is comparable to the direct measurement of ν_e , but it is not really better.

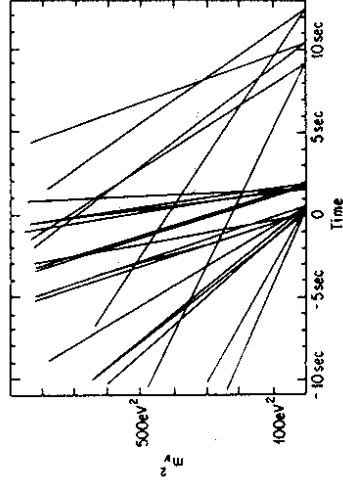


Fig. 35: 1σ contours of the pulse dispersion as a function of m_{ν_e} for the Kamiokande events, from [86].

Neutrino Mixing and the MSW Effect

This subject is controversial since it needs a statistical argument. Furthermore, if the components of mixing [87] are correct, then the MSW effect cannot be an explanation of the solar neutrino puzzle! I mentioned above that the cross section for the inverse beta decay process far exceeded the elastic electron scattering cross section. However, these two cross sections have quite different angular distributions for the produced leptons. The elastic scattering process $\nu_e e \rightarrow \nu_e e$ tends to produce leptons quite forward peaked in the direction of the incoming neutrinos, while for the inverse beta process one has a roughly isotropic distribution.

* In fact, the number of papers on this subject far exceeds the number of events!

Neutrinos originating from the supernova explosion have roughly the same fluxes for all kinds of neutrinos and antineutrinos, as shown in Figs. 36a and 36b below, except for an initial sharp burst of electron neutrinos arising from the conversion process $e^- p \rightarrow n \nu_e$, immediately after the core collapse [deleptonization burst].

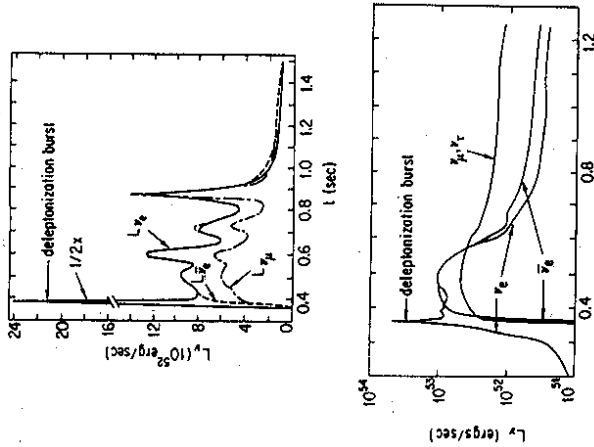


Fig. 36: Examples of two neutrino flux calculations from supernova collapse: a) from [88]; b) from [89].

Given the above facts, the interesting and debateable issue is whether the first two Kamiokande events, which both point towards the LMC, are $\nu_e e \rightarrow \nu_e e$ scattering events or not? Clearly, from the high forward peaking and their association with the earliest burst one may want to argue this way. However, from inferred neutrino energetics and from the number of events one estimate could arise from the deleptonization burst [90], one arrives at a contrary conclusion. If one assumes, anyway, that the events are really due to electron neutrinos, then one can severely constrain the allowed region for the MSW effect.

A careful analysis by Arafune et al [91], Nötzold [92] and Minakata et al [93] shows that only a small region around $\Delta m^2 \sim 10^{-6} \text{ eV}^2$, $\sin^2 2\theta \sim 0.3$ remains, for which the neutrinos from the supernova would either not have oscillated away or would have been reconverted in the earth.

The observation of the neutrinos from the collapse of SN 1987a is perhaps most important not for what it has taught us about neutrinos, but because it has confirmed the principal features of the theoretical picture of star collapse. I want to end my lectures by briefly discussing the standard collapse scenario [94] and indicate how SN 1987a has provided important checks on the theory.

Massive stars ($M > 10 M_\odot$) have increasing central temperatures and densities as a succession of nuclear fuels are burned, trying to stop the gravitational contraction. The different elements burned $H \rightarrow {}^4\text{He} \rightarrow {}^{12}\text{C} \rightarrow {}^{16}\text{O} \rightarrow {}^{28}\text{Si} \rightarrow {}^{56}\text{Fe}$ provide a shell-like structure for the star, as shown schematically in Fig. 37. Eventually, when the mass of the ${}^{56}\text{Fe}$ core exceeds the Chandrasekhar limit [$M_{ch} \approx 1.4 M_\odot$], where the fermion pressure cannot any longer overcome the gravitational attraction, gravitational collapse occurs and the star ends up as a neutron star (or a black hole).

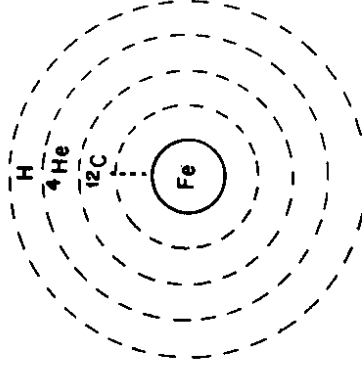


Fig. 37: Schematic shell-like structure of a collapsing star.

Clearly the energy release in this process is enormous, since the typical neutron star radius

A recent analysis by Burrows and Lattimer [95] of the Kamiokande data in this manner yields

$$T_{\text{eff}} = 2.72 \pm 0.26 \text{ MeV} \quad (282)$$

$$< E_{\nu} > = 8.57 \pm 0.82 \text{ MeV}$$

A more graphical analysis, which is shown in Fig. 38, due to Schramm [96], gives essentially the same answer for the combined data of IMB and Kamiokande.

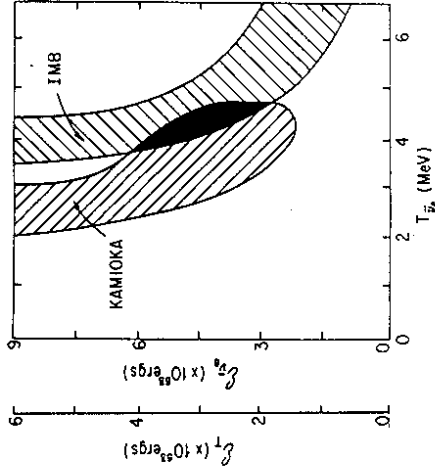


Fig. 38: Inferred energy release, versus effective neutrino temperature, for the neutrino events observed by the IMB and Kamiokande collaborations, from [96].

Acknowledgements

I am very grateful for the splendid hospitality and the friendly atmosphere of the Symposium. I especially would like to thank Prof. Kuang-Ta Chao for all his efforts in organizing such a stimulating meeting.

Part of the material presented here on neutrino counting is included in my lectures at the 1988 TASI school.

is of the order of 10 km :

$$\Delta E = G_N \frac{M_{\text{ch}}^2}{r_n} \simeq 2.7 \times 10^{53} \text{ ergs} \left(\frac{M}{M_{\odot}} \right)^2 \left(\frac{10 \text{ Km}}{r_n} \right) \quad (277)$$

Most of the energy released in the process of collapse is in the form of neutrinos ($\sim 95\%$), while the optical fireworks, for which supernovas are known, accounts for only about 1% of the energy emitted!

The first stage of this energy release via neutrinos is the deleptonization process we discussed above: $e^-p \rightarrow \nu_e n$. However, not all the neutrinos from deleptonization escape in the first shock wave. Rather, the majority of these neutrinos gets trapped in the collapsing core, due to the large nuclear NC scattering cross section, and form a neutrino-sphere [$R_{\nu} \sim 70 \text{ Km}$]. At a later stage, neutrinos (and antineutrinos) of all species are emitted from this neutrino-sphere in a black body way after the sphere is heated [$T \sim 10 \text{ MeV}$] by the shock wave bounce of the established neutron star. The time sequence for these two processes, deleptonization and black body emission, are quite different [cf Fig. 36], with the black body emission lasting around 5 - 10 sec, which is the relevant diffusion time.

The effective temperature of the neutrino sphere follows from the radiation law

$$T_{\text{eff}} = \left[\frac{\Delta E}{4\pi\sigma R_{\nu}^2} \left(\frac{1}{\frac{7}{4}N_{\nu}} \right) \right]^{\frac{1}{4}} \simeq 3 \text{ MeV} \quad (278)$$

with σ being the Stefan Boltzmann constant, and one finds for the average neutrino energy

$$\langle E_{\nu} \rangle \simeq 10 \text{ MeV} \quad (279)$$

These features are checked by the data of Kamiokande and IMB. The antineutrino flux is given by the Fermi-Dirac distribution

$$\Phi(\bar{\nu}_e) dE_{\bar{\nu}_e} = \frac{\left[\frac{1}{6}(\Delta E) \right]}{4\pi d^2} \cdot \frac{120 E_{\bar{\nu}_e}^2 dE_{\bar{\nu}_e}}{7\pi^4} \frac{E_{\bar{\nu}_e}}{1 + e^{T_{\text{eff}}/E_{\bar{\nu}_e}}} \quad (280)$$

so that the number of events expected is

$$N_{\text{events}} = N_{\text{protons}} \int_{E_{\text{th}}}^{\infty} \sigma_{\bar{\nu}_e p \rightarrow e^+ n} \Phi(\bar{\nu}_e) dE_{\bar{\nu}_e} \quad (281)$$

- A. Albrecht and P. Steinhardt, *Phys. Rev. Lett.* 48 (1982) 1220; For reviews see also Ref. [43]
- [60] For a review, see V. Trimble, *Ann. Rev. Astron. Astrophys.* 25 (1987) 425
- [61] See S. M. Faber and J. J. Gallagher, *Ann. Rev. Astron. Astrophys.* 17 (1979) 135 and Ref. [60]
- [62] J. Primack, B. Sadoulet and D. Seckel, *Ann. Rev. Nucl. Part. Sci.* 39 (1989); See also, K. Olive in *Proceedings of the XVIII Cracow School for Theoretical Physics, Zakopane, Poland, June 1988*
- [63] See for example, J. Uson and D. Wilkinson in *Inner Space/Outer Space*, eds. E. W. Kolb et al (Univ. of Chicago Press, Chicago 1986)
- [64] J. R. Bond, G. Efstathiou and J. Silk, *Phys. Rev. Lett.* 45 (1980); Ya. B. Zeldovich and R. A. Sunyaev, *Pisma Astr. Zh* 6 (1980) 457
- [65] Ya. B. Zeldovich, *Astron. Ap.* 5 (1970) 84
- [66] J. R. Bond and A. Szalay, *Ann NY Acad. Sci.* 82 (1984) 422; C. Frenk, S. White and M. Davis, *Astrophysical J.* 271 (1983) 417
- [67] A. Vilenkin, *Phys. Rept* 121 (1985) 1; N. Vittorio and D. Schramm, *Comm. on Nucl and Part. Phys.* 15 (1985) 1
- [68] V. DeLapparent, M. Geller and J. Huchra, *Astrophys. J.* 302 (1986) L1
- [69] K. Hirata et al, *Phys. Rev. Lett.* 58 (1987) 1490
- [70] R.M. Bionta et al, *Phys. Rev. Lett.* 58 (1987) 1494
- [71] J.K. Rowley, B.T. Cleveland and R. Davis Jr., in *Solar Neutrinos and Neutrino Astronomy AIP Conference Proceedings No. 126*, eds. M.L. Cherry, W. A. Fowler and K. Lande (AIP, New York, 1985)
- [72] J. N. Bahcall et al, *Rev. Mod. Phys.* 54 (1982) 767; J.N. Bahcall and R. K. Ulrich, *Rev. Mod. Phys.* 60 (1988) 297
- [73] R. Davis Jr., in *Proceedings of the Seventh Workshop on Grand Unification, ICOBAN 86, Toyoma, Japan* (Japanese Press, Tokyo, 1986)
- [74] See Bahcall and Ulrich, Ref. [72]
- [75] Y. Totsuka, to appear in the *Proceedings of the XXIV International Conference on High Energy Physics, Munich, August 1988*
- [76] R. Davis Jr., Ref. [73]. See, however, also J. Bahcall, G.B. Field and W. H. Press, *Astrophys. J.* 322 (1987) L69
- [77] For a discussion see, M. Fukugita in *Proceedings of the Enrico Fermi Summer School CIII, Varenna, Italy, July 1987*. See also Bahcall and Ulrich, Ref. [72]
- [78] L. Wolfenstein, *Phys. Rev. D* 17 (1978) 2369; D20 (1979) 2634
- [79] S. P. Mikheyev and A. Yu. Smirnov, *Nuovo Cim* 9C (1986) 17
- [80] See for example, M. Fukugita, Ref. [77]
- [81] H. A. Bethe, *Phys. Rev. Lett* 56 (1986) 1305
- [82] G. J. Mathews et al, *Phys. Rev. Lett.* 32 (1985) 796; See also Ref. [72]
- [83] S. J. Parke and T. P. Walker, *Phys. Rev. Lett.* 57 (1986) 2322
- [84] M. Aglietta et al., *Europhys. Lett.* 3 (1987) 1315, 1321
- [85] J.N. Bahcall, N. Cabibbo and A. Yahil, *Phys. Rev. Lett.* 28 (1972) 316
- [86] E. W. Kolb, A. J. Stebbins and M. S. Turner, *Phys. Rev.* 35 (1987) 3598
- [87] J. Arafune and M. Fukugita, *Phys. Rev. Lett.* 59 (1987) 367

- [88] R. Maysle, J. R. Wilson and D. N. Schramm, *Astrophysical J.* 318 (1987) 288
- [89] S. W. Bruenn, *Phys. Rev. Lett.* 59 (1987) 938
- [90] T. Walker and D. N. Schramm, *Phys. Lett.* 195B (1987) 331
- [91] J. Arafune et al, *Phys. Rev. Lett.* 59 (1987) 1864
- [92] D. Notzold, *Phys. Lett.* 196B (1987) 315
- [93] H. Minakata et al, *Mod. Phys. Lett.* A2 (1987) 827
- [94] For a very nice discussion, see for example N. Straumann, PSI preprint PR-88-06
- [95] A. Burrows and J. Lattimer, *Astrophys. J.* 318 (1987) L63
- [96] D. N. Schramm, in *Proceedings of the 1987 International Symposium on Lepton and Photon Interactions*, Hamburg, Ed. W. Bartel and R. Ruckl, *Nucl. Phys B (Proc. Suppl.)* 3 (1988) 471